Title

A CDC-42-regulated actin network is necessary for nuclear migration through constricted spaces in Caenorhabditis elegans

Permalink

https://escholarship.org/uc/item/1x7855x1

Author

Ho, Jamie

Publication Date

2023

Peer reviewed|Thesis/dissertation

A CDC-42-regulated actin network is necessary for nuclear migration through constricted spaces
in *Caenorhabditis elegans*

By

JAMIE HO
DISSERTATION

Submitted in partial satisfaction of the requirements for the degree of

DOCTOR OF PHILOSOPHY

in

Biochemistry, Molecular, Cellular and Developmental Biology

in the

OFFICE OF GRADUATE STUDIES

of the

UNIVERSITY OF CALIFORNIA

DAVIS

Approved:

Daniel A. Starr, Chair

Lesilee S. Rose

Mark Winey

Committee in Charge

2023

i

Acknowledgments

I want to thank my advisor Dan Starr for being a great and supportive mentor throughout my PhD. You believed in me especially during my imposter syndrome flare-ups and while your pep talks were not the best, the sentiments behind them were encouraging. Thank you for always being patient and making time to talk about my project or to just shoot the breeze. I'm grateful for the experience that I have had in your lab.

I would also like to thank my dissertation committee members Lesilee Rose and Mark Winey for their guidance and suggestions. I would also like to thank Hari Reddi for his support and kindness.

Thank you to my lab members in the Starr Lab. You were all so helpful and kind and willing to help me brainstorm and troubleshoot my experiments and I will always be eternally grateful for that. Special thanks to Linda Ma, Ellen Gregory, and Hongyan Hao for providing me with a lot of guidance, support, and friendship during my first couple years in the lab. You all really made me feel confident as a scientist and I truly appreciated that.

Thank you to all the friends I made within the Biochemistry, Molecular, Cellular and Developmental Biology (BMCDB) graduate group. Special shout out to Courtney Dreyer for your friendship, weeknight dinners, and chats about the struggles of graduate school.
I want to thank my old mentor William Pastor for giving me my first opportunity to become a scientist and for being patient with me during the learning process. My time as a lab technician under your tutelage is what pushed me to want to pursue a PhD and you helped me develop the necessary skills to do so.

Thank you to all the friends I've made while organizing for UAW2865. I appreciate all of you and I believe you all are some of the best people I will ever meet. You all gave me the opportunities to make actual change and I am so proud of what we achieved together.

Thank you to all my friends for their support and for constantly checking in on me. You all help remind me that my self-worth is not tied to the progress I make in grad school or how well my experiments turn out. Thank you for believing in me and for your constant reassurance about how I am progressing through life. Special shout out to Nicole Chuhak for your daily phone calls, weekend lunches, memes, and your ability to always cheer me up during the bad times. Thanks to my roommates Lauren and Jocelynn for supporting me when I found it difficult to support myself, taking care of me when I was down, and making sure I still appreciate the little things in life. I'm going to really miss our weekly horror movie nights.

Thank you, my adorable cat Quincy, for providing me with constant laughter and affection. You are the only highlight of the chaos that was the year 2020 and I am always grateful that I decided to adopt that year. You have made such a positive impact on my life and my mental health.

And the biggest thank you to my mother and my brother Johnny for being the reason why I've gotten this far in life. You guys are the reason why I do what I do and why I'm constantly trying to push myself to be better. Your constant support and love inspire me to always strive for things that bring me joy and fulfillment in life. Thank you for believing in me!

Abstract

Confined cell migration is a critical part of many biological processes. It is essential in developmental events such as neurogenesis, it's important during the immune response as immune cells must migrate through endothelial tissue, and it is also a hallmark of cancer metastasis. The rate of confined cell migration is usually limited by the rate of nuclear migration as the nucleus is usually the largest and most rigid organelle of the cell. There are several factors that contribute to nuclear deformability such as lamin composition, heterochromatin levels, and the cytoskeletal network. Much of what we know about confined nuclear migration and the factors that regulate this process comes from *in vitro* studies. Most of these *in vitro* experiments utilize fabricated 3D matrices with constrictions that cultured cells can migrate through. While these experiments have been vital in our understanding of how this process is regulated, it is still unclear how this process is modulated *in vivo*.

Our lab has developed an *in vivo* model to study nuclear migration through constricted spaces by observing hypodermal precursor cells called P cells in *Caenorhabditis elegans*. During the early L1 larval stage, P-cell nuclei have to move from a lateral position to a ventral position by migrating through a narrow constriction that is about 5% the diameter of the nucleus. If this process is successful, the P cells are able to divide and develop into vulval cells and GABA neurons. The canonical pathway for P-cell nuclear migration is through the **Li**nker of the **N**ucleoskeleton and **C**ytoskeleton (LINC), which is made up of the SUN protein (UNC-84) found at the inner nuclear membrane and the KASH protein (UNC-83) found at the outer nuclear membrane. UNC-84 binds to UNC-83 which is able to interact with microtubule motor proteins. I show that conditional knockdown of DHC-1 leads to a significant nuclear migration defect and therefore dynein is the main microtubule motor protein involved.

Our lab has shown that disruption of the LINC complex leads to a temperature sensitive phenotype, suggesting there is an alternative pathway that functions parallel to the LINC complex pathway. From a forward-genetics screen, we were able to identify several putative actin regulators that are involved in this alternative pathway, highlighting the major role that actin plays in P-cell nuclear migration. One of the genes identified is *cgef-1*, which codes for a GEF that is able to activate CDC-42. I hypothesized that CGEF-1 activates CDC-42, which indirectly activates the Arp2/3 complex to generate branched actin. I show that CDC-42, the Arp2/3 complex, and non-muscle myosin II (NMY-2) are required for P-cell nuclear migration in the absence of the LINC complex at the restrictive temperature. I also show constitutively active CDC-42 is able to partially rescue the nuclear migration defect of the *cgef-1(-); unc-84(-)* double mutant.

I propose future work to determine if other GEFs are involved in regulating CDC-42 and if CDC-42 regulates both the Arp2/3 complex and NMY-2. It would also be informative to observe localization of CGEF-1, CDC-42, the Arp2/3 complex, and NMY-2 to further understand the mechanism by which these proteins function. An area of interest for further studies would be to determine how much nuclear actin plays a role in confined nuclear migration.

Table of contents

Chapter I

<u>Introduction: Nuclear migration through constrictions</u>

Nuclear Migration through constrictions *in vivo*

Cell migration through constricted spaces is necessary for various processes such as migration of cells through the extracellular matrix during development, migration of immune cells through tissue to reach the site of inflammation, and migration of metastatic cancer cells (Bone & Starr, 2016; Denais et al., 2016; Thiam et al., 2016). The rate at which a cell is able to migrate through constricted spaces is limited by deformability of the nucleus as the nucleus is usually the largest and most rigid organelle of the cell (Friedl et al., 2011; Fu et al., 2012; Swift et al., 2013; Wolf et al., 2013).

There are many examples of nuclear migration through confined spaces. During mammalian brain development, newly born neurons must migrate from the germinal layers to the developing cortices (Trivedi & Solecki, 2011). These neurons have an elongated shape with a thin leading process extended to the final destination of the cell and a trailing process at the back of the migrating cell. During this process, the nucleus of the cell must migrate through the cytoplasm towards the leading process by moving through constrictions generated by the surrounding crowded neural tissue (Kalukula et al., 2022; Kengaku, 2018). This confined nuclear migration is driven in part by dynein and kinesin-1 through the LINC complex (Wu et al., 2018). Failure of neurons to migrate to their destination is associated with various brain disorders (Manzini & Walsh, 2011).

Leukocytes have to migrate through constricted spaces in order to rush to the site of inflammation, infection, and sites of injury. Leukocytes found in the blood stream move by passive rolling along the endothelium of the blood vessel, which allows to cell to make constant transient interactions with the wall. Once the leukocyte encounters an adhesion receptor of an inflamed blood vessel, it begins crawling along the endothelium until it detects a junction in

between endothelial cells, at which point it will insert a protrusion and migrate through the endothelium (Y. Li et al., 2022; Salvermoser et al., 2018). During this migration, the nuclei undergo drastic deformation in order to pass through the constriction. This is made possible because the nuclei of leukocytes have lower levels of lamin A/C than lamin B, making the nuclei softer and easily deformable(Manley et al., 2018; Rowat et al., 2013). Bone marrow derived dentritic cells on the other hand detect infectious agents at the site of inflammation and migrate into the lymphatic system. To do so, these cells also have to migrate through constrictions of the lymphatic vessels (Vargas et al., 2017). While leukocytes have lower levels of lamin A/C, dendritic cells appear to have higher levels of lamin A/C which may be to protect the nucleus from mechanical stress that can cause increased DNA damage (Lele et al., 2018). This nuclear deformation instead seems to be facilitated by branched actin generated by Arp2/3 to aid in nuclear migration through constricted spaces (Thiam et al., 2016). Thus, nuclear migration through constricted spaces is required for immune cells to carry out their function.

The nucleus also plays an important role in cancer metastasis as the nucleus is a major obstacle in a cancerous cell's ability to migrate in-between tissue and into the capillaries to reach their secondary location. Levels of lamin A/C have been implicated in nuclear migration of metastatic breast cancer cells (Fu et al., 2012). Lamin A/C levels in breast cancer cell lines are lower compared to that of epithelial cells suggesting a softer nuclei in these cells help the nucleus deform during migration (Bell et al., 2022). Overexpression of lamin A in certain breast cancer cells lines also resulted in slower migration compared to their cells where their lamin levels were not altered (Bell et al., 2022). Additionally, decreased heterochromatin in different cancer cell lines can affect the rate of nuclear migration (Shinchi et al., 2015). While decreased heterochromatin may affect nuclear stiffness, it's also important to note that changes in

chromatin structure can affect gene expression and expression of proteins that may play a role in nuclear migration (Shinchi et al., 2015). Mutations in LINC complex components such as Nesprin-1, Nesprin-2, and Sun2 are associated with ovarian cancer, breast cancer, colorectal cancer, and lung cancer (Bone & Starr, 2016). Furthermore, SUN1, SUN2, and Nesprin-2 are downregulated in human breast cancer tissues suggesting impaired LINC complex contribution to cancer progression (Matsumoto et al., 2015).

Regulators of Nuclear Deformability

There are three key factors that contribute to nuclear deformability: lamin composition, levels of heterochromatin, and cytoskeleton dynamics that act on the nucleus. Lamin is the main structural component of the nuclear lamina, which supports the integrity of the nucleus. There are two main types of lamins, lamin A/C and lamin B. Knockout of lamin A/C in mouse embryonic fibroblast cells led to increased nuclear deformability and lower levels of lamin A/C in metastatic breast cancer cells correlated with decreased nuclear stiffness (Bell et al., 2022; Davidson et al., 2014). Levels of lamin A, which correlates with nuclear stiffness, is in part regulated by the stiffness of the cell's environment. When human mesenchymal stem cells were cultured on stiff gels, their levels of lamin A increased compared to mesenchymal stem cells cultured on soft gels and had lower levels of lamin A (Swift et al., 2013). For migrating cells, this increase in lamin A and nuclear stiffness can impede migration through constricted spaces. In transwell assays where cells migrate through micro-porous filters with defined pore sizes, knockdown of lamin A in mesenchymal stem cells led to enhanced migration compared to wild-type (Harada et al., 2014).

Additionally, higher levels of heterochromatin in some cases results in increased nuclear stiffness. Mammalian cells treated with histone deacetylase inhibitors to decrease the levels of

heterochromatin led to a softer nucleus and nuclear blebbing (Stephens et al., 2018). Nuclear stiffness was measured by attaching micropipettes to isolated nuclei and measuring the force of deflection when providing a force on the nuclei. Levels of heterochromatin can also impact the rate of confined cell migration. When melanoma cells are treated with a drug to decondense chromatin and used in transwell assays, their rate of confined cell migration significantly decreased (Gerlitz & Bustin, 2010).

Lastly, nuclear deformability can be affected by mechanical forces, such as the cytoskeletal network (Thiam et al., 2016). The physical interaction between the nucleus and the cytoskeleton is through SUN (Sad1and UNC-84) proteins found at the inner nuclear membrane that interact with KASH (Klarsicht, ANC-1, Syne homology) proteins found at the outer nuclear membrane and together they form in the linker of nucleoskeleton and cytoskeleton (LINC) complexes (Malone et al., 1999; Starr et al., 2001). SUN proteins interact with the nuclear lamina while KASH proteins interact with elements of cytoskeleton such as microtubule motor proteins to create a bridge that spans the nuclear envelope (Starr & Fridolfsson, 2010).

Studying nuclear migration through constrictions *in vitro*

As described in the section above, nuclear migration through constricted spaces is important for many different cells to carry out their function and is a hallmark of cancer metastasis and thus makes this process critical to study. While many studies have been done to probe pathways that facilitate this process, most of these experiments were done *in vitro*.

Fibroblast migration has been extensively studied on 2D surfaces. While plated on culture plates, a monolayer of fibroblasts can be induced to polarize in preparation for migration if a single scratch is made across the plate. The nucleus becomes positioned rearward while the centrosome positions itself towards the direction of migration (Kupfer et al., 1982). Live imaging

of this process show that the nucleus moves rearward while the centrosome stays in the center of the cell and that this movement is regulated by CDC-42, MRCK, myosin, and actin (Gomes et al., 2005). Although using wound assays to probe migration mechanisms has been useful, cells in a multicellular organism rarely migrate on a 2D surface and thus researchers developed ways to study nuclear migration in 3D matrices, which is more physiologically relevant (Petrie & Yamada, 2015).

Using PDMS to create microchannels with constrictions can be used to study nuclear migration in a 3D environment. This method has been used by the Lammerding Lab, the Piel Lab, the Discher Lab, and the Sixt Lab to study nuclear migration in mammalian cells. The Lammerding Lab used this method to show that nuclear deformability in mouse embryonic fibroblasts (MEFs) is the rate-limiting step in cell migration through constricted spaces (Davidson et al., 2014). MEFs from lamin A/C-deficient mice were able to migrate through the constrictions in the microchannels faster than the wild-type controls, highlighting the importance of lamin levels as a determinant of nuclear deformability. This method was used by the Piel lab to study how mouse bone-marrow-derived dendritic cells are able to migrate through constrictions. Treatment of these cells with the Arp2/3 inhibitor drug CK666 or the actin depolymerizer latrunculin A prevents cells from migrating through the constrictions suggesting Arp2/3 is required for cellular migration of dendritic cells through constrictions (Thiam et al., 2016). Visualization of actin in these cells using LifeAct-GFP also show actin enrichment around the nucleus in the constriction. The lab also used this method to study the effects of nuclear deformation on the mechanical stability on the nucleus during migration. Mouse dendritic cells that expressed NLS-GFP were induced to migrate through a constriction and live cell imaging showed fluorescence signal decrease in the nucleus and increase in the cytoplasm suggesting

nuclear rupture occurs during nuclear migration. GFP-tagged CHMP4B, an ESCRT III complex subunit, was recruited to nuclear rupture sites in HeLa cells (Raab et al., 2016) and in mammalian tumor cells (Denais et al., 2016) suggesting the ESCRT III complex machinery repairs nuclear envelope rupture during nuclear migration through constricted spaces. In addition to using PDMS, labs such as the Yamada Lab use cell-derived matrix (CDM) and type I collagen to create 3D matrices to imitate complex tissue environment (Petrie et al., 2012). Using these matrices, the lab was able to determine that the intracellular hydrostatic pressure in human fibroblasts were elevated when migrating inside the 3D CDM compared to cells migrating on 2D CDM and this was mediated by actomyosin contractions. During migration, the nucleus gets pulled towards the leading edge of the cell like a piston, via nesprin 3, which results in an increase in hydrostatic pressure in the front of the cell. This difference in pressure between the front and back of the cell, with the nucleus in the middle, allows for efficient 3D cell migration (Petrie et al., 2014). While these 3D matrices have led to significant findings, they don't reflect the relevant landscape of tissue culture cells. To work around this issue, some labs have used mouse dermal explants as the 3D matrix for cells to migrate through (Petrie et al., 2012; Raab et al., 2016; Thiam et al., 2016). These dermal explants involve separating the dorsal and ventral halves of mouse ears, washed, and labeled with antibodies to mark structures of the tissue. Cultured cells were then plated onto the ear sheet and imaged at a later time.

There has also been many *in vitro* studies on nuclear stiffness that employ methods such as atomic force microscopy (AFM), traction force microscopy, and magnetic tweezers (Basoli et al., 2018). Of these methods, AFM is the most dominant method as the applied force can be controlled and the damage to the samples is minimal compared to the other methods (Luo et al., 2016). AFM instruments contain a cantilever that is pushed onto the cellular surface and the

resulting indentation and the deflection of the cantilever are registered. AFM was used to measure nuclear stiffness in the breast cancer cell lines MDA-MB-231 and MCF-7 and these cells were found to have higher nuclear stiffness than cytoskeletal stiffness (Fischer et al., 2020). Comparatively, nuclear stiffness of mammary epithelial cells was found to be lower than their cytoskeletal stiffness. Treatment of MCF-7 cells with the chromatin de-condensing reagent Trichostatin A reduced cytoskeletal and nuclear stiffness and the cell migration depths of these cells were increased in dense matrices. While some studies suggest a correlation between softer nuclei and increased cell motility, there has been other evidence that show cells with stiffer nuclei can have increased motility (Luo et al., 2016). This discrepancy highlights the drawbacks of studying nuclear migration *in vitro*.

Studying nuclear migration through constrictions *in vivo*

Nuclear migration through constricted spaces is important in so many processes and needs to be studied in more physiologically relevant conditions. While much has been learned from *in vitro* studies, there are many limitations. In order to study this process and to probe for biologically significant mechanisms at play, our lab is using *Caenorhabditis elegans* as a model organism to study confined nuclear migration, specifically observing nuclear migration of hypodermal precursor P cells. There are many advantages to using *C. elegans* as a model organism. They are useful in developmental studies because their embryonic cell lineages have all been mapped out (Horvitz & Sulston, 1980; Sulston & Horvitz, 1977, 1981), they can be easily imaged due to the transparency of the organism, and many genetic resources and tools have already been developed to genetically modify them (Sugi, 2016).

P cell development

P cells along with the seam cells and the hypodermal syncytium make up the epidermis. At hatching, the dorsal side of the animal is mostly occupied by a single epidermal cell called the hyp7 syncytium that contains 23 nuclei. There are six pairs of P cells (P1-12) and ten pairs of seam cells (H0-H2, V1-V6, and T) along each side of the animal, with the mid-body seam cells (V1-V6) in contact with the P cells along both lateral sides of the worm (Sulston & Horvitz, 1977).

Throughout the L1 stage, P cells undergo four developmental phases: attached, separation, narrowing, and migration (Figure 1.1)(Bone et al., 2016). At hatching, P cells are in a ventral-lateral position where the cell extends from the lateral side of the worm to the ventral side. All six pairs of P cells are attached and arranged along the anterior-posterior axis, with their nuclei found on the lateral side of the cell. At the separation stage, which occurs right after hatching, the P cells begin to separate from their neighbors on the lateral side starting with the most anterior pair all the way to the most posterior pair. This separation is aided by the seam cells, which asymmetrically divide into another seam cell and a hyp7 cell, which fill the gap in-between the separated P cells. After separating, the P cells begin to narrow along the anterior-posterior axis with hyp7 cells continuing to extend into the space in-between the narrowing P cells. At this point, the P cells still extend from the lateral side of the animal to the ventral cord, with their nuclei still located on the lateral side of the cell.

At the mid-L1 stage, P-cell nuclei begin to migrate from the lateral to the ventral side of the cell (Figure 1.2). This process occurs starting with the most anterior P cell pair to the most posterior pair (Sulston & Brenner, 1997; Sulston & Horvitz, 1977). During migration, the P-cell nuclei which is 3-4 μm in diameter must migrate through a narrow constriction of 200 nm in-between the cuticle and muscle to reach the ventral cord (Cox & Hardin, 2004; Francis &

Waterston, 1991). Prior to nuclear migration, this constriction is blocked by hemidesmosome-like, fibrous organelles that function to connect the cuticle to the body wall muscle. These structures are removed right before P-cell nuclear migration and re-formed after migration is completed (Bone et al., 2016; Francis & Waterston, 1991). After nuclear migration occurs, the cytoplasmic region of the cell on the lateral side retracts to the ventral cord, resulting in all twelve P cells aligned along the anterior-posterior axis on the ventral cord. If P-cell nuclear migration is successful, P cells rapidly divide and their progeny go on to develop into hypodermal cells, GABA motor neurons, and the vulva structure (Horvitz & Sulston, 1980; Sulston & Horvitz, 1981).

P-cell nuclear migration through the LINC complex

The best characterized molecular pathway for P-cell nuclear migration is through the UNC-84 and UNC-83 LINC complex (Figure 1.3)(Malone et al., 1999; Starr et al., 2001). UNC-84 is the SUN protein found at the inner nuclear membrane and recruits the KASH protein UNC-83 to the outer nuclear membrane (Starr & Fridolfsson, 2010). UNC-84 is able to interact with the lamin protein LMN-1 and UNC-83 is able to interact with cytoskeletal elements such as the microtubule motor proteins dynein and kinesin (Bone et al., 2014, 2016; Fridolfsson et al., 2010; Fridolfsson & Starr, 2010; Ho et al., 2018; Meyerzon et al., 2009). This resulting interaction allows for forces to be transferred from the cytoskeleton to the nucleus.

UNC-84 and UNC-83 are involved in nuclear migration in the embryonic hyp7 precursor by acting through kinesin, however during this P-cell nuclear migration, dynein is the major microtubule motor protein that functions through UNC-83 to migrate P-cell nuclei (Bone et al., 2016; Fridolfsson et al., 2010; Fridolfsson & Starr, 2010; Ho et al., 2018; Meyerzon et al., 2009). During nuclear migration, microtubules in P cells are polarized in the direction of migration with

the nucleus migrating towards the minus ends of microtubules (Bone et al., 2016). In Chapter 2 of this dissertation, I detail the results of conditionally knocking down DHC-1 and the effects that has on P-cell nuclear migration (Ho et al., 2018). While dynein seems to be the main motor protein, kinesin may play a smaller role in nuclear migration. Knockdown of both dynein and kinesin led to a worse nuclear migration defect than knockdown of dynein alone, suggesting kinesin may be involved possibly by pulling the nucleus in the opposite direction of migration if the nucleus encounters an obstacle (Bone et al., 2016).

Although the LINC complex plays an important role in facilitating nuclear migration in P cells, there are other less characterized pathways that are involved. Null mutations of *unc-83* or *unc-84* leads to a temperature sensitive defect (Sulston & Horvitz, 1981). Mutant animals at 25°C have a nuclear migration defect with less than 40% of P-cell nuclei successfully migrate to the ventral cord. However, mutant animals at 15°C have at least 90% of their nuclei able to successfully migrate (Malone et al., 1999; Starr et al., 2001). This suggests there is an additional pathway for P-cell nuclear migration that functions parallel to the LINC complex pathway (Figure 1.4).

P-cell nuclear migration pathway through actin-based mechanism

In order to identify players in this alternative P-cell nuclear migration pathway, our lab performed an unbiased, forward genetics screen to isolate genes that when mutated would enhance the nuclear migration defect of the *unc-84* null mutation (emu screen) (Chang et al., 2013). For the screen, the starting strain was *unc-84(n369)* with a GABA neuron marker (*unc-47::gfp*) which was used to indirectly quantify nuclear migration (McIntire et al., 1997). If P-cell nuclear migration is successful, they develop into GABA neurons. There are a total of nineteen GABA neurons, twelve of which are derived from P cells (McIntire et al., 1997; Sulston &

Horvitz, 1977). Because P cells develop into GABA neurons and the vulva structure, animals with a P-cell nuclear migration defect will have phenotypes such as uncoordinated movement (Unc) and egg-laying deficient (Egl) where the animals cannot lay eggs so their progeny hatch inside the mother resulting in a bag of worm phenotype (Horvitz & Sulston, 1980; Sulston & Horvitz, 1981). The mutagen EMS was used to introduce random mutations into this starting strain (Brenner, 1974). The mutagenized strains were grown at 15°C and their progeny were screened for Egl and Unc phenotypes, which would suggest that both the LINC complex pathway and the alternative pathway have been disrupted. GABA neurons of these mutants were also counted to quantify the nuclear migration defect (Chang et al., 2013).

Clonal lines of these mutants were generated and used for whole-genome sequencing in order to isolate the mutated gene. From this emu screen, the lab was able to identify *toca-1* and *fln-2* as necessary for P-cell nuclear migration at 15°C in the absence of *unc-84* (Chang et al., 2013). Transducer of Cdc-42-dependent actin assembly (TOCA)-1 has been implicated in organizing actin during endocytosis in mammalian cells (Bu et al., 2009). TOCA-1 contains an F-BAR domain and a CDC-42 binding domain and may function by localizing to the plasma membrane or nuclear membrane and inducing actin polymerization through CDC-42 to deform the nucleus. FLN-2 appears to be a divergent filamin and filamins generally function as actin crosslinkers and bundlers (DeMaso et al., 2011; Ma et al., unpublished data). The lab was also able to isolate *cgef-1* from the emu screen. CGEF-1 is a guanine nucleotide exchange factor that activates small G proteins by facilitating the exchange of GDP for GTP. CGEF-1 acts as a GEF for CDC-42 during early *C. elegans* embryogenesis (E. Chan & Nance, 2013). CDC-42 is a known regulator of actin organization (Etienne-Manneville, 2004). Chapter 3 will go into further detail about the role that CGEF-1 plays in P-cell nuclear migration.

Because all the genes that were isolated from the emu screen so far are putative actin regulators, I hypothesize that this alternative P-cell nuclear migration pathway is an actin-based pathway. During P-cell nuclear migration, actin cables can be seen extending throughout the cell and through the constriction with actin rings on the lateral side of some P cells supporting the idea of actin structures facilitating nuclear migration. In order to understand how actin may play a role in P-cell nuclear migration, it's pertinent to understand how actin is regulated and organized.

Actin Organization

Actin can be found in two states—globular actin (G-actin) and filamentous actin (F-actin). G-actin are actin monomers that polymerize into F-actin. Actin nucleation happens slowly and spontaneously when enough ATP-bound actin monomers assemble into a complex of small polymers from which elongation can occur from. Elongation of the filament is mainly driven by ATP activity of the actin monomers (Pollard, 2016). Like microtubules, actin filaments are also polarized with one end of the filament called the barbed end and the other end of the filament is called the pointed end. The barbed end of the filament recruits ATP-bound monomers and is the faster growing end while the pointed end of the filament involves the dissociation of ADP-bound monomers. If the rate of addition of monomers is the same as the rate of dissociation of monomers, the filament undergoes treadmilling, which results in a constant filament length (Lappalainen et al., 2022; Pollard, 2016; Wegner, 1976).

There are three main actin filament structures—branched actin, actin bundles, and actomyosin contractions (Lappalainen et al., 2022). The Arp2/3 complex is the nucleator that regulates branched actin. Arp2/3 binds to an existing actin filament and can be activated by the Wiskott-Aldrich syndrome protein (WASP) family and the WASP-family verprolin-homologous

protein (WAVE) family (Gautreau et al., 2022; Machesky et al., 1999). WASP/WAVE proteins

contain domains that can bind to actin monomers and a domain that can bind to Arp2/3 and bring

all of these units together to allow Arp2/3 to nucleate a new actin filament off the side of an

existing filament. These branches of actin filaments form at a 70° angle (Blanchoin et al., 2000;

Mullins et al., 1998; Smith et al., 2013). Formins are also regulatory proteins that facilitate

elongation of an existing actin filament and are involved in elongating filaments in branched

actin and in actin bundles (Lappalainen et al., 2022). Both actin polymerization in branched actin

and in actin bundles can produce force through a "Brownian ratchet" type of mechanism. When

the barbed end of an actin filament is facing a membrane, both the barbed end and the membrane

experience rapid thermal fluctuations, which causes a gap between the barbed end and the

membrane, during which a new actin monomer can be added to the barbed end leading to

elongation of the filament. This elongation pushes on the membrane and can cause membrane

deformation (Bieling et al., 2016; T.-D. Li et al., 2022; Mogilner & Oster, 2003). While

branched actin and actin bundles can generate a pushing force through elongation, actomyosin

contractions can provide a pulling force through myosin motors sliding along actin fibers (Livne

& Geiger, 2016).

All of these different organizations of actin play a role in migrating cells, such as in

lamellipodia-driven migration in mesenchymal cells and fibroblast cells (Innocenti, 2018;

Suraneni et al., 2012). In these cells, the lamellipodia is at the front of the migrating cell and is

driven by actin polymerization in the form of branched actin. Actin bundles can also be found at

the leading edge of the migrating cell in filopodia protrusions. Actomyosin contractions can be

found in the cell body and at the rear of the cell to pull the trailing end of the cell in the direction

of migration (Schaks et al., 2019; Seetharaman & Etienne-Manneville, 2020). These actin

structures are regulated by Rho GTPases (RhoA, Cdc-42, Rac1). Rho GTPases act as molecular switches and exist in an inactive GDP-bound stand and an active GTP-bound state. Once active, these proteins can activate downstream effectors to induce a signaling cascade that leads to a variety of intracellular responses, the best-characterized being regulation of actin organization (Lawson & Ridley, 2017; Parri & Chiarugi, 2010). During cell migration, Rac1 and Cdc-42 can be found at the leading edge (Nobes & Hall, 1995). Rac1 stimulates growth of branched actin by activating WAVE/WASP to activate Arp2/3 to generate the lamellipodia protrusion (Eden et al., 2002). Cdc-42 also promote actin polymerization in filopodia structures at the leading edge. RhoA functions at the rear of the cell and promote retraction of the trailing edge by activating Rho-associated serine/threonine kinase (ROCK). ROCK phosphorylates myosin light chain to induce myosin II activity in actomyosin contractions in order to pull the cell body in the direction of migration (Fukata et al., 2001; Totsukawa et al., 2000). Rho GTPases are regulated by guanine nucleotide exchange factors (GEFs) and GTPase-activating proteins (GAPs). GEFs activate Rho GTPases by facilitating the exchange of GDP bound to Rho GTPases for GTP while GAPs suppress Rho GTPases function by enhancing their GTPase activity (Rossman et al., 2005).

Actin during *C. elegans* development

A large component of my dissertation is focused on actin regulators and their role in P-cell nuclear migration and it's important to be aware of the crucial role actin plays in *C. elegans* development. Actin is especially important during early embryogenesis and is involved in patterning the embryo and facilitating significant tissue remodeling. Developmental events such as pronuclear migration, embryo polarization, neuroblast migration, ventral enclosure, dorsal intercalation, and elongation rely on actin in addition to other cytoskeletal elements (Chisholm & Hardin, 2005; Velarde et al., 2007).

After fertilization, the male and hermaphrodite pronuclei migrate towards each other before the zygote undergoes the first mitotic division. The site of the sperm entry defines the posterior end of the embryo. In addition to the pronuclei, the sperm also provides the only centrosome in the fertilized embryo. After fertilization, the microtubule aster from the sperm centrosome grows and pushes the male pronuclei towards the center of the embryo. The female pronuclei also moves towards the male pronuclei by grabbing onto the microtubules emanating from the sperm centrosome (Meaders & Burgess, 2020). This interaction is made through the LINC complex at the nuclear envelop of the female pronuclei. The KASH protein, ZYG-12, interacts with the SUN protein, SUN-1, to recruit dynein to the pronuclei (Malone et al., 2003; Minn et al., 2009; Zuela & Gruenbaum, 2016). Dynein is then able to pull the female pronuclei along the microtubules towards the male pronuclei (Malone et al., 2003). While this process has largely been characterized as an event driven by microtubule dynamics, depletion of the branched actin nucleator Arp2/3 results in reduced establishment of microtubules during pronuclear migration and also prevents migration of the male pronuclei, which suggests actin plays an important role in pronuclear migration in *C. elegans* (Xiong et al., 2011).

Around the same time as fertilization, the embryo also needs to establish the anterior-posterior (A/P) axis by asymmetrically distributing the partitioning PAR proteins at the one-cell stage embryo (Rose & Kemphues, 1998). Prior to symmetry breaking, anterior PARs (PAR-3/PAR-6/PKC-3) are found along the cortex while posterior PARs (PAR-1/PAR-2) are found distributed throughout the cytoplasm (Lang & Munro, 2017). During this time, a contractile actomyosin network can also be found at the cortex (Gan & Motegi, 2021). Symmetry breaking occurs after fertilization when the sperm centrosome approaches the posterior pole and it is regulated by the Aurora B kinase, AIR-1. AIR-1 is thought to diffuse from the centrosome to the

posterior cortex to disrupt local actomyosin network, possibly by regulated RHO-1 activity (Gan & Motegi, 2021; Klinkert et al., 2019). This leads to an asymmetrical contraction of the actomyosin network towards the anterior pole, which also moves the anterior PARs towards the anterior pole. With the posterior pole freed of the anterior PARs, PAR-2 is able to load onto the posterior cortex and PAR-2 is able to recruit PAR-1 to the posterior (Cuenca et al., 2003; Munro et al., 2004). This distribution of PAR-3/PAR-6/PKC-3 to the anterior and of PAR-2/PAR-1 to the posterior, which is mediated by actin structures, is important for components downstream of the PAR proteins to regulate asymmetric segregation of cell fate determinants that is necessary for embryonic development.

During the mid-to-late stage of *C. elegans* embryo morphogenesis, major processes such as neuroblast migration, ventral enclosure, and dorsal intercalation occur, all of which involve actin as a central player. By the end of the early stage, the ventral cleft has formed, which is a depression on the ventral side caused by ingression of endodermal and mesodermal precursors during gastrulation. Ventral neuroblast cells must migrate to fill in the ventral clef and provide a substrate for migrating epidermal cells. These bilateral epidermal cells migrate from the dorsal side to the ventral midline, covering the ventral side with a sheet of epidermal cells in a process called epiboly, or ventral enclosure (Chisholm & Hardin, 2005).

Actin seems to be playing a role in ventral neuroblast migration. RNAi knockdown of the SCAR/WAVE gene *wve-1*, or the WASP gene *wsp-1,* results in embryos with persistent ventral clefts and as a result a failure of ventral enclosure (Withee et al., 2004). Improper ventral cleft closure suggests ventral neuroblasts are unable to migrate normally due to the loss of function of these actin regulators. Many studies have been unable to distinguish the tissue-specific requirements of these actin regulators between ventral neuroblast migration and ventral

17

enclosure. More recent work favors the role of actin-myosin structures in ventral neuroblast migration. The non-muscle myosin, *nmy-2*, is required in neuroblasts in order for ventral enclosure to take place. Knockdown of *nmy-2* in neuroblast but not in epidermal cells led to failure to complete ventral enclosure and of the embryos that escaped this fate, about half of them experienced a delay in this process (Wernike et al., 2016). Adding to the importance of *nmy-2* in ventral neuroblast migration, anillin (*ani-1*), which has both an actin and myosin binding domain to coordinate actin-myosin contractions, is expressed in ventral neuroblasts but not in epidermal cells during ventral enclosure. ANI-1 is important for neuroblast cytokinesis and RNAi knockdown of ani-1 leads to misshapen neuroblast as well as ventral enclosure defects (Fotopoulos et al., 2013).

While defects in neuroblast migration can influence ventral enclosure, epidermal cells also rely on actin structures during this process. Ventral enclosure encompasses two phases and begins with two anterior leading cells on either side of the embryo migrating towards the midline. These cells contain actin-rich filopodia and treatment with cytochalasin D as well as laser inactivation of these cells halt migration (Williams-Masson et al., 1997). Early studies reveal the importance of numerous branched actin regulators. Loss of function of the Arp2/3 complex as well as the only SCAR/WAVE and WASP C. elegans homolog, *wve-1* and *wsp-1* respectively, results in failed migration of the leading cells (Patel et al., 2008; Sawa et al., 2003). Actin staining of these single mutants show a decrease in actin enrichment in the protrusions of the leading cells. For this first phase of ventral enclosure, two pathways work to generate branched actin in leading cells. In one pathway, CDC-42 activates WSP-1, which in turn activates the Arp2/3 complex to initiate branched actin (M.-H. Ouellette et al., 2016; Sawa et al., 2003). The Rho-GTPase activating protein (GAP) RGA-7 is able to regulate the distribution of

CDC-42 during this process (Ouellette et al., 2016). In the second pathway, CED-10/RAC-1 activates WVE-1, which in turn activates the Arp2/3 complex (Patel et al., 2008; Sawa et al., 2003). WVE-1 also recruits the VASP protein UNC-34 to promote F-actin elongation (Havrylenko et al., 2015; Withee et al., 2004). The second phase of ventral enclosure involves the more posterior epidermal cells known as "pocket cells." Pocket cells also rely on actin structures to cover the ventral axis, but use actin-myosin contractions instead of branched actin. NMY-2 localizes as a ring in the pocket cells leading to actin-myosin structures that undergo a purse-string-like mechanism to complete ventral enclosure (Wernike et al., 2016). Upstream of this mechanism is the small G protein, RHO-1, which activates LET-502/ROCK to activate myosin (Fotopoulos et al., 2013; Wernike et al., 2016). RHO-1 is regulated by the GAP protein HUM-7 and the guanine nucleotide exchange factor, ECT-2 (Fotopoulos et al., 2013; Wallace et al., 2018). Loss of function in any of these regulators in epidermal leading cells or pocket cells can lead to ventral enclosure failure or significantly slow down the process.

After ventral neuroblast migration but before ventral enclosure takes place, epidermal cells on the dorsal side of the embryo undergo a process called dorsal intercalation. Two rows of dorsal epidermal cells are found along the anterior-posterior axis and must elongate towards the dorsal midline. These cells extend in between the other row of epidermal cells and elongate until they reach the lateral edge on the opposite side, resulting in a single row of epidermal cells covering the dorsal midline. While it's clear actin is necessary for dorsal intercalation (Williams-Masson et al., 1997), early studies suggests branched actin regulators such as the Arp2/3 complex or CED-10/RAC-1 is not required for this process (Patel et al., 2008; Sawa et al., 2003), more recent studies reveal two parallel pathways are involved in generating branched actin for intercalation to take place (Walck-Shannon et al., 2015). While tissue-specific loss of function of

CED-10/RAC-1 only results in partial disruption of dorsal epidermal cell protrusions, knocking down both CED-10/RAC-1 and MIG-2/RHOG led to a more severe phenotype, suggesting both of these small G proteins act redundantly (Walck-Shannon et al., 2015). CED-10/RAC-1 and MIG-2/RHOG is able to activate WVE-1 and WSP-1, respectively, to initiate branched actin structures. The GEF UNC-73/TRIO is able to act upstream by regulating both CED-10/RAC-1 and MIG-2/RHOG (Walck-Shannon et al., 2015).

At the end of ventral enclosure, the embryo is a lima-bean shape and must elongate to the twofold stage by increasing in length by fourfold and decreasing in diameter by twofold in a process mainly driven by actomyosin contractility (Chisholm & Hardin, 2005). Actomyosin structures forms circumferential parallel bundles around the dorsal and ventral epidermal cells of the embryo. These actin structures are thought to squeeze the embryo radially to elongate the body, which elongate along the A/P through hydrostatic pressure (Priess & Hirsh, 1986; Vuong-Brender et al., 2016). Addition of the actin polymerization inhibitor cytochalasin D inhibits elongation (Priess & Hirsh, 1986). The activity of NMY-2 is regulated by the kinase LET-502, which is an effector of the RHO GTPase RHO-1 (Gally et al., 2009). RHO-1 is regulated by the GEF protein RHGF-2 and the guanine activator protein (GAP) RGA-2. Mutations in either *rhgf-2*, *let-502*, myosin light chain *mlc-4*, or *nmy-1/nmy-2* results in inability of the embryo to elongate and instead arrest at the two-fold stage or earlier in development. Mutations in *rga-2*, which would result in a hyperactive RHO-1, causes embryos to burst during elongation due to the increased pressure (B. G. Chan et al., 2015; Diogon et al., 2007; Vuong-Brender et al., 2016).

Summary of Dissertation

Because actin plays such a major role in cell migration, it most likely also plays a major role in nuclear migration through constricted spaces, which is shown from *in vitro* experiments

found in the literature and as described in the above sections. As mentioned previously, I propose to use P cells in C. elegans as an *in vivo* model to study how cytoskeletal dynamics influence nuclear migration through constricted spaces. In Chapter I, I detailed nuclear migration through constrictions in *in vivo* processes, the *in vitro* experiments done to determine the different pathways involved in this process, why P cells would be a good model to study this process, and why actin would be involved in this process. Chapter II will describe the role microtubules and dynein play in P-cell nuclear migration. Chapter III will dive into the impact CGEF-1, CDC-42, and non-muscle myosin II (NMY-2) on the actin pathway that facilitates P-cell nuclear migration. For Chapter IV, I will propose future experiments that can further our understanding of the actin pathway and P-cell nuclear migration.

Figures

Figure 1.1
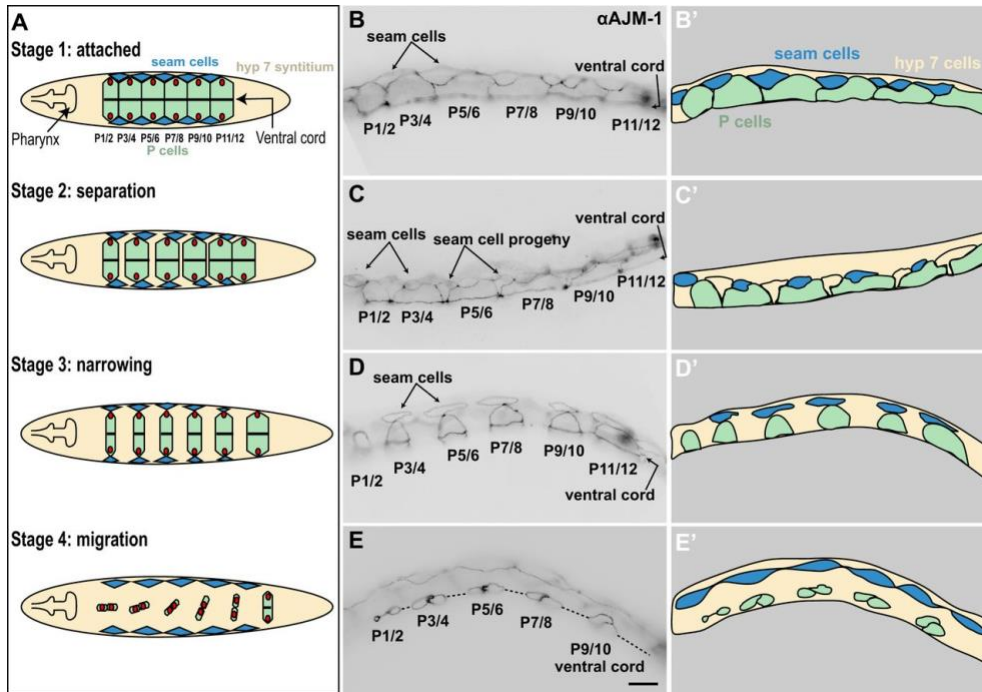
Figure 1.1: P-cell development during L1 stage (Bone et al., 2016). There are four stages of P-cell morphological changes: Attached, Separation, Narrowing, and Migration. Left column show animal from the dorsal side down at the ventral cord. Middle and right columns show animals from lateral side. (Top row) During the attached stage which occurs at hatching, six pairs of P cells are attached to each other in two rows, and they span both lateral sides of the worm to the ventral cord. The nuclei of each P cell are located on the lateral side. (Second row) P cell pairs begin to separate from their anterior and posterior neighbors. Seam cells (blue) give rise to hyp7 progeny (tan), which intercalate between the separating P cells (Figure 1C'). (Third row) During the narrowing stage, the P cell pairs continue to narrow and the hyp7 syncytium continues to expand and separate the P cell pairs. (Bottom row) Nuclear migration occurs during the mid-L1 stage. P-cell nuclei on the lateral side have to migrate to a ventral position starting with the most anterior pair and then continuing to consecutive pair all the way to the most posterior pair.
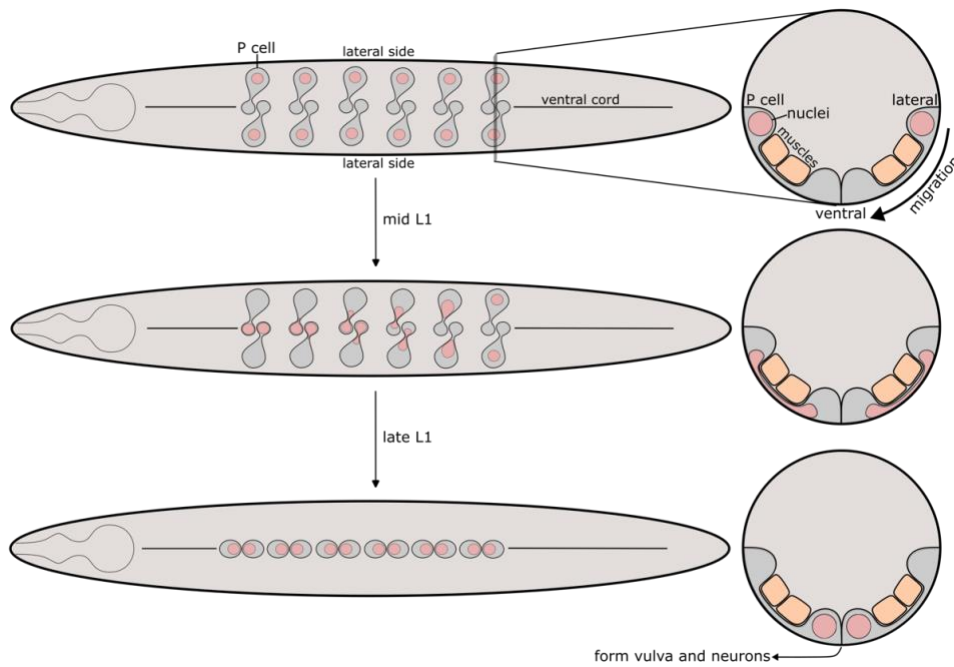
Figure 1.2

Figure 1.2: P-cell nuclear migration. Left side are images of the worm from a dorsal view looking down at the ventral cord. Right side images are cross-sections of the worm. (Top image) During the mid-L1 stage, there are six pairs of P cells (grey) along the anterior-posterior axis of the animal. Each P cell extend from the lateral side to the ventral side of the worm. The nuclei (pink) of each cell are found on the lateral side of the cell. There is a narrow constriction between the lateral and ventral portion of the cell that is created by the body wall muscle (orange) and the cuticle. (Middle image) During nuclear migration, the nuclei must migrate from the lateral to ventral side of the worm by squeezing through the narrow constriction. This process occurs with the most anterior pair and then followed by the next consecutive pair all the way to the most posterior pair. (Bottom image) When nuclear migration is complete, all the P-cell nuclei will be located along the ventral cord and the lateral portion of the cell also migrates to the ventral side resulting in the whole cell found only on the ventral side. These P cells go on to divide and develop into vulval cells and GABA neuron cells.
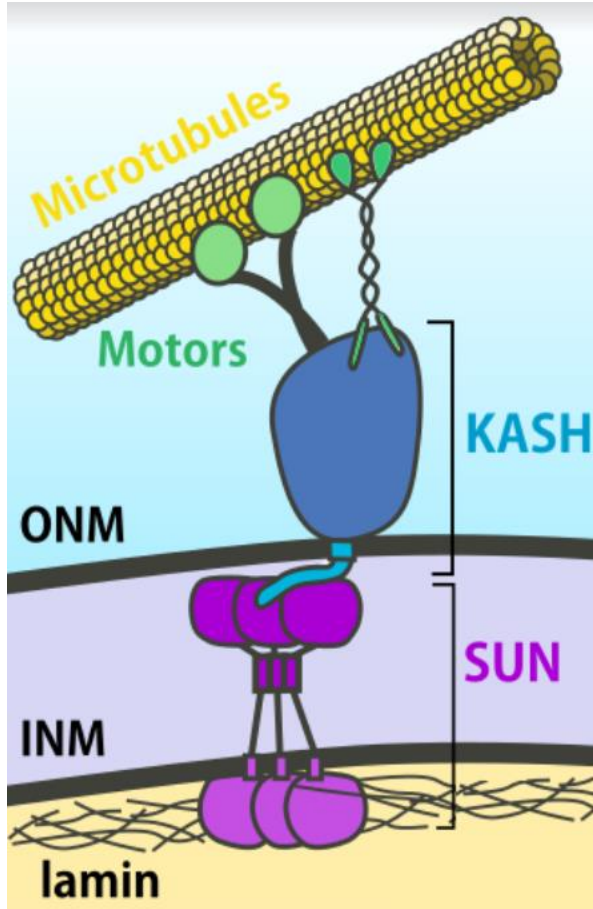
Figure 1.3

Figure 1.3: LINC complex. The Linker of the Nucleoskeleton and Cytoskeleton consists of the

SUN protein (magenta) found at the inner nuclear envelope and the SUN protein interacts with

the KASH protein (blue) which is found at the outer nuclear envelope. The KASH protein is able

to interact with microtubule motor proteins (green) to pull the nucleus along microtubules
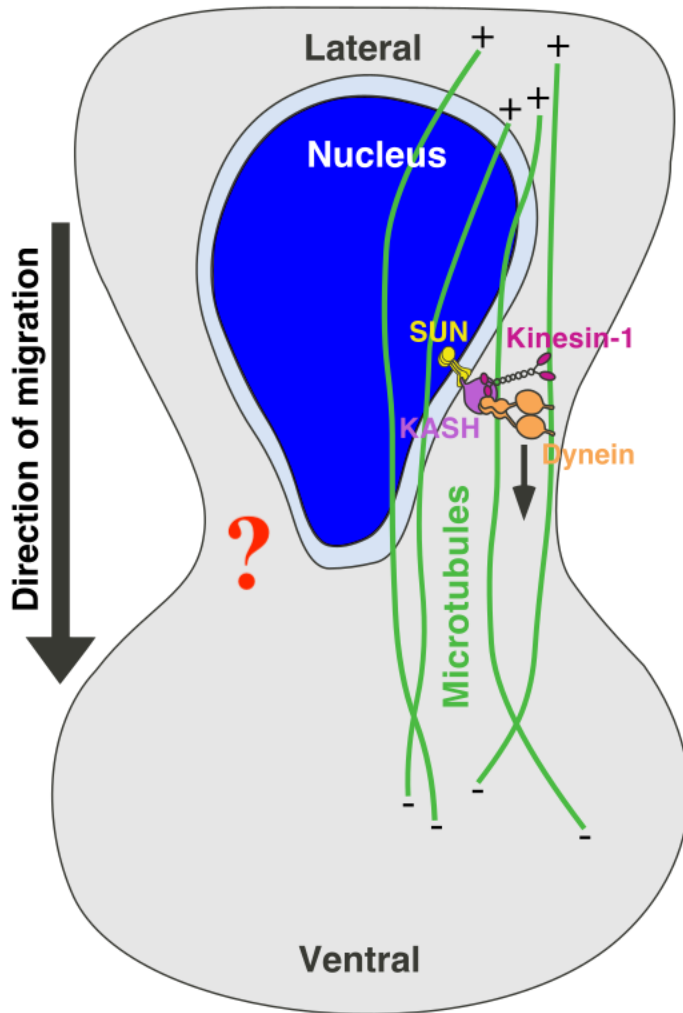
(yellow). Figure made by Ellen F. Gregory.

Figure 1.4

Figure 1.4: The LINC complex pathway and unknown parallel pathway for P-cell nuclear migration. The diagram shows a picture of a whole P cell that is undergoing nuclear migration. The canonical pathway for P-cell nuclear migration is the LINC complex pathway (right side of the nucleus) which consists of the interaction between the SUN protein, UNC-84, and the KASH protein, UNC-83, to generate the LINC complex. UNC-83 is able to interact with dynein to pull the nucleus towards the minus end of microtubules during nuclear migration. It is unclear what players are involved in the parallel pathway for nuclear migration (red question mark on the left side of the nucleus). Figure made by Ellen F. Gregory.

References

Basoli, F., Giannitelli, S. M., Gori, M., Mozetic, P., Bonfanti, A., Trombetta, M., & Rainer, A. (2018). Biomechanical Characterization at the Cell Scale: Present and Prospects. *Frontiers in Physiology*, *9*, 1449–1449. PubMed. https://doi.org/10.3389/fphys.2018.01449

Bell, E. S., Shah, P., Zuela-Sopilniak, N., Kim, D., Varlet, A.-A., Morival, J. L. P., McGregor, A. L., Isermann, P., Davidson, P. M., Elacqua, J. J., Lakins, J. N., Vahdat, L., Weaver, V. M., Smolka, M. B., Span, P. N., & Lammerding, J. (2022). Low lamin A levels enhance confined cell migration and metastatic capacity in breast cancer. *Oncogene*, *41*(36), 4211–4230. https://doi.org/10.1038/s41388-022-02420-9

Bieling, P., Li, T.-D., Weichsel, J., McGorty, R., Jreij, P., Huang, B., Fletcher, D. A., & Mullins, R. D. (2016). Force Feedback Controls Motor Activity and Mechanical Properties of Self-Assembling Branched Actin Networks. *Cell*, *164*(1), 115–127. https://doi.org/10.1016/j.cell.2015.11.057

Blanchoin, L., Amann, K. J., Higgs, H. N., Marchand, J.-B., Kaiser, D. A., & Pollard, T. D. (2000). Direct observation of dendritic actin filament networks nucleated by Arp2/3 complex and WASP/Scar proteins. *Nature*, *404*(6781), 1007–1011. https://doi.org/10.1038/35010008

Bone, C. R., Chang, Y.-T., Cain, N. E., Murphy, S. P., & Starr, D. A. (2016). Nuclei migrate through constricted spaces using microtubule motors and actin networks in C. elegans hypodermal cells. *Development*, *143*(22), 4193–4202. https://doi.org/10.1242/dev.141192

Bone, C. R., & Starr, D. A. (2016). Nuclear migration events throughout development. *Journal of Cell Science*, *129*(10), 1951–1961. https://doi.org/10.1242/jcs.179788

Bone, C. R., Tapley, E. C., Gorjánácz, M., & Starr, D. A. (2014). The Caenorhabditis elegans SUN protein UNC-84 interacts with lamin to transfer forces from the cytoplasm to the nucleoskeleton during nuclear migration. *Molecular Biology of the Cell*, *25*(18), 2853–2865. PubMed. https://doi.org/10.1091/mbc.E14-05-0971

Brenner, S. (1974). THE GENETICS OF CAENORHABDITIS ELEGANS. *Genetics*, *77*(1), 71–94. https://doi.org/10.1093/genetics/77.1.71

Bu, W., Chou, A. M., Lim, K. B., Sudhaharan, T., & Ahmed, S. (2009). The Toca-1-N-WASP Complex Links Filopodial Formation to Endocytosis. *Journal of Biological Chemistry*, *284*(17), 11622–11636. https://doi.org/10.1074/jbc.M805940200

Chan, B. G., Rocheleau, S. K., Smit, R. B., & Mains, P. E. (2015). The Rho guanine exchange factor RHGF-2 acts through the Rho-binding kinase LET-502 to mediate embryonic elongation in C. elegans. *Developmental Biology*, *405*(2), 250–259. https://doi.org/10.1016/j.ydbio.2015.07.010

Chan, E., & Nance, J. (2013). Mechanisms of CDC-42 activation during contact-induced cell polarization. *Journal of Cell Science*, *126*(7), 1692–1702. https://doi.org/10.1242/jcs.124594

Chang, Y.-T., Dranow, D., Kuhn, J., Meyerzon, M., Ngo, M., Ratner, D., Warltier, K., & Starr, D. A. (2013). Toca-1 Is in a Novel Pathway That Functions in Parallel with a SUN-KASH Nuclear Envelope Bridge to Move Nuclei in Caenorhabditis elegans. *Genetics*, *193*(1), 187–200. https://doi.org/10.1534/genetics.112.146589

Chisholm, A. D., & Hardin, J. (2005). Epidermal morphogenesis. *WormBook : The Online Review of C. Elegans Biology*, 1–22. PubMed. https://doi.org/10.1895/wormbook.1.35.1

Cowan, C. R., & Hyman, A. A. (2004). Centrosomes direct cell polarity independently of microtubule assembly in C. elegans embryos. *Nature*, *431*(7004), 92–96. https://doi.org/10.1038/nature02825

Cox, E. A., & Hardin, J. (2004). Sticky worms: Adhesion complexes in C. elegans. *Journal of Cell Science*, *117*(10), 1885–1897. https://doi.org/10.1242/jcs.01176

Cuenca, A. A., Schetter, A., Aceto, D., Kemphues, K., & Seydoux, G. (2003). Polarization of the C. elegans zygote proceeds via distinct establishment and maintenance phases. *Development*, *130*(7), 1255–1265. https://doi.org/10.1242/dev.00284

Davidson, P. M., Denais, C., Bakshi, M. C., & Lammerding, J. (2014). Nuclear Deformability Constitutes a Rate-Limiting Step During Cell Migration in 3-D Environments. *Cellular and Molecular Bioengineering*, *7*(3), 293–306. https://doi.org/10.1007/s12195-014-0342-y

DeMaso, C. R., Kovacevic, I., Uzun, A., & Cram, E. J. (2011). Structural and Functional Evaluation of C. elegans Filamins FLN-1 and FLN-2. *PLOS ONE*, *6*(7), e22428. https://doi.org/10.1371/journal.pone.0022428

Denais, C. M., Gilbert, R. M., Isermann, P., McGregor, A. L., te Lindert, M., Weigelin, B., Davidson, P. M., Friedl, P., Wolf, K., & Lammerding, J. (2016). Nuclear envelope rupture and repair during cancer cell migration. *Science*, *352*(6283), 353–358. https://doi.org/10.1126/science.aad7297

Diogon, M., Wissler, F., Quintin, S., Nagamatsu, Y., Sookhareea, S., Landmann, F., Hutter, H., Vitale, N., & Labouesse, M. (2007). The RhoGAP RGA-2 and LET-502/ROCK achieve a balance of actomyosin-dependent forces in C. elegans epidermis to control morphogenesis. *Development*, *134*(13), 2469–2479. https://doi.org/10.1242/dev.005074

Eden, S., Rohatgi, R., Podtelejnikov, A. V., Mann, M., & Kirschner, M. W. (2002). Mechanism of regulation of WAVE1-induced actin nucleation by Rac1 and Nck. *Nature*, *418*(6899), 790–793. https://doi.org/10.1038/nature00859

Etienne-Manneville, S. (2004). Cdc42—The centre of polarity. *Journal of Cell Science*, *117*(8), 1291–1300. https://doi.org/10.1242/jcs.01115

Fischer, T., Hayn, A., & Mierke, C. T. (2020). Effect of Nuclear Stiffness on Cell Mechanics and Migration of Human Breast Cancer Cells. *Frontiers in Cell and Developmental Biology*, *8*, 393–393. PubMed. https://doi.org/10.3389/fcell.2020.00393

Fotopoulos, N., Wernike, D., Chen, Y., Makil, N., Marte, A., & Piekny, A. (2013). Caenorhabditis elegans anillin (ani-1) regulates neuroblast cytokinesis and epidermal morphogenesis during embryonic development. *Developmental Biology*, *383*(1), 61–74. https://doi.org/10.1016/j.ydbio.2013.08.024

Francis, R., & Waterston, R. H. (1991). Muscle cell attachment in Caenorhabditis elegans. *Journal of Cell Biology*, *114*(3), 465–479. https://doi.org/10.1083/jcb.114.3.465

Fridolfsson, H. N., Ly, N., Meyerzon, M., & Starr, D. A. (2010). UNC-83 coordinates kinesin-1 and dynein activities at the nuclear envelope during nuclear migration. *Developmental Biology*, *338*(2), 237–250. https://doi.org/10.1016/j.ydbio.2009.12.004

Fridolfsson, H. N., & Starr, D. A. (2010). Kinesin-1 and dynein at the nuclear envelope mediate the bidirectional migrations of nuclei. *The Journal of Cell Biology*, *191*(1), 115–128. PubMed. https://doi.org/10.1083/jcb.201004118

Friedl, P., Wolf, K., & Lammerding, J. (2011). Nuclear mechanics during cell migration. *Cell Structure and Dynamics*, *23*(1), 55–64. https://doi.org/10.1016/j.ceb.2010.10.015

Fu, Y., Chin, L. K., Bourouina, T., Liu, A. Q., & VanDongen, A. M. J. (2012). Nuclear deformation during breast cancer cell transmigration. *Lab on a Chip*, *12*(19), 3774–3778. https://doi.org/10.1039/C2LC40477J

Fukata, Y., Kaibuchi, K., Amano, M., & Kaibuchi, K. (2001). Rho–Rho-kinase pathway in smooth muscle contraction and cytoskeletal reorganization of non-muscle cells. *Trends in Pharmacological Sciences*, *22*(1), 32–39. https://doi.org/10.1016/S0165-6147(00)01596-0

Gally, C., Wissler, F., Zahreddine, H., Quintin, S., Landmann, F., & Labouesse, M. (2009). Myosin II regulation during C. elegans embryonic elongation:LET-502/ROCK, MRCK-1 and PAK-1, three kinases with different roles. *Development*, *136*(18), 3109–3119. https://doi.org/10.1242/dev.039412

Gan, W. J., & Motegi, F. (2021). Mechanochemical Control of Symmetry Breaking in the Caenorhabditis elegans Zygote. *Frontiers in Cell and Developmental Biology*, *8*. https://doi.org/10.3389/fcell.2020.619869

Gautreau, A. M., Fregoso, F. E., Simanov, G., & Dominguez, R. (2022). Nucleation, stabilization, and disassembly of branched actin networks. *Trends in Cell Biology*, *32*(5), 421–432. https://doi.org/10.1016/j.tcb.2021.10.006

Gerlitz, G., & Bustin, M. (2010). Efficient cell migration requires global chromatin condensation. *Journal of Cell Science*, *123*(13), 2207–2217. https://doi.org/10.1242/jcs.058271

Gomes, E. R., Jani, S., & Gundersen, G. G. (2005). Nuclear Movement Regulated by Cdc42, MRCK, Myosin, and Actin Flow Establishes MTOC Polarization in Migrating Cells. *Cell*, *121*(3), 451–463. https://doi.org/10.1016/j.cell.2005.02.022

Harada, T., Swift, J., Irianto, J., Shin, J.-W., Spinler, K. R., Athirasala, A., Diegmiller, R., Dingal, P. C. D. P., Ivanovska, I. L., & Discher, D. E. (2014). Nuclear lamin stiffness is a barrier to 3D migration, but softness can limit survival. *Journal of Cell Biology*, *204*(5), 669–682. https://doi.org/10.1083/jcb.201308029

Havrylenko, S., Noguera, P., Abou-Ghali, M., Manzi, J., Faqir, F., Lamora, A., Guérin, C., Blanchoin, L., & Plastino, J. (2015). WAVE binds Ena/VASP for enhanced Arp2/3 complex–based actin assembly. *Molecular Biology of the Cell*, *26*(1), 55–65. https://doi.org/10.1091/mbc.e14-07-1200

Ho, J., Venecia A. Valdez, Ma, L., & Starr, D. A. (2018). *Characterizing Dynein's Role in P-cell Nuclear Migration using an Auxin-Induced Degradation System*. https://doi.org/10.17912/W2W96J

Horvitz, H. R., & Sulston, J. E. (1980). ISOLATION AND GENETIC CHARACTERIZATION OF CELL-LINEAGE MUTANTS OF THE NEMATODE CAENORHABDITIS ELEGANS. *Genetics*, *96*(2), 435–454. https://doi.org/10.1093/genetics/96.2.435

Innocenti, M. (2018). New insights into the formation and the function of lamellipodia and ruffles in mesenchymal cell migration. *Cell Adhesion & Migration*, *12*(5), 401–416. https://doi.org/10.1080/19336918.2018.1448352

Kalukula, Y., Stephens, A. D., Lammerding, J., & Gabriele, S. (2022). Mechanics and functional consequences of nuclear deformations. *Nature Reviews. Molecular Cell Biology*, *23*(9), 583–602. PubMed. https://doi.org/10.1038/s41580-022-00480-z

Kengaku, M. (2018). Cytoskeletal control of nuclear migration in neurons and non-neuronal cells. *Proceedings of the Japan Academy. Series B, Physical and Biological Sciences*, *94*(9), 337–349. PubMed. https://doi.org/10.2183/pjab.94.022

Klinkert, K., Levernier, N., Gross, P., Gentili, C., von Tobel, L., Pierron, M., Busso, C., Herrman, S., Grill, S. W., Kruse, K., & Gönczy, P. (2019). Aurora A depletion reveals centrosome-independent polarization mechanism in Caenorhabditis elegans. *ELife*, *8*, e44552. https://doi.org/10.7554/eLife.44552

Kupfer, A., Louvard, D., & Singer, S. J. (1982). Polarization of the Golgi apparatus and the microtubule-organizing center in cultured fibroblasts at the edge of an experimental wound. *Proceedings of the National Academy of Sciences*, *79*(8), 2603–2607. https://doi.org/10.1073/pnas.79.8.2603

Lang, C. F., & Munro, E. (2017). The PAR proteins: From molecular circuits to dynamic self-stabilizing cell polarity. *Development*, *144*(19), 3405–3416. https://doi.org/10.1242/dev.139063

Lappalainen, P., Kotila, T., Jégou, A., & Romet-Lemonne, G. (2022). Biochemical and mechanical regulation of actin dynamics. *Nature Reviews Molecular Cell Biology*, *23*(12), 836–852. https://doi.org/10.1038/s41580-022-00508-4

Lawson, C. D., & Ridley, A. J. (2017). Rho GTPase signaling complexes in cell migration and invasion. *Journal of Cell Biology*, *217*(2), 447–457. https://doi.org/10.1083/jcb.201612069

Lele, T. P., Dickinson, R. B., & Gundersen, G. G. (2018). Mechanical principles of nuclear shaping and positioning. *Journal of Cell Biology*, *217*(10), 3330–3342. https://doi.org/10.1083/jcb.201804052

Li, T.-D., Bieling, P., Weichsel, J., Mullins, R. D., & Fletcher, D. A. (2022). The molecular mechanism of load adaptation by branched actin networks. *ELife*, *11*, e73145. https://doi.org/10.7554/eLife.73145

Li, Y., Chen, M., & Chang, W. (2022). Roles of the nucleus in leukocyte migration. *Journal of Leukocyte Biology*, *112*(4), 771–783. https://doi.org/10.1002/JLB.1MR0622-473RR

Livne, A., & Geiger, B. (2016). The inner workings of stress fibers − from contractile machinery to focal adhesions and back. *Journal of Cell Science*, *129*(7), 1293–1304. https://doi.org/10.1242/jcs.180927

Luo, Q., Kuang, D., Zhang, B., & Song, G. (2016). Cell stiffness determined by atomic force microscopy and its correlation with cell motility. *Biochimica et Biophysica Acta (BBA) - General Subjects*, *1860*(9), 1953–1960. https://doi.org/10.1016/j.bbagen.2016.06.010

Machesky, L. M., Mullins, R. D., Higgs, H. N., Kaiser, D. A., Blanchoin, L., May, R. C., Hall, M. E., & Pollard, T. D. (1999). Scar, a WASp-related protein, activates nucleation of actin filaments by the Arp2/3 complex. *Proceedings of the National Academy of Sciences*, *96*(7), 3739–3744. https://doi.org/10.1073/pnas.96.7.3739

Malone, C. J., Fixsen, W. D., Horvitz, H. R., & Han, M. (1999). UNC-84 localizes to the nuclear envelope and is required for nuclear migration and anchoring during C. elegans development. *Development*, *126*(14), 3171–3181. https://doi.org/10.1242/dev.126.14.3171

Malone, C. J., Misner, L., Le Bot, N., Tsai, M.-C., Campbell, J. M., Ahringer, J., & White, J. G. (2003). The C. elegans Hook Protein, ZYG-12, Mediates the Essential Attachment between the Centrosome and Nucleus. *Cell*, *115*(7), 825–836. https://doi.org/10.1016/S0092-8674(03)00985-1

Manley, H. R., Keightley, M. C., & Lieschke, G. J. (2018). The Neutrophil Nucleus: An Important Influence on Neutrophil Migration and Function. *Frontiers in Immunology*, *9*, 2867–2867. PubMed. https://doi.org/10.3389/fimmu.2018.02867

Manzini, M. C., & Walsh, C. A. (2011). What disorders of cortical development tell us about the cortex: One plus one does not always make two. *Molecular and Genetic Bases of Disease*, *21*(3), 333–339. https://doi.org/10.1016/j.gde.2011.01.006

Matsumoto, A., Hieda, M., Yokoyama, Y., Nishioka, Y., Yoshidome, K., Tsujimoto, M., & Matsuura, N. (2015). Global loss of a nuclear lamina component, lamin A/C, and LINC complex components SUN1, SUN2, and nesprin-2 in breast cancer. *Cancer Medicine*, *4*(10), 1547–1557. https://doi.org/10.1002/cam4.495

McIntire, S. L., Reimer, R. J., Schuske, K., Edwards, R. H., & Jorgensen, E. M. (1997). Identification and characterization of the vesicular GABA transporter. *Nature*, *389*(6653), 870–876. https://doi.org/10.1038/39908

Meaders, J. L., & Burgess, D. R. (2020). Microtubule-Based Mechanisms of Pronuclear Positioning. *Cells*, *9*(2). https://doi.org/10.3390/cells9020505

Meyerzon, M., Fridolfsson, H. N., Ly, N., McNally, F. J., & Starr, D. A. (2009). UNC-83 is a nuclear-specific cargo adaptor for kinesin-1-mediated nuclear migration. *Development*, *136*(16), 2725–2733. https://doi.org/10.1242/dev.038596

Minn, I., Rolls, M. M., Hanna-Rose, W., & Malone, C. J. (2009). SUN-1 and ZYG-12, Mediators of Centrosome–Nucleus Attachment, Are a Functional SUN/KASH Pair in Caenorhabditis elegans. *Molecular Biology of the Cell*, *20*(21), 4586–4595. https://doi.org/10.1091/mbc.e08-10-1034

Mogilner, A., & Oster, G. (2003). Polymer Motors: Pushing out the Front and Pulling up the Back. *Current Biology*, *13*(18), R721–R733. https://doi.org/10.1016/j.cub.2003.08.050

Mullins, R. D., Heuser, J. A., & Pollard, T. D. (1998). The interaction of Arp2/3 complex with actin: Nucleation, high affinity pointed end capping, and formation of branching networks of filaments. *Proceedings of the National Academy of Sciences*, *95*(11), 6181–6186. https://doi.org/10.1073/pnas.95.11.6181

Munro, E., Nance, J., & Priess, J. R. (2004). Cortical Flows Powered by Asymmetrical Contraction Transport PAR Proteins to Establish and Maintain Anterior-Posterior Polarity in the Early C. elegans Embryo. *Developmental Cell*, *7*(3), 413–424. https://doi.org/10.1016/j.devcel.2004.08.001

Nobes, C. D., & Hall, A. (1995). Rho, Rac, and Cdc42 GTPases regulate the assembly of multimolecular focal complexes associated with actin stress fibers, lamellipodia, and filopodia. *Cell*, *81*(1), 53–62. https://doi.org/10.1016/0092-8674(95)90370-4

Ouellette, M.-H., Martin, E., Lacoste-Caron, G., Hamiche, K., & Jenna, S. (2016). Spatial control of active CDC-42 during collective migration of hypodermal cells in Caenorhabditis elegans. *Journal of Molecular Cell Biology*, *8*(4), 313–327. https://doi.org/10.1093/jmcb/mjv062

Parri, M., & Chiarugi, P. (2010). Rac and Rho GTPases in cancer cell motility control. *Cell Communication and Signaling*, *8*(1), 23. https://doi.org/10.1186/1478-811X-8-23

Patel, F. B., Bernadskaya, Y. Y., Chen, E., Jobanputra, A., Pooladi, Z., Freeman, K. L., Gally, C., Mohler, W. A., & Soto, M. C. (2008a). The WAVE/SCAR complex promotes polarized cell movements and actin enrichment in epithelia during C. elegans embryogenesis. *Developmental Biology*, *324*(2), 297–309. https://doi.org/10.1016/j.ydbio.2008.09.023

Patel, F. B., Bernadskaya, Y. Y., Chen, E., Jobanputra, A., Pooladi, Z., Freeman, K. L., Gally, C., Mohler, W. A., & Soto, M. C. (2008b). The WAVE/SCAR complex promotes polarized cell movements and actin enrichment in epithelia during C. elegans embryogenesis. *Developmental Biology*, *324*(2), 297–309. https://doi.org/10.1016/j.ydbio.2008.09.023

Petrie, R. J., Gavara, N., Chadwick, R. S., & Yamada, K. M. (2012). Nonpolarized signaling reveals two distinct modes of 3D cell migration. *Journal of Cell Biology*, *197*(3), 439–455. https://doi.org/10.1083/jcb.201201124

Petrie, R. J., Koo, H., & Yamada, K. M. (2014). Generation of compartmentalized pressure by a nuclear piston governs cell motility in a 3D matrix. *Science*, *345*(6200), 1062–1065. https://doi.org/10.1126/science.1256965

Petrie, R. J., & Yamada, K. M. (2015). Fibroblasts Lead the Way: A Unified View of 3D Cell Motility. *Trends in Cell Biology*, *25*(11), 666–674. https://doi.org/10.1016/j.tcb.2015.07.013

Pollard, T. D. (2016). Actin and Actin-Binding Proteins. *Cold Spring Harbor Perspectives in Biology*, *8*(8), a018226. PubMed. https://doi.org/10.1101/cshperspect.a018226

Priess, J. R., & Hirsh, D. I. (1986). Caenorhabditis elegans morphogenesis: The role of the cytoskeleton in elongation of the embryo. *Developmental Biology*, *117*(1), 156–173. https://doi.org/10.1016/0012-1606(86)90358-1

Raab, M., Gentili, M., de Belly, H., Thiam, H.-R., Vargas, P., Jimenez, A. J., Lautenschlaeger, F., Voituriez, R., Lennon-Duménil, A.-M., Manel, N., & Piel, M. (2016). ESCRT III repairs nuclear envelope ruptures during cell migration to limit DNA damage and cell death. *Science*, *352*(6283), 359–362. https://doi.org/10.1126/science.aad7611

Rose, L. S., & Kemphues, K. J. (1998). EARLY PATTERNING OF THE C. ELEGANS EMBRYO. *Annual Review of Genetics*, *32*(1), 521–545. https://doi.org/10.1146/annurev.genet.32.1.521

Rossman, K. L., Der, C. J., & Sondek, J. (2005). GEF means go: Turning on RHO GTPases with guanine nucleotide-exchange factors. *Nature Reviews Molecular Cell Biology*, *6*(2), 167–180. https://doi.org/10.1038/nrm1587

Rowat, A. C., Jaalouk, D. E., Zwerger, M., Ung, W. L., Eydelnant, I. A., Olins, D. E., Olins, A. L., Herrmann, H., Weitz, D. A., & Lammerding, J. (2013). Nuclear Envelope Composition Determines the Ability of Neutrophil-type Cells to Passage through Micron-scale Constrictions*. *Journal of Biological Chemistry*, *288*(12), 8610–8618. https://doi.org/10.1074/jbc.M112.441535

Salvermoser, M., Begandt, D., Alon, R., & Walzog, B. (2018). Nuclear Deformation During Neutrophil Migration at Sites of Inflammation. *Frontiers in Immunology*, *9*, 2680–2680. PubMed. https://doi.org/10.3389/fimmu.2018.02680

Sawa, M., Suetsugu, S., Sugimoto, A., Miki, H., Yamamoto, M., & Takenawa, T. (2003). Essential role of the C. elegans Arp2/3 complex in cell migration during ventral enclosure. *Journal of Cell Science*, *116*(8), 1505–1518. https://doi.org/10.1242/jcs.00362

Schaks, M., Giannone, G., & Rottner, K. (2019). Actin dynamics in cell migration. *Essays in Biochemistry*, *63*(5), 483–495. https://doi.org/10.1042/EBC20190015

Seetharaman, S., & Etienne-Manneville, S. (2020). Cytoskeletal Crosstalk in Cell Migration. *Trends in Cell Biology*, *30*(9), 720–735. https://doi.org/10.1016/j.tcb.2020.06.004

Shinchi, Y., Hieda, M., Nishioka, Y., Matsumoto, A., Yokoyama, Y., Kimura, H., Matsuura, S., & Matsuura, N. (2015). SUV420H2 suppresses breast cancer cell invasion through down regulation of the SH2 domain-containing focal adhesion protein tensin-3. *Invited Reviews: Molecular Motors*, *334*(1), 90–99. https://doi.org/10.1016/j.yexcr.2015.03.010

Smith, B. A., Padrick, S. B., Doolittle, L. K., Daugherty-Clarke, K., Corrêa, I. R., Jr, Xu, M.-Q., Goode, B. L., Rosen, M. K., & Gelles, J. (2013). Three-color single molecule imaging shows WASP detachment from Arp2/3 complex triggers actin filament branch formation. *ELife*, *2*, e01008. https://doi.org/10.7554/eLife.01008

Starr, D. A., & Fridolfsson, H. N. (2010). Interactions Between Nuclei and the Cytoskeleton Are Mediated by SUN-KASH Nuclear-Envelope Bridges. *Annual Review of Cell and Developmental Biology*, *26*(1), 421–444. https://doi.org/10.1146/annurev-cellbio-100109-104037

Starr, D. A., Hermann, G. J., Malone, C. J., Fixsen, W., Priess, J. R., Horvitz, H. R., & Han, M. (2001). Unc-83 encodes a novel component of the nuclear envelope and is essential for proper nuclear migration. *Development*, *128*(24), 5039–5050. https://doi.org/10.1242/dev.128.24.5039

Stephens, A. D., Liu, P. Z., Banigan, E. J., Almassalha, L. M., Backman, V., Adam, S. A., Goldman, R. D., & Marko, J. F. (2018). Chromatin histone modifications and rigidity affect

nuclear morphology independent of lamins. *Molecular Biology of the Cell*, *29*(2), 220–233. https://doi.org/10.1091/mbc.E17-06-0410

Sugi, T. (2016). Genome Editing in C. elegans and Other Nematode Species. *International Journal of Molecular Sciences*, *17*(3), 295–295. PubMed. https://doi.org/10.3390/ijms17030295

Sulston, J. E., & Brenner, S. (1997). Post-embryonic development in the ventral cord of Caenorhabditis elegans. *Philosophical Transactions of the Royal Society of London. B, Biological Sciences*, *275*(938), 287–297. https://doi.org/10.1098/rstb.1976.0084

Sulston, J. E., & Horvitz, H. R. (1977). Post-embryonic cell lineages of the nematode, Caenorhabditis elegans. *Developmental Biology*, *56*(1), 110–156. https://doi.org/10.1016/0012-1606(77)90158-0

Sulston, J. E., & Horvitz, H. R. (1981). Abnormal cell lineages in mutants of the nematode Caenorhabditis elegans. *Developmental Biology*, *82*(1), 41–55. https://doi.org/10.1016/0012-1606(81)90427-9

Suraneni, P., Rubinstein, B., Unruh, J. R., Durnin, M., Hanein, D., & Li, R. (2012). The Arp2/3 complex is required for lamellipodia extension and directional fibroblast cell migration. *Journal of Cell Biology*, *197*(2), 239–251. https://doi.org/10.1083/jcb.201112113

Swift, J., Ivanovska, I. L., Buxboim, A., Harada, T., Dingal, P. C. D. P., Pinter, J., Pajerowski, J. D., Spinler, K. R., Shin, J.-W., Tewari, M., Rehfeldt, F., Speicher, D. W., & Discher, D. E. (2013). Nuclear Lamin-A Scales with Tissue Stiffness and Enhances Matrix-Directed Differentiation. *Science*, *341*(6149), 1240104. https://doi.org/10.1126/science.1240104

Thiam, H.-R., Vargas, P., Carpi, N., Crespo, C. L., Raab, M., Terriac, E., King, M. C., Jacobelli, J., Alberts, A. S., Stradal, T., Lennon-Dumenil, A.-M., & Piel, M. (2016). Perinuclear Arp2/3-driven actin polymerization enables nuclear deformation to facilitate cell migration through complex environments. *Nature Communications*, *7*(1), 10997. https://doi.org/10.1038/ncomms10997

Totsukawa, G., Yamakita, Y., Yamashiro, S., Hartshorne, D. J., Sasaki, Y., & Matsumura, F. (2000). Distinct Roles of Rock (Rho-Kinase) and Mlck in Spatial Regulation of Mlc Phosphorylation for Assembly of Stress Fibers and Focal Adhesions in 3t3 Fibroblasts. *Journal of Cell Biology*, *150*(4), 797–806. https://doi.org/10.1083/jcb.150.4.797

Trivedi, N., & Solecki, D. J. (2011). Neuronal migration illuminated. *Cell Adhesion & Migration*, *5*(1), 42–47. https://doi.org/10.4161/cam.5.1.13609

Vargas, P., Barbier, L., Sáez, P. J., & Piel, M. (2017). Mechanisms for fast cell migration in complex environments. *Cell Dynamics*, *48*, 72–78. https://doi.org/10.1016/j.ceb.2017.04.007

Velarde, N., Gunsalus, K. C., & Piano, F. (2007). Diverse roles of actin in C. elegans early embryogenesis. *BMC Developmental Biology*, *7*, 142–142. PubMed. https://doi.org/10.1186/1471-213X-7-142

Vuong-Brender, T. T. K., Yang, X., & Labouesse, M. (2016). Chapter Thirty-Five—C. elegans Embryonic Morphogenesis. In P. M. Wassarman (Ed.), *Current Topics in Developmental Biology* (Vol. 116, pp. 597–616). Academic Press. https://doi.org/10.1016/bs.ctdb.2015.11.012

Walck-Shannon, E., Reiner, D., & Hardin, J. (2015a). Polarized rac-dependent protrusions drive epithelial intercalation in the embryonic epidermis of c. Elegans. *Development (Cambridge)*, *142*(20), 3549–3560. https://doi.org/10.1242/dev.127597

Walck-Shannon, E., Reiner, D., & Hardin, J. (2015b). Polarized Rac-dependent protrusions drive epithelial intercalation in the embryonic epidermis of C. elegans. *Development*, *142*(20), 3549–3560. https://doi.org/10.1242/dev.127597

Wallace, A. G., Raduwan, H., Carlet, J., & Soto, M. C. (2018). The RhoGAP HUM-7/myo9 integrates signals to modulate RHO-1/RhoA during embryonic morphogenesis in caenorhabditis elegans. *Development (Cambridge)*, *145*(23). https://doi.org/10.1242/dev.168724

Wegner, A. (1976). Head to tail polymerization of actin. *Journal of Molecular Biology*, *108*(1), 139–150. https://doi.org/10.1016/S0022-2836(76)80100-3

Wernike, D., Chen, Y., Mastronardi, K., Makil, N., & Piekny, A. (2016). Mechanical forces drive neuroblast morphogenesis and are required for epidermal closure. *Developmental Biology*, *412*(2), 261–277. https://doi.org/10.1016/j.ydbio.2016.02.023

Williams-Masson, E. M., Malik, A. N., & Hardin, J. (1997). An actin-mediated two-step mechanism is required for ventral enclosure of the C. elegans hypodermis. *Development*, *124*(15), 2889–2901. https://doi.org/10.1242/dev.124.15.2889

Withee, J., Galligan, B., Hawkins, N., & Garriga, G. (2004a). Caenorhabditis elegans WASP and Ena/VASP proteins play compensatory roles in morphogenesis and neuronal cell migration. *Genetics*, *167*(3), 1165–1176. https://doi.org/10.1534/genetics.103.025676

Withee, J., Galligan, B., Hawkins, N., & Garriga, G. (2004b). Caenorhabditis elegans WASP and Ena/VASP Proteins Play Compensatory Roles in Morphogenesis and Neuronal Cell Migration. *Genetics*, *167*(3), 1165–1176. https://doi.org/10.1534/genetics.103.025676

Wolf, K., te Lindert, M., Krause, M., Alexander, S., te Riet, J., Willis, A. L., Hoffman, R. M., Figdor, C. G., Weiss, S. J., & Friedl, P. (2013). Physical limits of cell migration: Control by ECM space and nuclear deformation and tuning by proteolysis and traction force. *Journal of Cell Biology*, *201*(7), 1069–1084. https://doi.org/10.1083/jcb.201210152

Wu, Y. K., Umeshima, H., Kurisu, J., & Kengaku, M. (2018). Nesprins and opposing microtubule motors generate a point force that drives directional nuclear motion in migrating neurons. *Development*, *145*(5), dev158782. https://doi.org/10.1242/dev.158782

Xiong, H., Mohler, W. A., & Soto, M. C. (2011). The branched actin nucleator Arp2/3 promotes nuclear migrations and cell polarity in the C. elegans zygote. *Developmental Biology*, *357*(2), 356–369. https://doi.org/10.1016/j.ydbio.2011.07.008

Zuela, N., & Gruenbaum, Y. (2016). Matefin/SUN-1 Phosphorylation on Serine 43 Is Mediated by CDK-1 and Required for Its Localization to Centrosomes and Normal Mitosis in C. elegans Embryos. *Cells*, *5*(1). https://doi.org/10.3390/cells5010008

Chapter II

<u>Characterizing Dynein's Role in P-cell Nuclear Migration using an Auxin-Induced Degradation System</u>

Jamie Ho[1], Venecia A. Valdez[1], Linda Ma[1], and Daniel A. Starr[1]

[1]Department of Molecular and Cellular Biology, University of California, Davis, CA, USA

Jamie Ho carried out the experiments and wrote the manuscript. Venecia A. Valdez generated the strains. Daniel A. Starr and Linda Ma designed the experiments.

Characterizing Dynein's Role in P-cell Nuclear Migration using an Auxin-Induced Degradation System

Jamie Ho[1], Venecia A. Valdez[1], Linda Ma[1], and Daniel A. Starr[1]

[1]Department of Molecular and Cellular Biology, University of California, Davis, CA 95616, USA
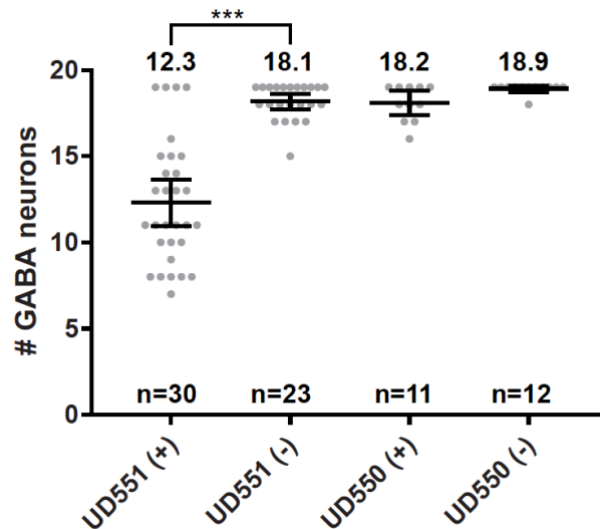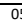
Figure 1. Auxin-induced degradation of dynein causes a P-cell nuclear migration defect. Average number of GABA neurons in L4 animals that express the TIR1 gene (an auxin-induced E3 ubiquitin ligase; Zhang et al., 2015) specifically in P cells. Animals either expressed the DHC-1 degron tag (UD551) or did not express the DHC-1 degron tag (UD550). These animals (UD551 and UD550) were either exposed to auxin (+) or not (-) as L1 animals. Statistical significance calculated by t-test with p-value<0.0001. The mean is marked with error bars denoting 95% CI.

Description

Nuclear migration limits the rate of cellular migration through narrow spaces due to the large size and stiffness of the nucleus (Ungricht and Kutay, 2017). Using *Caenorhabditis elegans* as a model organism, we can observe P-cell nuclear migration *in vivo*. During the mid-L1 stage, P-cell nuclei that are about 3-4μm in diameter must migrate from a lateral to ventral position. This migration occurs through a constricted space ~ 200nm wide, about 5% of the diameter of the relaxed nucleus, between body wall muscle and cuticle (Cox and Hardin, 2004). If this migration succeeds, P-cells develop into vulval cells and GABA neurons. Failure of P-cell nuclear migration leads to cell death and missing P-cell lineages, leading to egg laying defective (Egl) and uncoordinated (Unc) animals because of missing vulval cells and GABA neurons, respectively (Sulston and Horvitz, 1981). Two proteins that are known to be involved in P-cell nuclear migration are UNC-84 and UNC-83. These proteins make up the LINC complex to form a bridge between the nucleus and the cytoplasm. Disruption of the LINC complex leads to nuclear migration defects in P-cells (Starr et al., 2001). Previously, our lab showed that P-cell nuclei migrate towards the minus ends of microtubules through the microtubule motor, dynein. Dynein is essential in embryogenesis (Gonczy et al., 1999), therefore our research was previously limited to viable, partial loss-of-function alleles of dynein or dynein-interacting proteins. Animals expressing a hypomorphic allele of dynein, *dhc-1(js319)*, had an average of ~3 P-cells that failed to migrate (Bone et al., 2016).

Here, we tested the hypothesis that the *unc-83/unc-84* pathway works through dynein to move P-cell nuclei using the auxin-inducible degradation system (AID) to knock down dynein specifically during P-cell nuclear migration

(Zhang et al., 2015). The *Arabidopsis thaliana* TIR1 gene was expressed downstream of the *C. elegans* P-cell specific *hlh-3* promoter (Bone et al., 2016) in the strain UD550 (*oxIs12[unc-47::GFP]; ycEx253[p$_{hlh-3}$::TIR-1::mRuby; odr-1::rfp]*). Next, UD550 was crossed to a strain with *dhc-1(ie28[dhc-1::degron::GFP])* (Zhang et al., 2015) to make UD551 (*dhc-1(ie28[dhc-1::degron::GFP]) I; oxIs12[unc-47::GFP] X; ycEx253[p$_{hlh-3}$::TIR-1::mRuby; odr-1::rfp]*). UD550 and UD551 animals were synchronized to mid L1 as previously described (Bone et al., 2016) and exposed to 1mM auxin for five hours at 25°C. P-cell nuclear migration defects were quantified by counting GABA neurons marked with UNC-47::GFP by fluorescence microscopy in L4 animals after the auxin treatment. Wild-type animals have 19 GABA neurons and missing GABA neurons indicate that P-cell nuclear migration failed (Chang et al., 2013; Bone et al., 2016). As a negative control, UD550 animals, which lack the *dhc-1* degron tag, had no P-cell nuclear migration defects when exposed to auxin. This result is similar to UD551 animals that were not exposed to auxin (Figure 1). In support of our hypothesis, larvae exposed to auxin that expressed both the TIR1 gene in P cells and the *dhc-1* degron tag (UD551) had an average of 12.3 GABA neurons compared to sibling larvae not exposed to auxin that had an average of 18.1 GABA neurons (Figure 1). Thus, the dynein-degraded larvae had an average of 5.8 missing GABA neurons (p<0.0001), indicative of a severe P-cell nuclear migration defect. These results further strengthen our model that dynein plays a major role in generating forces to move nuclei in P-cells through constricted spaces. Finally, the *p$_{hlh-3}$::TIR1* line will be a valuable reagent to knock down other essential proteins to determine their roles during P-cell nuclear migration.
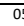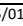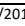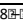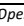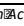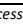
Reagents

The *Arabidopsis thaliana* TIR1 gene was amplified from pLZ31 (pCFJ151_Peft-3_TIR1_linker_mRuby_unc-54 3'UTR; a gift from Abby Dernburg; Addgene plasmid # 71720; Zhang et al., 2015) and cloned downstream of the P-cell specific *hlh-3* promoter in pSL780 (Bone et al., 2016) to make pSL814. 2ng/ml of pSL814 and 100ng/ml of *odr-1::rfp* were injected into a strain with *oxIs12[unc-47::GFP]* to make the strain UD550: *oxIs12[unc-47::GFP]; ycEx253[p$_{hlh-3}$::TIR-1::mRuby; odr-1::rfp]*. UD550 was crossed to CA1207: *dhc-1(ie28[dhc-1::degron::GFP])*, a gift from Abby Dernburg (Zhang et al., 2015), to make UD551: *dhc-1(ie28[dhc-1::degron::GFP]) I; oxIs12[unc-47::GFP] X; ycEx253[p$_{hlh-3}$::TIR-1::mRuby; odr-1::rfp]*. Auxin (Sigma #I2886) was added to NGM plates to a final concentration of 1 mM.

References

Bone CR, Chang YT, Cain NE, Murphy SP, Starr DA. 2016. Nuclei migrate through constricted spaces using microtubule motors and actin networks in C. elegans hypodermal cells. Development (Cambridge, England) **143**: 4193-202.

Chang YT, Dranow D, Kuhn J, Meyerzon M, Ngo M, et al. 2013. toca-1 is in a novel pathway that functions in parallel with a SUN-KASH nuclear envelope bridge to move nuclei in Caenorhabditis elegans. Genetics **193**: 187-200.

Cox EA, Hardin J. 2004. Sticky worms: adhesion complexes in C. elegans. J Cell Sci **117**: 1885-97.

Gonczy P, Pichler S, Kirkham M, Hyman AA. 1999. Cytoplasmic dynein is required for distinct aspects of MTOC positioning, including centrosome separation, in the one cell stage Caenorhabditis elegans embryo. J Cell Biol **147**: 135-50.

Starr DA, Hermann GJ, Malone CJ, Fixsen W, Priess JR, et al. 2001. unc-83 encodes a novel component of the nuclear envelope and is essential for proper nuclear migration. Development (Cambridge, England) **128**: 5039-50.

Sulston JE, Horvitz HR. 1981. Abnormal cell lineages in mutants of the nematode Caenorhabditis elegans. Developmental biology **82**: 41-55.

Ungricht R, Kutay U. 2017. Mechanisms and functions of nuclear envelope remodelling. Nat Rev Mol Cell Biol **18**: 229-45.

Zhang L, Ward JD, Cheng Z, Dernburg AF. 2015. The auxin-inducible degradation (AID) system enables versatile conditional protein depletion in C. elegans. Development (Cambridge, England) **142**: 4374-84.

Funding
This work was funded by the National Institutes of Health grant RO1 GM073874 to D.A.S.

Citation: Ho, J; Valdez, VA; Ma, L; Starr, DA. (2018): Characterizing Dynein's Role in P-cell Nuclear Migration using an Auxin-Induced Degradation System. Micropublication:biology. Dataset. https://doi.org/10.17912/W2W96J

Chapter III

<u>A CDC-42-regulated actin network is necessary for nuclear migration through constricted spaces</u>

<u>in *C. elegans*</u>

Jamie Ho[1], Leslie A. Guerrero[1], Diana Libuda[2], GW Gant Luxton[1], and Daniel A Starr[1]

[1]Department of Molecular and Cellular Biology, University of California, Davis, CA, USA

[2]Department of Biology, University of Oregon, Eugene, OR, USA

Abstract

Confined nuclear migration is a necessary process for proper development to take place and is a property of cancer metastasis. Successful nuclear migration through constricted spaces relies on the ability of the nucleus to deform. While there have been numerous *in vitro* studies done to understand this process, not much is known of how this takes place *in vivo*. Our lab has developed an *in vivo* system to study confined nuclear migration by observing P-cell nuclear migration in *C. elegans* larvae. The best characterized pathway for P-cell nuclear migration is through the LINC complex. The SUN protein, UNC-84, and KASH protein, UNC-83, interact with lamin and dynein, respectively, to pull nuclei towards the minus ends of microtubules through constrictions. However, null mutations of *unc-84* lead to a temperature-dependent phenotype, with nuclear migration defects at higher temperatures but not at lower temperatures, suggesting the presence of a parallel pathway that functions in addition to the LINC complex pathway. Using a forward genetics screen for components involved in the parallel SUN/KASH pathway, we identified putative actin regulators, including *cgef-1* (**C**DC-42 **G**uanine Nucleotide **E**xchange **F**actor). Mutations in the *cgef-1d* isoform and expression of *cgef-1d* promoter reporter in P-cells confirm *cgef-1d* is the *cgef-1* isoform involved. CGEF-1 functions by activating CDC-42 during embryogenesis but it's unclear if CGEF-1 activates CDC-42 for P-cell nuclear migration. Conditional knockdown of CDC-42 in the absence of the LINC complex led to a P-cell nuclear migration defect and expression of constitutively active CDC-42 in *cgef-1; unc-84* double mutants resulted in a partial rescue of the nuclear migration defect suggesting CDC-42 functions downstream of CGEF-1. Knockdown of the Arp2/3 complex or non-muscle myosin II (NMY-2) in *unc-84* mutants led to a P-cell nuclear migration defect, suggesting branched actin and actomyosin structures are involved in migrating P-cell nuclei. In our model, CGEF-1

activates CDC-42, which is recruited to the nuclear periphery where it induces actin

polymerization through the Arp2/3 complex to deform the nucleus during nuclear migration.

NMY-2 mediated actomyosin contractions at the rear of the nucleus provides a pushing force to

push the nucleus through confined spaces.

Introduction

Cell migration is an essential process for development of multicellular organisms and is

also important for wound healing throughout life. When migrating, cells have to undergo

dramatic morphological changes to aid in this process (Raftoppoulou & Hall, 2004; Ridley,

2015). From studying fibroblast migration, we know these morphological changes are due to

reorganization of the actin cytoskeleton which is regulated by the RhoGTPases—RhoA, Rac1,

and Cdc42 process (Lawson & Ridley, 2017; Raftoppoulou & Hall, 2004; Ridley, 2015).

RhoGTPases function as molecular switches by switching between a GTP-bound active state and

a GDP-bound inactive state (Rossman et al., 2005; Schmidt & Hall, 2002). Once activated, these

proteins can go on to activate downstream effectors to regulate a variety of intracellular

responses (Etienne-Manneville, 2004; Hall, 1998). During fibroblast migration, Rac1 is localized

to the front of the migrating cell to regulate actin polymerization and drive extension of the

leading-edge protrusion. RhoA is found at the cell body and the rear of the migrating cell to drive

actomyosin contractility to promote retraction at the cell rear. Cdc42 is found at the front of the

migrating cell and is important in establishing cell polarity and directionality of migration

(Lawson & Ridley, 2017).

In addition to the importance of actin structures in cell migration, nuclear positioning has

also been shown to contribute to effective cell migration. During migration, the nucleus of

fibroblasts is positioned rearwards with the centrosome at the center of the cell (Zhu et al., 2018).

This movement is modulated by the LINC (**Li**nker of the **N**ucleoskeleton and **C**ytoskeleton) complex, which acts as a bridge, transferring forces generated by the cytoskeleton in the cytoskeleton to structures inside the nucleus (Zhu et al., 2018). The LINC complex is composed of the SUN (**S**ad1 and **UN**C-84) protein found at the inner nuclear membrane which interacts with the KASH (**K**larsicht, **A**NC-1, **S**yne **h**omology) protein found at the outer nuclear membrane (Starr & Fridolfsson, 2010). Rearward translocation of the nucleus in migrating fibroblasts is facilitated by the SUN protein SUN2 and the KASH protein nesprin-2G (Luxton et al., 2010). Nesprin-2G binds to rearward moving actin cables to translocate the nucleus through these transmembrane actin-associated nuclear (TAN) lines. This process of orienting the centrosome towards the leading edge and the nucleus to the rear is important for productive fibroblast migration, highlighting the role the nucleus plays during cell migration.

Cellular migration through constricted spaces is a process that occurs during the immune response, neuronal development, and cancer metastasis (Bone & Starr, 2016; Denais et al., 2016; Thiam et al., 2016). During mammalian brain development, newly born neurons must migrate from the germinal layers to the developing cortices by migrating through constrictions generated by the surrounding neural tissue (Kalukula et al., 2022; Kengaku, 2018). Additionally, during the immune response, neutrophils in the blood stream must migrate through the endothelial monolayer of the blood vessels to rush to the site of inflammation or tissue injury (Liu et al., 2021; Salvermoser et al., 2018). The rate of cellular migration through narrow spaces is limited by nuclear deformability as the nucleus is the largest and most rigid organelle of the cell (Friedl et al., 2011; Fu et al., 2012; Swift et al., 2013; Wolf et al., 2013). Nuclear deformability is dependent on several factors such as lamin composition, levels of heterochromatin, and cytoskeletal dynamics. Low expression or knockdown of laminA/C or low levels of

heterochromatin results in increased nuclear deformability (Bell et al., 2022; Davidson et al., 2014, 2015; Stephens et al., 2018). Additionally, cytoskeletal forces applied to nuclei can affect nuclear deformability (Renkawitz et al., 2019; Thiam et al., 2016). Mouse dendritic cells that are induced to migrate through constrictions are unable to undergo successful nuclear migration when the actin-nucleating Arp2/3 complex is inhibited (Thiam et al., 2016), highlighting the importance of actin in this process. In addition, nuclear migration through constricted spaces lead to nuclear envelope rupture and increased DNA damage (Denais et al., 2016; Raab et al., 2016; Thiam et al., 2016). Most of these findings were made using *in vitro* systems of cells migrating through manufactured constricted spaces. A system where mouse dendritic cells are imaged migrating through the extra-cellular matrix of explanted mouse ears has been used to find more *in vivo* relevance (Raab et al., 2016). While we have gained much insight on the mechanisms that govern confined nuclear migration, most of these studies have been done in an in vitro setting and can lead to discrepancies between mechanisms found in cultured cells versus a multicellular organism. For example, while TAN lines are important in fibroblast migration, these structures have yet to be observed in a tissue context. Therefore, how cells and nuclei migrate through constricted spaces as a normal part of development *in vivo* is poorly understood.

Our lab has developed an *in vivo* model to study nuclear migration through constricted spaces using larval hypodermal precursor cells called P cells in *Caenorhabditis elegans* (Fig. 3.1A)(Bone et al., 2016; Chang et al., 2013). During the early L1 larval stage, twelve P cells organized into six pairs of P cells span the lateral side to the ventral side, with the nuclei located on the lateral side of the animal (Sulston & Horvitz, 1977). During the mid-L1 development, P-cell nuclei, which are 3-4 μm in diameter, migrate from their lateral positions to the ventral cord by squeezing through a narrow space of ~200 nm between the body wall muscles and the cuticle

(Bone et al., 2016; Cox & Hardin, 2004; Francis & Waterston, 1991). This constriction is about 5% the diameter of the nucleus. If P-cell nuclei successfully migrate, the P cells will divide and develop into vulval cells and GABA neurons. Failed nuclear migration results in P-cell death and a lack of a vulva and GABA neurons, leading to **egg l**aying deficient (Egl) and **unc**oordinated (Unc) phenotypes (Horvitz & Sulston, 1980; Sulston & Horvitz, 1981).

P-cell nuclear migration is regulated by the SUN protein UNC-84 and the KASH protein UNC-83 (Malone et al., 1999; Starr et al., 2001). UNC-84, located at the inner nuclear membrane, interacts with UNC-83 to recruit it to the out nuclear membrane (McGee et al., 2006). Together, UNC-84 and UNC-83 form a LINC complex to transfer forces generated by the cytoskeleton in the cytoplasm to structures inside the nucleus (Starr & Fridolfsson, 2010). UNC-83 is then able to interact with microtubule motor proteins kinesin and dynein to move nuclei (Fridolfsson et al., 2010; Fridolfsson & Starr, 2010; Meyerzon et al., 2009). In larval P-cells, dynein is the major motor necessary to move nuclei toward the minus ends of microtubules in the ventral cord (Bone et al., 2016; J. Ho et al., 2018). Null mutations in *unc-83* or *unc-84* lead to a temperature-sensitive nuclear migration defect in P cells. When these mutants are grown at 25°C, less than 40% of P-cell nuclei successfully migrate to a ventral position. However, when the LINC complex is disrupted at 15°C, at least 90% of P-cell nuclei migrate successfully (Malone et al., 1999; Starr et al., 2001). This leads to our central model that there is an additional pathway that functions parallel to the SUN/KASH pathway to move P-cell nuclei through constricted spaces.

To identify players in this alternative nuclear migration pathway, our lab previously conducted an unbiased forward genetics screen for **e**nhancers of the nuclear **m**igration defect of *u*nc-84 (*emu*) at 15°C (Chang et al., 2013). Eight *emu* mutations were isolated in these screens

and one was identified as a lesion in *toca-1* (Transducer of Cdc-42 dependent actin assembly) (Chang et al., 2013). TOCA-1 is predicted to have an F-BAR domain, a domain that interacts with the Rho GTPase Cdc42, and a domain that interacts with actin-nucleating WASP proteins (Fricke et al., 2009; Giuliani et al., 2009; H.-Y. H. Ho et al., 2004). One model is that TOCA-1 functions by binding to the nuclear membrane, recruiting Cdc42 and WASP to nucleate actin, and deforming the nucleus to aid in migration.

Here we report the identification of a second *emu* allele in *cgef-1* which is predicted to encode a guanine nucleotide exchange factor (GEF) for CDC-42 (Chan & Nance, 2013). GEFs function by activating G-proteins, which are molecular switches involved in regulating signaling cascades. G-proteins can be found in an "inactive" GDP-bound state and an "active" GTP-bound state. GEFs activate G-proteins by facilitating the exchange of GDP for GTP (Rossman et al., 2005; Schmidt & Hall, 2002). The Rho-GTPase family of G-proteins include RhoA, Rac, and Cdc42, which function by regulating polarity establishment, cell movement, and actin cytoskeleton dynamics (Etienne-Manneville, 2004; Hall, 1998). *C. elegans* orthologs are RHO-1, CED-10 (Rac), MIG-2 (Rac), and CDC-42 (Reiner & Lundquist, 2018). CGEF-1 acts as GEF for CDC-42 during early embryonic development (Chan & Nance, 2013), but its role outside of embryogenesis is unclear. We hypothesize CGEF-1 activates CDC-42, which then regulates actin networks to help nuclei migrate through constricted spaces in a pathway that functions parallel to the LINC-dynein pathway. To test this hypothesis, we examined the roles of CGEF-1, CDC-42, and other actin regulators during P-cell nuclear migration.

Results

Mutations in *cgef-1* enhance the P-cell nuclear migration defect of *unc-84(null)*

The *yc3* and *yc21* alleles were found in an *emu* screen and the homozygous mutants significantly enhance the nuclear migration defect of *unc-84* (Chang et al., 2013). To quantify P-cell nuclear migration, we expressed the GABA neuronal marker $p_{unc-47}::gfp$ and counted the number of GABA neurons at the L4 stage as an indicator of successful P-cell nuclear migration (Fridolfsson et al., 2018; McIntire et al., 1997). At 15°C, *unc-84(n369)* mutants were missing an average of 2.1 GABA neurons, slightly above wildtype (Fig. 3.1B-C). *yc3* single mutants had no phenotype on their own, missing an average of 1.3 GABA neurons. However, *yc3, unc-84(n369)* double mutants had an average of 4.4 missing GABA neurons (p<0.00005). *yc3* also enhanced the nuclear migration defect of *unc-84(n369)* at 20°C and at 25°C (Fig. 3.1D-E).

To identify the molecular lesion underlying *emu* alleles, we performed whole genome sequencing of seven different *emu* mutant strains isolated in our previous screen (Chang et al., 2013). We cataloged single nucleotide polymorphisms (SNPs) that were predicted to cause severe disruptions to open reading frames. SNPs that were found in all the strains were eliminated because they were likely in the background of the UD87 strain that was used for mutagenesis. We focused on a SNP predicted to cause a premature stop codon in the *cgef-1* gene that was identified in both the *yc3* and *yc21* alleles. Nucleotide X:2798063 in the penultimate exon of *cgef-1* was mutated from a G to an A, causing the tryptophan 345 of CGEF-1a to change to a premature stop codon (Fig. 3.2A).

To confirm that the premature stop codon in *cgef-1(yc3)* is the molecular lesion responsible for enhancing the nuclear migration defect of *unc-84*, we tested whether other alleles of *cgef-1* also enhance the P-cell nuclear migration defect of *unc-84(n369)* null mutants. *Cgef-1(gk261)* is a likely null allele. It is a 318 bp deletion that removes the entire third exon in *cgef-1a* and is predicted to result in a frame shift (Fig. 3.2A) (C. elegans Deletion Mutant Consortium,

2012). *Cgef-1(gk261) unc-84(n369)* double mutants had significant P-cell nuclear migration defects at 15°C, 20°C, and 25°C compared to the single mutants (Fig. 3.1C-E). Likewise, *cgef-1(RNAi)* significantly enhanced the nuclear migration defects of *unc-84(n369)* (Fig. 3.1C-E). Thus, multiple alleles and RNAi of *cgef-1* all had similar phenotypes.

To confirm that the *yc3* phenotype is due to the molecular lesion in *cgef-1* and not some other mutation in the genome, we expressed *cgef-1* extra-chromosomal rescue arrays in *yc3, unc-84(n369)* double mutants. A fosmid covering the longest isoforms of *cgef-1*(WRM0622bA03) was able to rescue the nuclear migration defect in three independent lines (P<0.0005) (Fig. 3.1F). Together, these data suggest that lesions in *cgef-1* are responsible for the nuclear migration defects in *yc3* and *yc21* and that *cgef-1* functions in parallel with the LINC complex to facilitate P-cell nuclear migration.

The *cgef-1d* isoform is necessary for LINC-dependent P-cell nuclear migration

CGEF-1 activates CDC-42 in early embryogenesis (Chan & Nance, 2013; Kumfer et al., 2010). There are at least four *cgef-1* predicted isoforms (Fig. 3.2A) (Ziel et al., 2009; Wormbase). All four isoforms have the last four exons in common that are predicted to encode Dbl homology (DH) catalytic and pleckstrin homology (PH) domains (Chan & Nance, 2013; Ziel et al., 2009). *Cgef-1a* and *cgef-1c* are the shortest isoforms, encoding proteins 462 and 464 residues respectively, that differ at their N termini. A longer isoform *cgef-1d* encodes a 641-residue protein and the longest isoform, *cgef-1b*, is predicted to be 1055 residues. Expression of a fosmid (WRM0627cD01) that only spans the *cgef-1a, c,* and *d* isoforms was sufficient to rescue the *cgef-1(yc3) unc-84* nuclear migration defect at 15°C, indicating exons 1 – 11 of *cgef-1b* are not necessary for P-cell nuclear migration (Fig. 3.1G).

To further determine which isoform of *cgef-1* is necessary for this process, we generated new alleles in each isoform using the CRISPR-Cas9 system, either an early stop codon in the first or second exon of an isoform or a deletion mutation that resulted in a predicted frameshift (Fig. 3.2A). Predicted severe alleles of the long isoforms, *cgef-1b(yc101)* and *cgef-1b(yc102)*, did not enhance the nuclear migration defect of *unc-84(n369)* at 15 or 20°C (Fig. 3.2B-C). In contrast, the *cgef-1d(yc103)* early stop codon and *cgef-1d(yc104)* frame-shift deletions mutations significantly enhanced the nuclear migration defect of *unc-84(n369)* at 15 and 20°C (Fig. 3.2C). Mutations in the shortest isoforms, *cgef-1a,c(yc109)* and *cgef-1a,c(yc110)*, also enhanced the nuclear migration defect of *unc-84(n369)* at 20°C but not at 15°C. We conclude that *cgef-1b* is dispensable for P-cell nuclear migration while *cgef-1d* and *cgef-1a,c* are necessary for nuclear migration when the LINC complex is disrupted.

We next determined the extent to which the *cgef-1a,c* and *cgef-1d* isoforms are expressed in P-cells during nuclear migration. We used previously published 5'*cis*-regulatory element reporter strains that drive nuclear GFP under control of promoters for or *cgef-1d* and *cgef-1a,c* (Ziel et al., 2009) (Fig. 3.2A) and looked for GFP expression in L1 larval P-cells, which were marked with a tdTomato nuclear marker expressed from the P-cell specific promoter of *hlh-3* (Bone et al., 2016; Chang et al., 2013). The *cgef-1d* reporter expressed GFP in larval P cells. However, the *cgef-1a,c* reporter did not express detectable GFP above background in larval P cells. Thus, *cgef-1d* appears to be the main isoform expressed in P-cells and necessary for LINC-dependent nuclear migration.

CGEF-1 activates CDC-42 during P-cell nuclear migration.

Since CGEF-1 activates the small GTPase CDC-42 in early embryogenesis (Chan & Nance, 2013; Kumfer et al., 2010), we hypothesized *cdc-42* is also necessary for P-cell nuclear

migration in the absence of *unc-84*. To test this, we knocked-down *cdc-42* specifically in larval P

cells at the time of nuclear migration using the auxin-inducible degradation (AID) system (J. Ho

et al., 2018; Zhang et al., 2015). We tagged the endogenous *cdc-42* locus with a 44-amino acid

degron using CRISPR/Cas9 engineering and expressed the TIR-1 E3 ubiquitin ligase under

control of the P-cell specific *hlh-3* promoter. This combination of tissue-specific expression of

TIR-1 and the addition of auxin during the mid-L1 larval stage, when P-cell nuclear migration

occurs, allowed for spatial and temporal control of CDC-42 protein degradation. We found that

degrading CDC-42 in otherwise wild-type L1 larvae had no effect on P-cell nuclear migration

(Fig. 3.3A). However, CDC-42 auxin-induced degradation significantly enhanced the *unc-

84(null)* nuclear migration defect at both 15 and 25°C (Fig. 3.3A-B), suggesting CDC-42 is

necessary for P-cell nuclear migration in the absence of LINC complexes.

We next tested whether *cdc-42* is in the same pathway as *cgef-1* by degrading CDC-42 in

cgef-1, unc-84 double mutants. Degradation of CDC-42 in *cgef-1(gk261), unc-84(n369)* double

mutant L1 larvae significantly enhanced the P-cell nuclear migration defects of the double

mutant alone (Fig. 3.3C-D). Because cgef-1(gk261) is a predicted null, this result suggests that

CGEF-1 and CDC-42 have partially independent roles and that other RhoGTPases or GEFs may

function during P-cell nuclear migration.

To test the roles of other small RhoGTPases, we expressed constitutively active *cdc-42,

rho-1, mig-2,* or *ced-10* (Alan et al., 2013; Gujar et al., 2019; Norris et al., 2014) to see if they

suppressed the nuclear migration defects of *cgef-1(yc3), unc-84(n369)* double mutants. When

constitutively active *cdc-42(G12V)* was expressed from an extrachromosomal array under

control of the P-cell specific *hlh-3* promoter, it was able to partially rescue the nuclear migration

defect of *cgef-1(yc3), unc-84(n369)* double mutants (Fig. 3.4A-B). However, in similar

experiments where constitutively active *rho-1(G14V), mig-2(G16V),* or *ced-10(G12V)* were expressed in P cells, none rescued the nuclear migration defect of *cgef-1(yc3), unc-84(n369)* mutants (Fig. 3.4C-E). We conclude that CGEF-1 activates CDC-42, however, it is still unclear if CGEF-1 does activate the other RhoGTPases.

Branched actin and actin-myosin networks are necessary for P-cell nuclear migration

While it is clear that CDC-42 is necessary for nuclear migration, how it functions is unclear. CDC-42 has been known to regulate many downstream effectors such as proteins that are involved in regulating cell polarity, branched-actin networks, and actomyosin contractions. CDC-42 interacts with PAR-6 and PKC-3 during polarization events in early embryogenesis (Aceto et al., 2006; Gotta et al., 2001; Rodriguez et al., 2017; Wang et al., 2017) and to regulate non-centrosomal microtubule arrays in larval epidermal epithelium (Castiglioni et al., 2020). We therefore hypothesized that CDC-42 functions through PAR-6 and PKC-3 during P-cell nuclear migration. We used the AID system to knock down PAR-6 and PKC-3 in P cells during nuclear migration (Castiglioni et al., 2020). Degradation of PAR-6 slightly enhanced the *unc-84(n369)* nuclear migration defect at 15C° but not at 20C° (Fig. 3.5A-B). However, this defect was mild compared to degrading CDC-42 in *unc-84(n369)* mutants. Furthermore, degradation of PKC-3 did not significantly enhance the nuclear migration defect of *unc-84(n369)* (Fig. 3.5C-D). Together, these data suggest that PAR-6 and PKC-3 play only minor roles in P-cell nuclear migration and that CDC-42 is functioning through an alternative pathway.

CDC-42 regulates branched-actin networks (Carlier et al., 1999; Ma et al., 1998; Rohatgi et al., 1999). To test the hypothesis that branched-actin networks function during P-cell nuclear migration, we used the AID system to degrade a component of the Arp2/3 complex. ARX-3, the *C. elegans* homolog of mammalian Arp3, is one of the seven subunits that make up the ARP2/3

complex (Sawa et al., 2003). Degradation of ARX-3 in L1 larvae at the time of P-cell nuclear migration had no defect on its own, again supporting the hypothesis that the LINC complex pathway is sufficient to move P-cell nuclei (Fig. 3.6A-B). However, degrading ARX-3 significantly enhanced the *unc-84(n369)* nuclear migration defect (Figure 3.6A-B). We conclude that the Arp2/3 complex is necessary for the movement of P-cell nuclei in the absence of LINC complexes.

We next hypothesized that myosin may be working with actin networks to exert pushing or pulling forces on P-cell nuclei. To test this hypothesis, we used the AID system by adding a degron tag onto the N terminus of the non-muscle myosin heavy chain *(nmy-2)* gene. Degradation of NMY-2 in an *unc-84(n369)* background resulted in a significantly worse nuclear-migration defect than the *unc-84(n369)* single mutant larvae (Fig. 3.6C-E). Therefore, CDC-42, ARX-3, and NMY-2 are all necessary to migrate P-cell nuclei in the absence of LINC complexes.

Discussion

In our model, there are two pathways that facilitate P-cell nuclear migration—the LINC pathway and an actin-based pathway (Fig. 3.7). For the LINC pathway, the SUN protein UNC-84 interacts with the KASH protein UNC-83 in the nuclear envelope. The cytoplasmic domain of UNC-83 interacts with microtubule motors kinesin-1 and dynein (Fridolfsson et al., 2010; Fridolfsson & Starr, 2010; Meyerzon et al., 2009). In P-cell nuclear migration, UNC-83 recruits dynein to the nuclear envelope where it is the main motor protein to pull the nucleus towards the minus ends of microtubules (Bone et al., 2016; J. Ho et al., 2018). Here, we focus on the actin-based pathway. In our model, CGEF-1D is a GEF, which activates the small GTPase CDC-42 during P-cell nuclear migration. CDC-42 then interacts with WAVE/WASP to activate the Arp2-

3 complex and nucleate branched actin. Additionally, NMY-2-induced actomyosin contractions provide force on the nucleus to help it squeeze through narrow constrictions. Whether or not CDC-42 plays a part in regulating NMY-2 in this process is unclear. There are thick actin cables along the direction of migration and some cells have actin rings on the lateral side of the cell during P-cell nuclear migration (Bone et al., 2016). While branched actin is implicated in nuclear migration, it is not clear where in the cell branched actin and actomyosin specific structures are required to move nuclei. One possibility is that branched actin could be localized at the leading edge of the nucleus to deform it as it enters the constriction. Alternatively, actin could act all around the nucleus to deform it. A third possibility is that actomyosin contractions could localize to the back of the nucleus to provide a pushing force on the nucleus in the diction of migration. Studies on mouse dendritic cells induced to migrate through fabricated constrictions show actin enrichment within the constriction during nuclear migration (Thiam et al., 2016). Actomyosin contractions also provide the force that is needed for dendritic cells to migrate through confined environments with myosin enrichment at the cell rear during contraction (Barbier et al., 2019; Lämmermann et al., 2008).

Because CDC-42 can indirectly regulate the Arp2/3 complex and NMY-2 (Gally et al., 2009; Kumfer et al., 2010; Raduwan et al., 2020; Ramesh et al., 1997; Rohatgi et al., 1999, 2000; Watson et al., 2017), further studies will need to be done to determine if CDC-42 regulates NMY-2 in this context. The roles of RhoGAPs are also not understood in P-cell nuclear migration. GAPs help localize RhoGTPase activity by inactivating them in certain areas of the cell. Furthermore, our data suggest that CGEF-1D regulates CDC-42 in addition to other RhoGTPases during nuclear migration. RHO-1 plays important roles in P-cell development. *rho-1* mutants have P-cell migration defects, but unlike in LINC complex mutants, P-cell nuclei do

not even attempt to migrate in *rho-1* mutants and the P-cells remain alive in ectopic positions on the lateral side of larvae, leading to the ectopic development of GABA neurons and pseudovulvae (Spencer et al., 2001). UNC-73 is the main GEF for RHO-1 in early larval P cells (Spencer et al., 2001).

An alternative model that involves actin structures could be nuclear actin. Nuclear actin has been shown to affect transcription, chromatin organization, and nuclear stiffness and deformation (Kelpsch & Tootle, 2018). Either cytoplasmic or nuclear actin could help prevent nuclear rupture and the resulting DNA damage. Heterochromatin also plays an important role in regulating nuclear mechanics during migration. Global chromatin condensation is required for efficient cell migration (Gerlitz, 2020). Future studies are required to precisely localize the mechanisms of how actin helps P-cell nuclei migrate through constricted spaces.
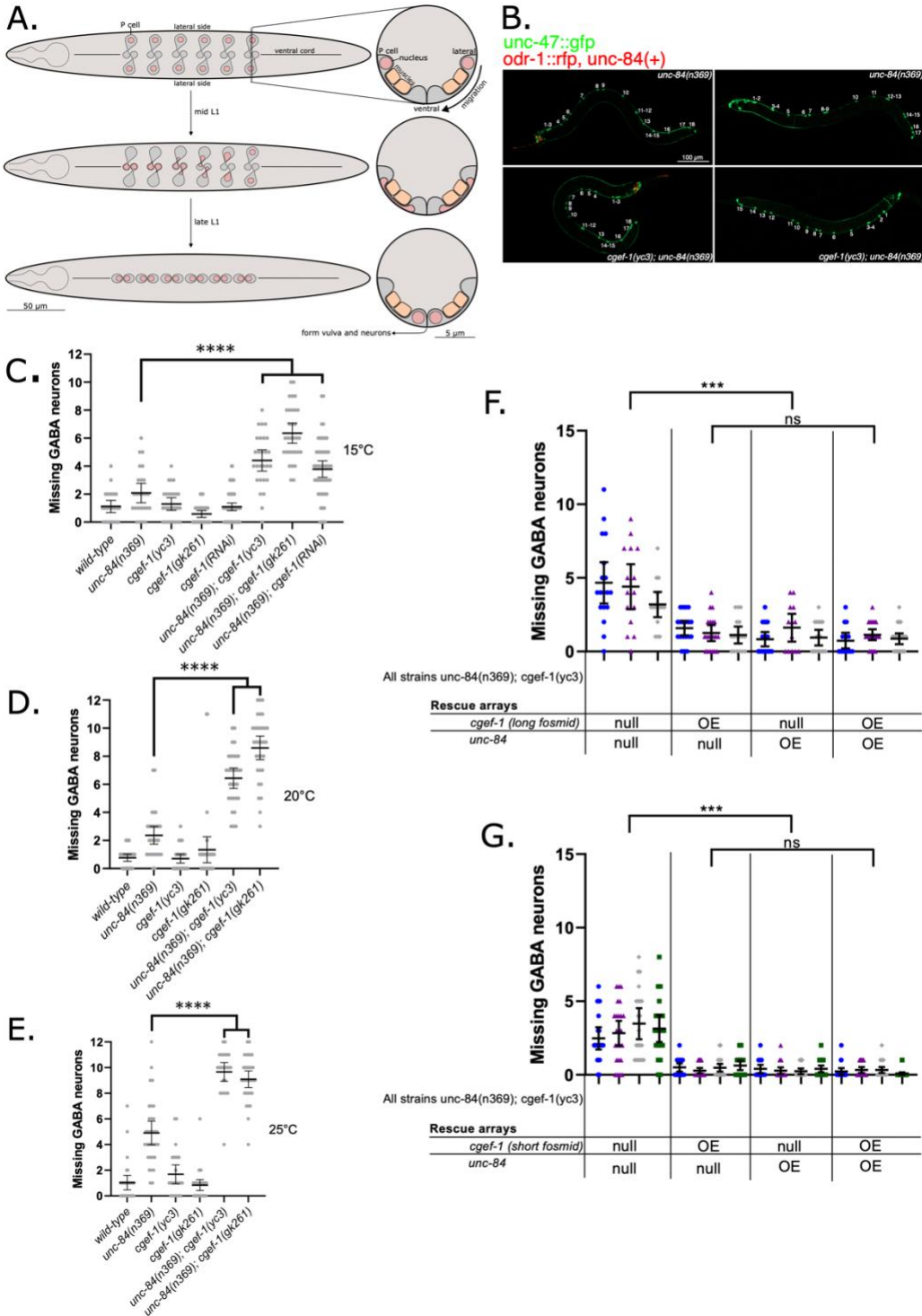
Figures

Figure 3.1

Figure 3.1. Mutations in *cgef-1* enhance the P-cell nuclear migration defect of *unc-84(null)*.
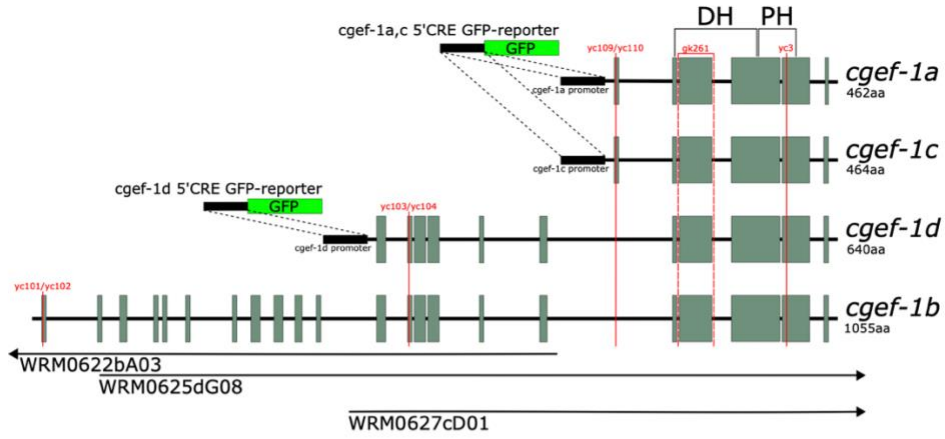
(A). Schematic of P-cell nuclear migration. On the left are ventral views of L1 larva during P-cell nuclear migration. Anterior is on the left where a pharynx is drawn. The ventral cord is marked with a line down the center of the larvae. On the right are cross sections of analogous stages with ventral down. (Top) Before the onset of P-cell nuclear migration, P cells (grey) span from the lateral to the ventral side of the worm, with the nuclei (pink circles) located laterally. The P cell is partitioned into a lateral and ventral region by a narrow constriction between body wall muscles (orange in cross section) and the cuticle. (Middle) When nuclear migration begins, P-cell nuclei migrate through the constriction towards the ventral region. This process starts with the most anterior pair of P cells and is followed by the consecutive pairs. (Bottom) P-cell nuclear migration ends when all twelve nuclei have migrated to the ventral cord.

(B). Images of L4 animals expressing *unc-47::gfp* in ventral cord GABA neurons in *unc-84(n369)* (top panels) and *unc-84(n369, cgef-1(yc3)* double mutants (bottom panels). Animals expressing an *unc-84(+)* rescue array also express *odr-1::rfp* in the head (left panels). L4 larvae are shown from the lateral side with anterior to the left and ventral down. **(C).** Number of missing GABA neurons at 15°C, **(D).** 20°C, **(E).** and 25°C of the *unc-84(n369), oxIs12(unc-47::gfp); ycEx60(odr-1::rfp,WRM0617cH07)* and *cgef-1(yc3)* single and double mutants. **(F).** Number of missing GABA neurons when both *WRM0625dG08* and *WRM0622bA03* fosmids (long fosmids) are expressed at 15°C. Each color represents an independent line with a total of three independent lines assayed for P-cell nuclear migration defects. **(G).** Number of missing GABA neurons when *WRM0627cD01* fosmid (short fosmid) is expressed at 15°C. Each color represents an independent line with a total of four independent lines assayed for P-cell nuclear migration defects. "OE" denotes overexpression of the indicated transgene. Error bars are 95%
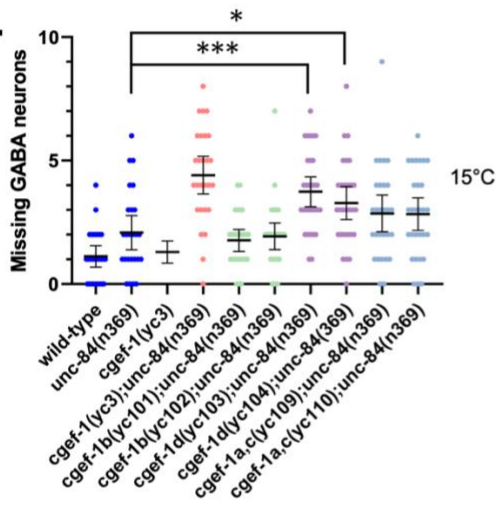
confidence intervals and statistical analysis was done using student t-tests. *** indicates a P-value < 0.001 and **** indicates a P-value < 0.0001.

Figure 3.2

A.

cgef-1a,c 5'CRE GFP-reporter

GFP

yc109/yc110

DH PH

gk261 yc3

cgef-1a promoter

cgef-1a
462aa

cgef-1c promoter

cgef-1c
464aa

cgef-1d 5'CRE GFP-reporter

GFP

yc103/yc104

cgef-1d promoter

cgef-1d
640aa

yc101/yc102

cgef-1b
1055aa

WRM0622bA03

WRM0625dG08

WRM0627cD01

B.

Missing GABA neurons

15°C

***
*

wild-type
unc-84(n369)
cgef-1(yc3)
cgef-1(yc3);unc-84(n369)
cgef-1b(yc101);unc-84(n369)
cgef-1b(yc102);unc-84(n369)
cgef-1d(yc103);unc-84(n369)
cgef-1d(yc104);unc-84(n369)
cgef-1a,c(yc109);unc-84(n369)
cgef-1a,c(yc110);unc-84(n369)

C.

Missing GABA neurons

20°C

****
****
****
***

wild-type
unc-84(n369)
cgef-1(yc3)
cgef-1(yc3);unc-84(n369)
cgef-1b(yc101);unc-84(n369)
cgef-1b(yc102);unc-84(n369)
cgef-1d(yc103);unc-84(n369)
cgef-1d(yc104);unc-84(n369)
cgef-1a,c(yc109);unc-84(n369)
cgef-1a,c(yc110);unc-84(n369)

D.

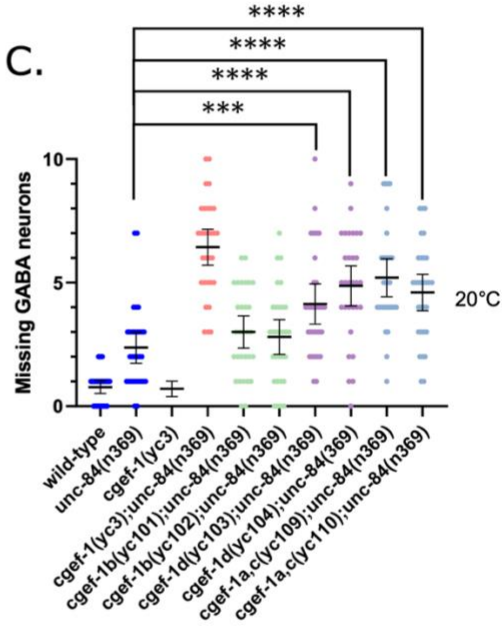5'CRE::gfp   nls::tdTomato   merge
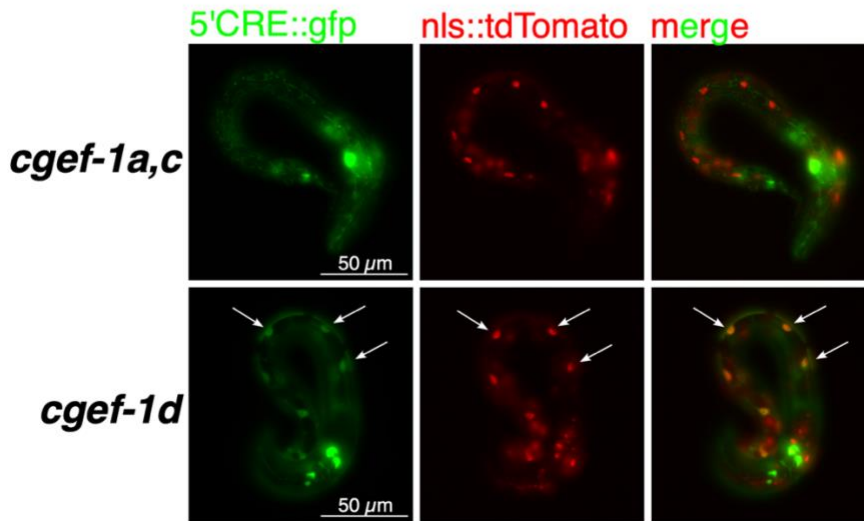
cgef-1a,c

50 μm

cgef-1d

50 μm

Figure 3.2. The *cgef-1d* isoform is required in P-cell nuclear migration

(A). Intron (black lines) and exon (green boxes) schematics for the four known *cgef-1* isoforms are shown. All isoforms share the same 3' end and that encodes Dbl homology (DH) and Pleckstrin homology (PH) domains. The red vertical lines that run perpendicular to the diagrams show where the labeled mutations are located. The regions that the *WRM0625dG08, WRM0622bA03,* and *WRM0627cD01* fosmids overlap are indicated at the bottom and the arrows indicate the fosmids continue beyond the genomic region shown in the diagram. *cgef-1a,c* and *cgef-1d* 5'*cis*-regulatory element (5'CRE) GFP-reporters are shown. These constructs were generated by using 2.5kb region upstream of each isoform transcript to drive GFP expression.

(B). Number of missing GABA neurons at 15°C and at **(C).** 20°C of *cgef-1* isoform mutations.

(D). Images of *phlh-3::nls::tdTomato* (red) and *cgef-1a,c* 5'CRE GFP-reporter (top row) and *cgef-1d* 5'CRE GFP-reporter (bottom row). White arrows indicate areas of co-localization. All error bars are 95% confidence intervals and all statistical analysis was done using student t-tests. * indicates a P-value <0.05, *** indicates a P-value < 0.001, and **** indicates a P-value < 0.0001.
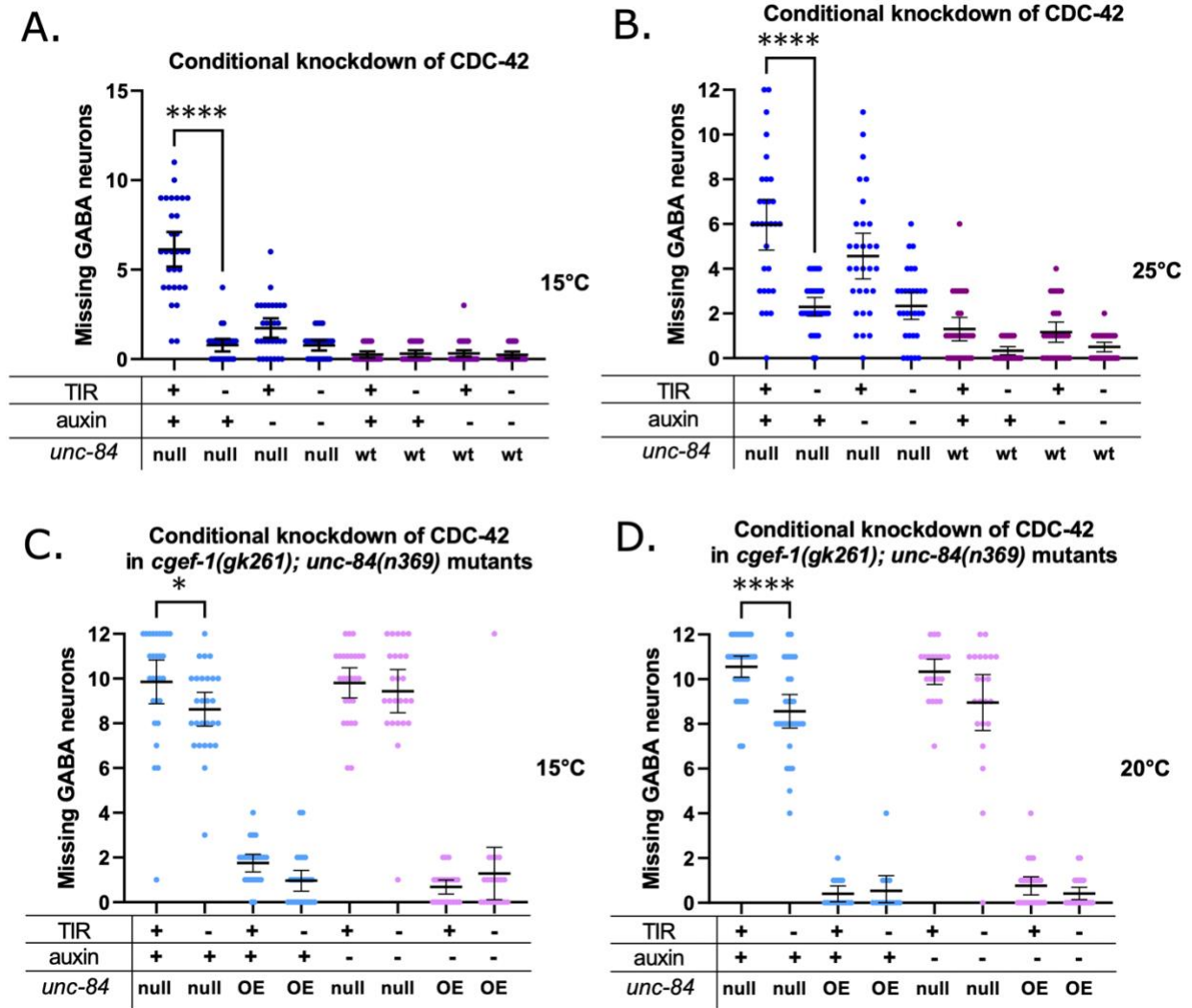
Figure 3.3

Figure 3.3: CDC-42 is necessary for P-cell nuclear migration

(A). Auxin inducible degradation (AID) system was used to knock down CDC-42 in P cells at

15C° and **(B).** 25C°. *degron::GFP11::cdc-42; unc-84(n369), oxIs12(unc-47::gfp);*

ycEx266(Pmyo-2::mCherry;phlh-3::TIR-1::mRuby) shown in blue dots and

degron::GFP11::cdc-42; oxIs12(unc-47::gfp); ycEx266(Pmyo-2::mCherry;phlh-3::TIR-

1::mRuby) shown in purple dots were treated with auxin during P-cell nuclear migration. The y-

axis shows the number of missing GABA neurons. **(C).** AID was used to knockdown CDC-42 in

P cells of *degron::GFP11::cdc-42*; *unc-84(n369), cgef-1(gk261), oxIs12(unc-47::gfp);*

ycEx300(odr-1::gfp,WRM0617cH07); ycEx266(Pmyo-2::mCherry;phlh-3::TIR-1::mRuby)

mutants at 15C° and at **(D).** 20C°. Light blue dots indicate strains that were exposed to auxin and

pink dots indicate strains that were not exposed to auxin. For all the graphs, "OE" and "null" for

unc-84 indicates *unc-84(n369)* null mutation with expression of the *unc-84* rescue array

(*ycEx60(odr-1::rfp,WRM0617cH07)*) and no expression of the rescue array, respectively. "wt"

indicates no *unc-84(n369)* mutation. All error bars are 95% confidence intervals and all

statistical analysis was done using student t-tests. **** indicates a P-value < 0.0001.

Figure 3.4

A.
Expressing constitutively active *cdc-42(G12V)* in *cgef-1(yc3); unc-84(n369)* mutants
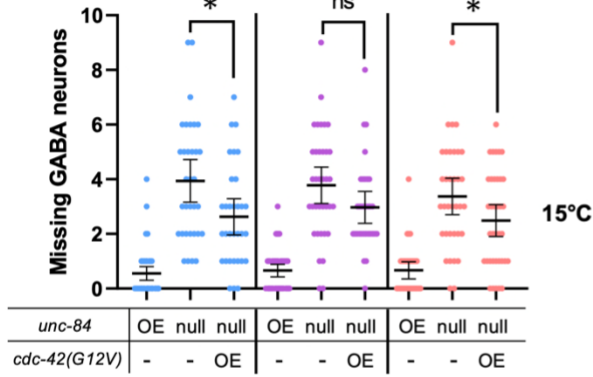
B.
Expressing constitutively active *cdc-42(G12V)* in *cgef-1(yc3); unc-84(n369)* mutants
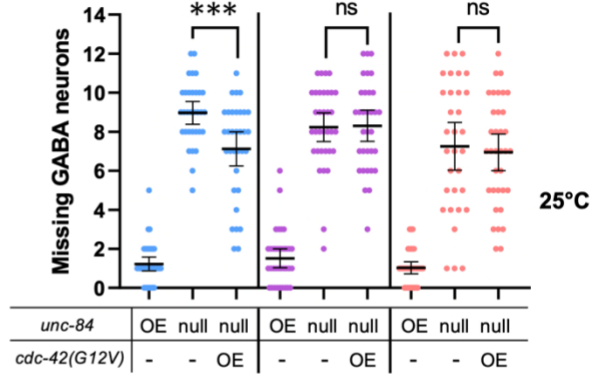
C.
Expressing constitutively active *rho-1(G14V)* in *cgef-1(yc3); unc-84(n369)* mutants
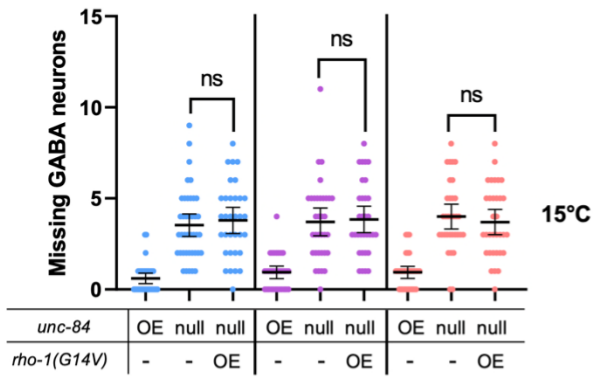
D.
Expressing constitutively active *mig-2(G16V)* in *cgef-1(yc3); unc-84(n369)* mutants
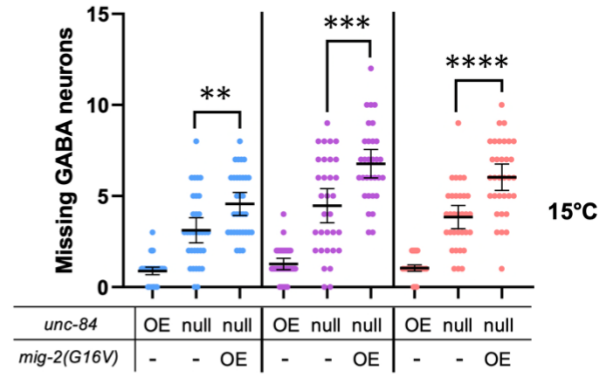
E.
Expressing constitutively active *ced-10(G12V)* in *cgef-1(yc3); unc-84(n369)* mutants
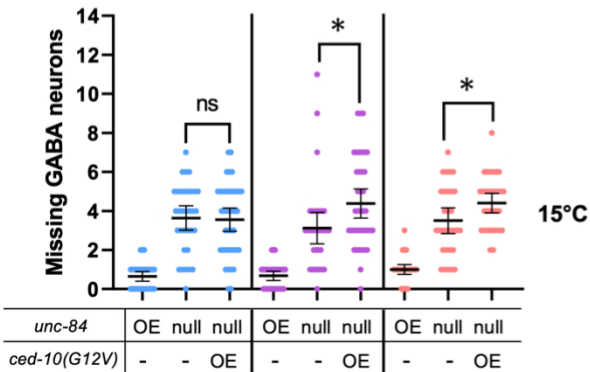
Figure 3.4: CGEF-1 activates CDC-42 during P-cell nuclear migration.

(A). *phlh-3::2xHA::cdc-42(G12V); odr-1::gfp* construct was expressed in *unc-84(n369);cgef-1(yc3);oxIs12(unc-47::gfp);ycEx60(odr-1::rfp,WRM0617cH07)* in three independent lines as indicated by the different colors. Worms were grown at 15C° and **(B).** 25C° and assayed for P-cell nuclear migration. The y-axis shows the number of missing GABA neurons. **(C).** *phlh-3::2xHA::rho-1(G14V); odr-1::gfp*, **(D).** *phlh-3::2xHA::mig-2(G16V); odr-1::gfp*, **(E).** and *phlh-3::2xHA::ced-10(G12V); odr-1::gfp* constructs were expressed in *unc-84(n369);cgef-1(yc3);oxIs12(unc-47::gfp);ycEx60(odr-1::rfp,WRM0617cH07)* in three independent lines as indicated by the different colors. Worms were grown at 15C° and assayed for P-cell nuclear migration. The y-axis shows the number of missing GABA neurons. For all the graphs, "OE" and "null" for *unc-84* indicates expression of the *unc-84* rescue array (*ycEx60(odr-1::rfp,WRM0617cH07)*) and no expression of the rescue array, respectively. "OE" for the other transgene indicate overexpression of the indicated transgene. All error bars are 95% confidence intervals and all statistical analysis was done using student t-tests. * indicates a P-value <0.05, ** indicates a P-value < 0.01, *** indicates a P-value < 0.001, and **** indicates a P-value < 0.0001.

Figure 3.5
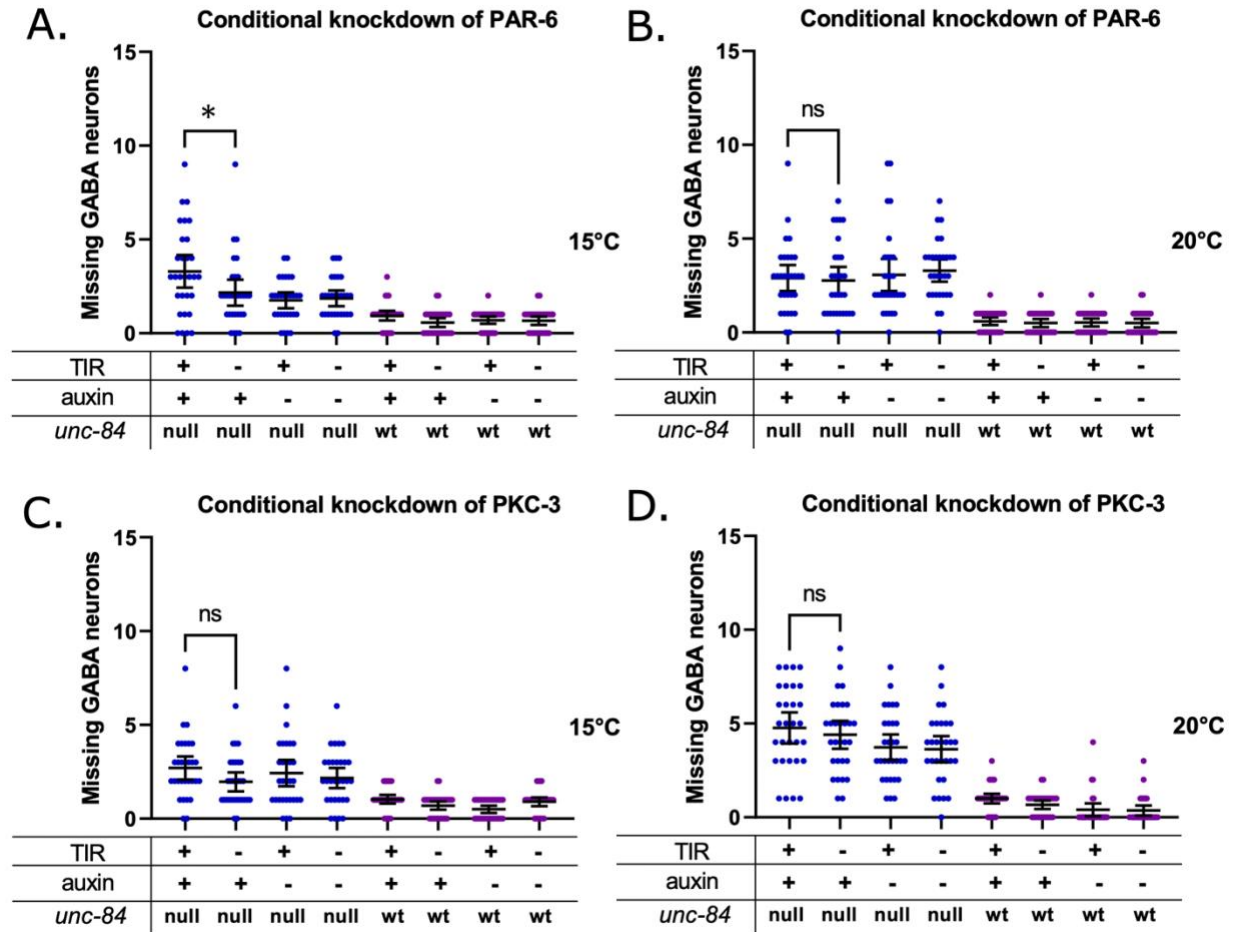
Figure 3.5: PAR-6 and PKC-3 are not involved in P-cell nuclear migration

(A). AID was used to knock down PAR-6 in P cells at 15C° and **(B).** 20C°. *par-6::degron::egfp;*
unc-84(n369), oxIs12(unc-47::gfp); ycEx266(Pmyo-2::mCherry;phlh-3::TIR-1::mRuby) shown
in blue dots and *par-6::degron::egfp; oxIs12(unc-47::gfp); ycEx266(Pmyo-2::mCherry;phlh-*
3::TIR-1::mRuby) shown in purple dots were treated with auxin during P-cell nuclear migration.
The y-axis shows the number of missing GABA neurons. **(C).** AID was used to knock down
PKC-3 in P cells at 15C° and **(D).** 20C°. *egfp::degron::pkc-3; unc-84(n369), oxIs12(unc-*
47::gfp); ycEx266(Pmyo-2::mCherry;phlh-3::TIR-1::mRuby) shown in blue dots and
egfp::degron::pkc-3; oxIs12(unc-47::gfp); ycEx266(Pmyo-2::mCherry;phlh-3::TIR-1::mRuby)

shown in purple dots were treated with auxin during P-cell nuclear migration. The y-axis shows

the number of missing GABA neurons. For all the graphs, "OE" and "null" for *unc-84* indicates

unc-84(n369) null mutation with expression of the *unc-84* rescue array (*ycEx60(odr-*

1::rfp,WRM0617cH07)) and no expression of the rescue array, respectively. "wt" indicates no

unc-84(n369) mutation. All error bars are 95% confidence intervals and all statistical analysis

was done using student t-tests. * indicates a P-value <0.05

Figure 3.6

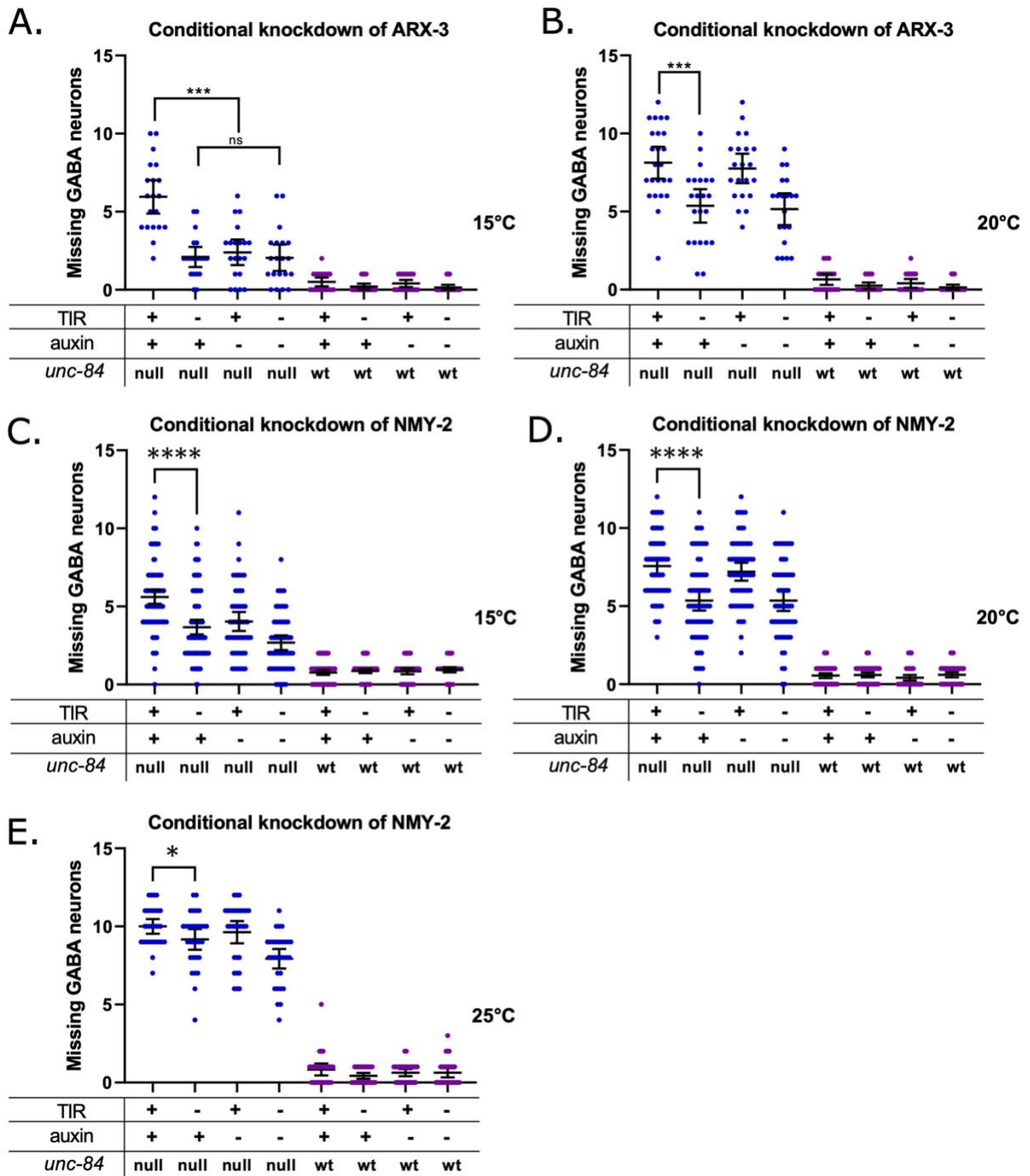**Figure 3.6: Branched actin and actin-myosin contractions are involved in P-cell nuclear migration**

(A-B). Auxin inducible degradation system was used to knock down ARX-3 in P cells at 15°C (A) or 20°C (B). *degron::arx-3; unc-84(n369), oxIs12(unc-47::gfp); ycEx253(odr-1::rfp;phlh-3::TIR-1::mRuby)* shown in blue dots and *degron::arx-3; oxIs12(unc-47::gfp); ycEx253(odr-1::rfp;phlh-3::TIR-1::mRuby)* shown in purple dots were treated with auxin during P-cell nuclear migration. The y-axis shows the number of missing GABA neurons. **(C).** Auxin inducible degradation system was used to knock down NMY-2 in P cells at 15C°, **(D).** 20C°, and **(E).** 25C°. *degron::GFP11::nmy-2; unc-84(n369), oxIs12(unc-47::gfp); ycEx266(Pmyo-2::mCherry;phlh-3::TIR-1::mRuby)* shown in blue dots and *degron::GFP11::nmy-2; oxIs12(unc-47::gfp);ycEx266(Pmyo-2::mCherry;phlh-3::TIR-1::mRuby)* shown in purple dots were treated with auxin during P-cell nuclear migration. The y-axis shows the number of missing GABA neurons. For all the graphs, "OE" and "null" for *unc-84* indicates *unc-84(n369)* null mutation with expression of the *unc-84* rescue array (*ycEx60(odr-1::rfp,WRM0617cH07)*) and no expression of the rescue array, respectively. "wt" indicates no *unc-84(n369)* mutation. All error bars are 95% confidence intervals and all statistical analysis was done using student t-tests. * indicates a P-value <0.05, *** indicates a P-value < 0.001, and **** indicates a P-value < 0.0001.

Figure 3.7

Figure 3.7: Model for both pathways involved in P-cell nuclear migration.

In the LINC complex pathway (right side of cell), UNC-84 (yellow) interacts with UNC-83 (light green) at the nuclear envelope. UNC-83 interacts with both kinesin and dynein, but uses dynein as the main microtubule motor protein to pull the nucleus towards the minus ends of microtubules (green lines). The actin-based pathway described in this paper is drawn on the left of the cell. In the inset, CGEF-1D activates CDC-42 by exchanging the nucleotide for GTP. CDC-42 in the GTP form activates WAVE/WASP, which then activates the Arp2/3 complex to

generate branched actin. CDC-42 may also be involved in indirectly activating NMY-2 (back of the nucleus) which can then induce actomyosin contractions. Branched actin functions by exerting force onto the nucleus to deform it and actomyosin contractions provide a pushing/pulling force to the nucleus to facilitate confined nuclear migration.

Materials and Methods

Table 1 (Strains)

Strain	Genotype	Reference
	Figure 1	
N2	Bristol, wild type	(Brenner, 1974)
EG1285	*oxIs12[p_{unc-47}::gfp] X*	(McIntire et al., 1997)
UD87	*unc-84(n369), oxIs12 X; ycEx60[odr-1::rfp, WRM0617cH07]*	(Chang et al., 2013)
UD279	*cgef-1(yc21), unc-84(n369), oxIs12 X; ycEx60*	(Chang et al., 2013)
UD285	*cgef-1(yc3), unc-84(n369), oxIs12 X; ycEx60*	(Chang et al., 2013)
VC506	*cgef-1(gk261) X*	(Kumfer et al., 2010)
UD923	*cgef-1(gk261), unc-84(n369), oxIs12 X; ycEx60*	This study
UD524	*cgef-1(yc3), unc-84(n369), oxIs12 X; ycEx60; ycEx250[100 ng/ul odr-1::gfp; 5 ng/ul WRM0625dG08; 5 ng/ul WRM0622bA03]*	This study
UD525	*cgef-1(yc3), unc-84(n369), oxIs12 X; ycEx60; ycEx250[100 ng/ul odr-1::gfp; 5 ng/ul WRM0625dG08; 5 ng/ul WRM0622bA03]*	This study
UD526	*cgef-1(yc3), unc-84(n369), oxIs12 X; ycEx60; ycEx250[100 ng/ul odr-1::gfp; 5 ng/ul WRM0625dG08; 5 ng/ul WRM0622bA03]*	This study
UD718	*cgef-1(yc3), unc-84(n369), oxIs12 X; ycEx60; ycEx267[100ng/uL odr-1; 5ng/uL WRM0627cD01]*	This study
UD719	*cgef-1(yc3), unc-84(n369), osIs12 X; ycEx60; ycEx268[100ng/uL odr-1; 5ng/uL WRM0627cD01]*	This study
UD720	*cgef-1(yc3), unc-84(n369), osIs12 X; ycEx60; ycEx269[100ng/uL odr-1; 5ng/uL WRM0627cD01]*	This study
UD721	*cgef-1(yc3), unc-84(n369), oxIs12 X; ycEx60; ycEx270[100ng/uL odr-1; 5ng/uL WRM0627cD01]*	This study
	Figure 2	
UD814	*cgef-1b(yc101[S14*]), unc-84(n369), oxIs12 X; ycEx60*	This study
UD815	*cgef-1b(yc102[Δ50 nt in exon 1]), unc-84(n369), oxIs12 X; ycEx60*	This study
UD818	*cgef-1d(yc103[G13*]), unc-84(n369), oxIs12 X; ycEx60*	This study
UD819	*cgef-1d(yc104[Δ49 nt in exon 2]), unc-84(n369), oxIs12 X; ycEx60*	This study

UD822	*cgef-1a,c(yc109[P6*]), unc-84(n369), oxIs12 X; ycEx60*	This study
UD823	*cgef-1a,c(yc110[Δ52 nt exon 1]), unc-84(n369), oxIs12 X; ycEx60*	This study
NK774	*qyEx116 [p$_{cgef-1b}$::GFP + unc-119(+)]*	(Ziel et al., 2009)
NK775	*qyEx117 [pcgef-1a,c::GFP + unc-119(+)].*	(Ziel et al., 2009)
UD725	*qyEx116[p$_{cgef-1b}$::GFP + unc-119(+)]; ycEx244 [odr-1::gfp; p$_{hlh-3}$::nls::tdTomato]*	This study
UD726	*qyEx117[p$_{cgef-1a,c}$::GFP + unc-119(+)]; ycEx244 [odr-1::gfp; p$_{hlh-3}$::nls::tdTomato]*	This study
Figure 3		
AFS222	*zen-4(cle10) IV*	(Farboud et al., 2019)
UD716	*cdc-42(yc100[degron::GFP11::cdc-42]) II; oxIs12 X; ycEx266[p$_{myo-2}$::mCherry; p$_{hlh-3}$::TIR-1::mRuby]*	This study
UD717	*cdc-42(yc100) II; unc-84(n369), oxIs12 X; ycEx266*	This study
UD989	*cdc-42(yc100[degron::GFP11::cdc-42]) II; cgef-1(gk261), unc-84(n369), oxIs12 X; ycEx300[odr-1::GFP, unc-84 (+)]; ycEx266[p$_{myo-2}$::mCherry; p$_{hlh-3}$::TIR-1::mRuby]*	This study
Figure 4		
UD925	*cgef-1(yc3), unc-84(n369), oxIs12 X; ycEx60; ycEx285[100ng/uL odr-1::gfp; 2ng/uL pSL884]*	This study
UD926	*cgef-1(yc3), unc-84(n369), oxIs12 X; ycEx60; ycEx286[100ng/uL odr-1::gfp; 2ng/uL pSL884]*	This study
UD927	*cgef-1(yc3), unc-84(n369), oxIs12 X; ycEx60; ycEx287[100ng/uL odr-1::gfp; 2ng/uL pSL884]*	This study
UD932	*cgef-1(yc3), unc-84(n369), oxIs12 X; ycEx60; ycEx288[100ng/uL odr-1::gfp; 2ng/uL pSL885]*	This study
UD933	*cgef-1(yc3), unc-84(n369), oxIs12 X; ycEx60; ycEx289[100ng/uL odr-1::gfp; 2ng/uL pSL885]*	This study
UD934	*cgef-1(yc3), unc-84(n369), oxIs12 X; ycEx60; ycEx290[100ng/uL odr-1::gfp; 2ng/uL pSL885]*	This study
UD935	*cgef-1(yc3), unc-84(n369), oxIs12 X; ycEx60; ycEx291[100ng/uL odr-1::gfp; 2ng/uL pSL886]*	This study
UD936	*cgef-1(yc3), unc-84(n369), oxIs12 X; ycEx60; ycEx292[100ng/uL odr-1::gfp; 2ng/uL pSL886]*	This study

UD937	*cgef-1(yc3), unc-84(n369), oxIs12 X; ycEx60; ycEx293[100ng/uL odr-1::gfp; 2ng/uL pSL886]*	This study
UD938	*cgef-1(yc3), unc-84(n369), oxIs12 X; ycEx60; ycEx294[100ng/uL odr-1::gfp; 2ng/uL pSL887]*	This study
UD939	*cgef-1(yc3), unc-84(n369), oxIs12 X; ycEx60; ycEx295[100ng/uL odr-1::gfp; 2ng/uL pSL887]*	This study
UD940	*cgef-1(yc3), unc-84(n369), oxIs12 X; ycEx60; ycEx296[100ng/uL odr-1::gfp; 2ng/uL pSL887]*	This study
Figure 5		
BOX409	*par-6(mib30[par-6::degron::egfp-loxp]) I; mibIs49[p_{wrt-2}::TIR-1::tagBFP2-Lox511::tbb-2-3'UTR, IV:5014740-5014802 (cxTi10882 site)]) IV*	(Castiglioni et al., 2020)
BOX607	*pkc-3(mib78[egfp-loxp::degron::pkc-3]) II; mibIs49[p_{wrt-2}::TIR-1::tagBFP2-Lox511::tbb-2-3'UTR, IV:5014740-5014802(cxTi10882 site)]) IV*	(Castiglioni et al., 2020)
UD829	*par-6(mib30[par-6::degron::egfp-loxp]) I; oxIs12 X; ycEx266[p_{myo-2}::mCherry; p_{hlh-3}::TIR-1::mRuby]*	This study
UD830	*par-6(mib30[par-6::degron::egfp-loxp]) I; unc-84(n369), oxIs12 X; ycEx266[p_{myo-2}::mCherry; p_{hlh-3}::TIR-1::mRuby]*	This study
UD831	*pkc-3(mib78[egfp-loxp::aid::pkc-3]) II; oxIs12 X; ycEx266[p_{myo-2}::mCherry; p_{hlh-3}::TIR-1::mRuby]*	This study
UD832	*pkc-3(mib78[egfp-loxp::aid::pkc-3]) II; unc-84(n369), oxIs12 X; ycEx266[p_{myo-2}::mCherry; p_{hlh-3}::TIR-1::mRuby]*	This study
Figure 6		
DLW29	*dpy-10, wLZ32[p_{sun-1}::TIR-1::mRuby, Cbr-unc-119(+)]; arx-3(lib7[degron::arx-3] III, unc-119(ed3))*	(Zhang et al., 2015)
UD709	*arx-3(lib7[degron::arx-3]) III; oxIs12 X; ycEx253[odr-1::rfp; p_{hlh-3}::TIR-1::mRuby]*	This study
UD710	*arx-3(lib7[degron::arx-3]) III; unc-84(n369), oxIs12 X; ycEx253[odr-1::rfp; p_{hlh-3}::TIR-1::mRuby]*	This study
UD825	*nmy-2(yc111[degron::GFP11::nmy-2]) I; oxIs12 X; ycEx266[p_{myo-2}::mCherry; p_{hlh-3}::TIR-1::mRuby]*	This study
UD826	*nmy-2(yc111[degron::GFP11::nmy-2]) I; unc-84(n369), oxIs12 X; ycEx266[p_{myo-2}::mCherry; p_{hlh-3}::TIR-1::mRuby]*	This study

Table 2 (CRISPR cRNA/Repair Templates)

New Alleles	Starting Strain	crRNA	DNA repair template [1,2]
arx-3(lib7[degron::arx-3] III	wLZ32[psun-1::TIR-1::mRuby, Cbr-unc-119(+)]	AGTTTTCAGgcgATGTCGTC	AAAGTTCCAGTGGAGAACGGGAACGCCGGACGACTTCACGAACGCCGCCGCCTCCGGGCCACCGCTTGATTTTTGGCAGGAAACCATCACGTTCTTCCGGTATGATCTCACCGGTGGCCATCCCACAACTTGTGCCTTGGCCGGAGGTTTGGCTGGATCTTTAGGCATcgcCTGAAAACTGACCTAAACTCACAAAAAAT
cdc-42 (yc100[degron::GFP11::cdc-42]) II	ASF222	ACGATCAAGTGCGTCGTCGT	taaagacgtaattttaatactttattcattttttttttcaggcgaaATGCCTAAAGATCCAGCCAAACCTCCGGCCAAGGCACAAGTTGTGGGATGGCCACCGGTGAGATCATACCGGAAGAACGTGATGGTTTCCTGCCAAAAATCAAGCGGTGGCCCGGAGGCGGCGGCGTTCGTGAAGTCAGGAGCTAGCGGAGCCAGAGATCACATGGTTCTTCATGAATATGTAAATGCAGCTGGAATTACAGGAGGTTCTGGCGGATCAGGAGCTAGCGGAGCCCAGACGATCAAGTGTGTGGTGGTGGGAGATGGAGCTGTCGGTAAAACTTGTCTCCTGATCAGCTATACCAC
cgef-1b (yc101[cgef-1b(S14*)]) X	N2	ACCATGCTGCCGTAGCAGGA	gagagtggagggcctcacgaatcgagtgtttgaaATGCAGGCGGCTCCGTCATGTTATGGCAGCATGGTAGCTTGAACATCAGAAGAAGTCACAACATCCACATTATCGCGGGGACCAATGACCAT
cgef-1d (yc103[cgef-1d(G13* exon 2)]) X	N2	CGAGTTGATGAGATCTTCTC	gaacatttttgcagGAAGAAGTTGAAGCCTCGCGAAATCTCAAAAAAGCTTGAGAAGATCTTATCAACTCGAATGAAGCCGAGgtgaacaagacaacaaaatgactttcttg
cgef-1a,c (yc109[cgef-1a,c(P6*)]) X	N2	AGGTTCCTGTCGTTCCGGCG	acctaccagcaactctggagcaccagaccgcttttATGAAGCGAACACTTTAAAGGTTCCTGTCGTTCCGGCGCTCAAAGCGTAGGCTCATCACTTCAGTATC
nmy-2 (yc111[degron::GFP11::nmy-2]) I	AFS222	GATGATGTCATtattaccgc	ccgccttttattccatttaactttcagctaattgattacaacaacagctccagcggtaataATGCCTAAAGATCCAGCCAAACCTCCGGCCAAGGCACAAGTTGTGGGATGGCCACCGGTGAGATCATACCGGAAGAACGTGATGGTTTCCTGCCAAAAATCAAGCGGTGGCCCGGAGGCGGCGGCGTTCGTGAAGTCAGGAGCTAGCGGAGCCAGAGATCACATGGTTCTTCATGAATATGTAAATGCAGCTGGAATTACAGGAGGTTCTGGCGGATCAGGAGCTAGCGGAGCCACATCATCTCGACAAAAAGATGATGAGATTGACCAATTGAGAgtatgtttcttcaaat

72

zen-4(cle10) IV	AFS222	UGAUGGA AGCUAAC UACCAG	GACCATCTTCAACTCTTCTTACTATGATTC GCCAATACATGATGGAAGCAGACTACCAG CGAGTAGAGATTGCACGTCTCAAAGATTC TCTAAACGACAAGGATG
cgef-1b(yc102[cgef-1b(D50 nt in exon1)]) X	N2	ACCATGCT GCCGTAGC AGGA	**CTGCTACGGCAGCATGGTTGCTAGCAC ATCAGAAGAAGTCACAACATCCA**
cgef-1d(yc104[cgef-1d(D49 nt in exon 2)]) X	N2	CGAGTTGA TGAGATCT TCTC	**GAAGATCTCATCAACTCGAATGAAGCC GAGgtgaacaagacaacaaaat**
cgef-1a,c(yc110[cgef-1a,c(D52 nt in exon 1)) X	N2	AGGTTCCT GTCGTTCC GGCG	**TCCAAGGTTCCTGTCGTTCCGGCGCTCA AAGCGTAGGCTCATCACTTCAGTA**

[1] Lowercase letters indicate nucleotides in intronic regions and uppercase letters indicate

nucleotides in the coding regions.

[2] Bolded letters indicate nucleotides in deleted region

Table 3 (Reagents)

Reagent Type	Name	Source or reference	Additional Information
Escherichia. coli	OP50	Caenorhabditis Genetics Center (CGC)	
Recombinant DNA reagent	pSL619	(Chang et al., 2013)	p$_{hlh-3}$::nls::tdTOMATO
Recombinant DNA reagent	pSL814	(J. Ho et al., 2018)	p$_{hlh-3}$::TIR-1::mRuby
Recombinant DNA reagent	pSL830	This paper	p$_{hlh-3}$::GFP(1-10)
Recombinant DNA reagent	pSL884	This paper	p$_{hlh-3}$::2xHA::cdc-42(G12V)
Recombinant DNA reagent	pSL885	This paper	p$_{hlh-3}$::2xHA::mig-2(G16V)
Recombinant DNA reagent	pSL886	This paper	p$_{hlh-3}$::2xHA::ced-10(G12V)
Recombinant DNA reagent	pSL887	This paper	p$_{hlh-3}$::2xHA::rho-1(G14V)
Recombinant DNA reagent	pLZ31	(Zhang et al., 2015)	p$_{eft-3}$::TIR-1::mRuby

Recombinant DNA reagent	pEL298	(Alan et al., 2013)	p_{osm-6}::cdc-42(G12V)::GFP
Recombinant DNA reagent	pEL656	(Norris et al., 2014)	p_{unc-25}::mig-2(G16V)::GFP
Recombinant DNA reagent	pEL777	(Norris et al., 2014)	p_{unc-25}::ced-10(G12V)::GFP
Recombinant DNA reagent	pEL1021	(Gujar et al., 2019)	p_{unc-25}::rho-1(G14V)::GFP

Table 4 (Primers)

Primer	Gene	Purpose	Sequence
DLO689	*arx-3*	Forward primer to amplify degron::arx-3. Use with ods2402.	AGGCTTCTCCAACGTACC
DLO690	*arx-3*	Reverse primer to amplify degron::arx-3. Use with ods2401.	CGATTAAAGCGGACGAGC
ods2450	*unc-84*	Forward primer to amplify region of unc-84 that contains n369 mutation. Use with ods2451.	CAGACCATACGCAACCAACTACAC
ods2451	*unc-84*	Reverse primer to amplify region of unc-84 that contains n369 mutation. To be used with ods2450.	CCGGTTGCGAATGAGAGCTGTAC
ods2669	*cgef-1*	Forward primer to sequence yc3 mutation. Use with ods2670.	GCGTCAGCAATCCAGGAACTAC
ods2670	*cgef-1*	Reverse primer to sequence yc3 mutation. Use with ods2669.	CTTGCGTCGTCTGTGTATTCCC
ods2803	*cgef-1b*	Amplify region in cgef-1b that contains early stop codon. Use with ods2804.	CGAGCACCGAGGAGTCTTG
ods2804	*cgef-1b*	Amplify region in cgef-1b that contains early stop codon. Use with ods2803.	GATTACGCGGCGATGTCTTC
ods2805	*cgef-1d*	Amplify region in cgef-1d with early stop codon. Use with ods2806.	CTCGAAACCTCTCAAGCGC
ods2806	*cgef-1d*	Amplify region in cgef-1d with early stop codon. Use with ods2805.	GTTTAAGACAATCGCCTCGACG
ods2807	*par-6*	Screen for par-6::degron::egfp. Use with ods2808 to identify the construct and with ods2809 to identify the WT.	GACCGTCACAACAAGGAACAC
ods2808	*par-6*	Screen for par-6::degron::egfp. Use with ods2807.	CATTGGACTCCGTAAGTGAAGG
ods2809	*par-6*	Screen for WT par-6 to differentiate from par-6::degron::egfp. Use with ods2807.	GTGTGTGTGGTTTTAGCGAG

ods2810	*pkc-3*	Screen for egfp::degron::pkc-3. Use with ods2811 to screen for egfp::degron::pkc-3.	GGCCGACAAGCAAA AGAACG
ods2811	*pkc-3*	Screen for egfp::degron::pkc-3. Use with ods2810 to screen for egfp::degron::pkc-3 and with ods2812 to screen for WT.	CTCACCTGTCCTTGA AACCTCG
ods2812	*pkc-3*	Screen for WT pkc-3 to differentiate from egfp::degron::pkc-3. Use with ods2811.	GCATCGTCGTCCTGT ACAGTG
ods2827	*cdc-42*	Forward primer to amplify degron::GFP11::cdc-42. Use with ods2828.	GTGTGCGTGCACATT TATGTGACTCATCC
ods2828	*cdc-42*	Reverse primer to amplify degron::GFP11::cdc-42. Use with ods2827.	CCTAATGTGTATGGC TCGCCACCGATC
ods2861	*cgef-1a,c*	Forward primer to screen for cgef-1a,c premature stop mutation. Use with ods2862.	GCGGTCCAGTCAAA CTGAC
ods2862	*cgef-1a,c*	Reverse primer to screen for cgef-1a,c premature stop codon. Use with ods2861.	CGCGCAGACTAGTG CAAC
ods2864	*nmy-2*	Forward primer to screen for degron::GFP11::nmy-2. Use with ods2865.	CAGATGGGACAAGC AGATTAC
ods2865	*nmy-2*	Reverse primer to screen for degron::GFP11::nmy-2. Use with ods2864.	GAGGAAGTCTGTCT TGGCc
ods3136	*cgef-1d*	Forward primer to screen for cgef-1d split-GFP11. Forward primer to screen for cgef-1d split-GFP11 on N-terminus.	CATTCATCGCAGATT TTCCTCGG
ods3137	*cgef-1d*	Reverse primer to screen for cgef-1d split-GFP11. Reverse primer to screen for cgef-1d split-GFP11 on N-terminus.	CGCCTTCTGCGTATT GTCTGTG
ods3154	*cdc-42*	Forward primer to clone cdc-42(G12V) from pEL298 from the Lundquist Lab into pSL830 under the hlh-3 promoter. ~20bp overlaps. Use with ods3155. Forward primer to clone cdc-42(G12V) under hlh-3 promoter.	CCTTGCTTGGAGGGT ACCCCATGCAGACG ATCAAGTGCGTC
ods3155	*cdc-42*	Reverse primer to clone cdc-42(G12V) from pEL298 from the Lundquist Lab into pSL830 under the hlh-3 promoter. ~20bp overlaps. Use with ods3154. Reverse primer to clone cdc-42(G12V) under hlh-3 promoter.	GTTGGAATTCCTACT TCACTCTAGAGAAT ATTGCACTTCTTC
ods3156	*rac-1/ced-10*	Forward primer to clone rac-1/ced-10(G12V) from pEL777 from the Lundquist Lab into pSL830 under the hlh-3 promoter. ~20bp overlaps. Use with ods3157. Forward primer to clone ced-10(G12V) under hlh-3 promoter.	CCTTGCTTGGAGGGT ACCCCATGCAAGCG ATCAAATGTGTC

ods3157	*rac-1/ced-10*	Reverse primer to clone rac-1/ced-10(G12V) from pEL777 from the Lundquist Lab into pSL830 under the hlh-3 promoter. ~20bp overlaps. Use with ods3156. Reverse primer to clone ced-10(G12V) under hlh-3 promoter.	GTTGGAATTCCTACT TCACTTTAGAGCACC GTACACTTGC
ods3158	*mig-2*	Forward primer to clone mig-2(G16V) from pEL656 from the Lundquist Lab into pSL830 under the hlh-3 promoter. ~20bp overlaps. Use with ods3159. Forward primer to clone mig-2(G16V) under hlh-3 promoter.	CCTTGCTTGGAGGGT ACCCCATGTCTTCAC CGTCGAGGCAG
ods3159	*mig-2*	Reverse primer to clone mig-2(G16V) from pEL656 from the Lundquist Lab into pSL830 under the hlh-3 promoter. ~20bp overlaps. Use with ods3158. Reverse primer to clone mig-2(G16V) under hlh-3 promoter.	GTTGGAATTCCTACT TCACTTTACATAATA TTGCAAGACTTC
ods3160	*rho-1*	Forward primer to clone rho-1(G14V) from pEL1021 from the Lundquist Lab into pSL830 under the hlh-3 promoter. ~20bp overlaps. Use with ods3161. Forward primer to clone rho-1(G14V) under hlh-3 promoter.	CCTTGCTTGGAGGGT ACCCCATGGCTGCG ATTAGAAAGAAG
ods3161	*rho-1*	Reverse primer to clone rho-1(G14V) from pEL1021 from the Lundquist Lab into pSL830 under the hlh-3 promoter. ~20bp overlaps. Use with ods3160. Reverse primer to clone rho-1(G14V) under hlh-3 promoter.	GTTGGAATTCCTACT TCACTTTACAAAATC ATGCACTTGC
ods3162	*cdc-42*	Forward primer to clone HA-HA-cdc-42(G12V) from pEL298 from the Lundquist Lab into pSL830 under the hlh-3 promoter. ~20bp overlaps. Use with ods3155. Forward primer to clone HA-HA-cdc-42(G12V) under hlh-3 promoter.	CCTTGCTTGGAGGGT ACCCCATGTACCCAT ATGATGTCCCGGATT ACGCTTACCCATATG ATGTCCCGGATTAC GCTGGATCAGGATC ACAGACGATCAAGT GCGTCGTC
ods3163	*rac-1/ced-10*	Forward primer to clone HA-HA-rac-1/ced-10(G12V) from pEL777 from the Lundquist Lab into pSL830 under the hlh-3 promoter. ~20bp overlaps. Use with ods3157. Forward primer to clone HA-HA-ced-10(G12V) under hlh-3 promoter.	CCTTGCTTGGAGGGT ACCCCATGTACCCAT ATGATGTCCCGGATT ACGCTTACCCATATG ATGTCCCGGATTAC GCTGGATCAGGATC ACAAGCGATCAAAT GTGTCGTC
ods3164	*mig-2*	Forward primer to clone HA-HA-mig-2(G16V) from pEL656 from the Lundquist Lab into pSL830 under the hlh-3 promoter. ~20bp	CCTTGCTTGGAGGGT ACCCCATGTACCCAT ATGATGTCCCGGATT

		overlaps. Use with ods3158. Reverse primer to clone HA-HA-mig-2(G16V) under hlh-3 promoter.	ACGCTTACCCATATG ATGTCCCGGATTAC GCTGGATCAGGATC ATCTTCACCGTCGAG GCAGATC
ods3165	*rho-1*	Forward primer to clone HA-HA-rho-1(G14V) from pEL1021 from the Lundquist Lab into pSL830 under the hlh-3 promoter. ~20bp overlaps. Use with ods3160. Reverse primer to clone HA-HA-rho-1(G14V) under hlh-3 promoter.	CCTTGCTTGGAGGGT ACCCCATGTACCCAT ATGATGTCCCGGATT ACGCTTACCCATATG ATGTCCCGGATTAC GCTGGATCAGGATC AGCTGCGATTAGAA AGAAGTTG

Whole-genome sequencing of strains from the *enhancer of the nuclear migration defect of unc-84* screen

Strains carrying the *yc3*, *yc15*, *yc16*, *yc18*, *yc20*, and *yc21* alleles were previously isolated as described from a chemical mutagenesis screen for *enhancers of the nuclear migration defect of unc-84 (emu)*. We collected genomic DNA from each homozygous mutant strain for whole-genome sequencing to identify candidate lesions underlying the nuclear migration phenotypes. Genomic DNA preps were made with the Qiagen DNeasy Blood and Tissue kit as previously described (Herrera & Starr, 2018). Genomic DNA was fragmented and made into libraries for Illumina HiSeq2500 sequencing by the Functional Genomics Laboratory at UC Berkeley. RAPID Sequencing where 150 bp PE reads were generated. We processed raw reads using the default settings of the CloudMap pipeline for Galaxy (Minevich et al., 2012). For each mutant line, we generated a list of variants that did not match the reference N2 genome. We excluded variants found in common between mutant lines as they were likely to be variants present in our starting strain used for the mutagenic screen (Doitsidou et al., 2016). We focused on early stop codon mutations that were present in just one or two of the six sequenced strains and identified a single nucleotide polymorphism (SNP) in the *yc3* and *yc21* strains but not the other four

sequenced strains. The SNP was predicted to cause an early stop codon in *cgef-1*. No other unique mutations predicted to cause stop codons were identified in the six strains.

C. elegans **strains and genetics**

C. elegans animals were grown on NGM plates seeded with OP50 at their specified temperatures (Brenner, 1974). Some *C. elegans* strains used in this study were provided by the Caenorhabditis Genetics Center (CGC) which is funded by the National Institutes of Health Office of Research Infrastructure Programs (P40OD010440). The strains used in this study are described in Table 1.

For the cgef-1 RNAi experiments, clone X-2A03 from the Ahringer RNAi library (Source Bioscience) (Kamath et al., 2003) was used to create dsRNA *in vitro*, which was then injected into UD87 as described (Chang et al., 2013; Fire et al., 1998).

Fosmids used in the *cgef-1* rescue experiments were from the *C. elegans* Fosmid Library (Source BioScience) and were amplified in bacteria using CopyControl Induction Solution (Lucigen, #CCIS125) and purified using a DNA midi prep kit (Thermo Scientific, #K0481). Fosmid injection mixes contained 5 ng/µl of each indicated fosmid and 100 ng/µl of *odr-1::gfp* plasmid (L'Etoile & Bargmann, 2000) and were injected into UD285.

CRISPR/Cas9 gene editing

cgef-1 isoform mutants were generated using *dpy-10* as a co-CRISPR marker (Arribere et al., 2014; Paix et al., 2015, 2017). The CRISPR injection mix was generated as described (Hao et al., 2021). The same guides were used to create the deletion mutations of each isoforms but without the addition of the repair templates. Deletion mutations were screened by amplifying the region around the guide and PCR products that show a lower band size were sent in for sanger sequencing.

All crRNA and ssODN repair templates are listed in Table 2. Degron and GFP11 insertions for *cdc-42* and *nmy-2* were generated by using *zen-4(+)* as a co-CRISPR marker (Farboud et al., 2019). Single stranded repair templates for insertions contained 50nt homology arms (Genewiz). The CRISPR injection mix contained 0.084 µl *zen-4* crRNA (0.6mM), 0.21 µl target gene crRNA (0.6mM), 1.033 µl tracr (0.17mM), 4.39 µl Cas9 (40µM), 0.28 µl ssODN *zen-4(+)* repair template (500ng/µl), and 4 µl ssDNA repair template (500 ng/µl). Injection mix was injected into germline of temperature sensitive *zen-4(cle10)* mutant young adults and screened as described (Farboud et al., 2019).

An auxin-induced degron was inserted to the 5' end of *arx-3*, replacing the native start codon. No linker sequence was used. The tag was inserted with a ssDNA oligo (Table 2). A *dpy-10* co-CRISPR strategy was used to identify successful injections and CRISPR repair activity (Arribere et al., 2014). The strain wLZ32[p_{sun-1}::TIR-1::mRuby, Cbr-unc-119(+)] an unnamed strain from Abby Dernburg that expresses single copy TIR1 in the germline, was used for injections. Protein Cas9 and synthetic RNA was generated by IDT.

Cloning constitutively active constructs

To generate plasmid pSL884 (*p_{hlh-3}::2xHA::cdc-42(G12V)::unc-54 3'UTR*), the *cdc-42(G12V)* open reading frame was amplified from pEL298 (Alan et al., 2013) with homology arms to add a 2xHA tag after the *cdc-42* start codon. To generate plasmid pSL885 (*p_{hlh-3}::2xHA::mig-2(G16V)::unc-54 3'UTR*), the *mig-2(G16V)* open reading frame was amplified from pEL656 (Norris et al., 2014) with homology arms to add a 2xHA tag after the *mig-2* start codon. To generate plasmid pSL886 (*p_{hlh-3}::2xHA::ced-10(G12V)::unc-54 3'UTR*), the *ced-10(G12V)* open reading frame was amplified from pEL777 (Norris et al., 2014) with homology arms to add a 2xHA tag after the *ced-10* start codon. To generate plasmid pSL887 (*p_{hlh-}*

3::2xHA::rho-1(G14V)::unc-54 3'UTR), the *rho-1(G14V)* open reading frame was amplified

from pEL1021 (Gujar et al., 2019) with homology arms to add a 2xHA tag after the *rho-1* start

codon. The backbone of pSL830 including the promoter of *hlh-3* and the *unc-54 3'UTR* was

amplified, and the HiFi DNA Assembly Cloning Kit (New England Biolabs) was used to

assemble pSL884, pSL885, pSL886, and pSL887. Injection mixes containing 2 ng/μl of a

plasmid encoding a constitutively active construct and 100 ng/μl of plasmid *odr-1::gfp* (L'Etoile

& Bargmann, 2000) as a co-injection marker were injected into UD285. A list of plasmids for

transgenic constructs are listed in Table 3.

P-cell nuclear migration assay

For the P-cell nuclear migration assays, *oxIs12[p_{unc-47}::gfp]* transgenic worms (EG1285)

were used as the wild type control (McIntire et al., 1997). *oxIs12* was used as a reporter for P-

cell derived GABA neurons to assay for P-cell nuclear migration defects. L4 animals were

mounted onto 2% agarose slides in 1mM tetramisole solution. Slides were viewed using a wide-

field epifluorescent Leica DM6000 microscope and a 63x Plan Apo 1.40 NA objective. UNC-

47::GFP-positive GABA neurons were counted in the ventral cord. Neurons normally outside the

ventral cord in the nerve ring and the most posterior neuron in the tail are not decedents of P

cells and were not counted. 19 GABA neurons (12 derived from P cells) were scored for each

animal as described (Fridolfsson et al., 2018).

Synchronization and auxin assay

We synchronized *C. elegans* larvae in the mid L1 stage at approximately the time of P-

cell nuclear migration for the auxin experiments. 50-100 L4s were picked and grown at 20°C for

24-48 hours so that animals reached the adult stage. Adult animals were transferred onto a fresh

NGM plate and allowed to lay eggs at 20°C for 1 hour. After 1 hour, the adult animals were removed, leaving synchronized embryos behind.

Conditional knock-down of proteins of interest was done using the auxin-inducible degradation system (Zhang et al., 2015). TIR-1 was amplified from plasmid pLZ31 (Zhang et al., 2015) (Addgene #71720) and cloned under control of the *hlh-3* promoter in pSL780 (Bone et al., 2016) with Gibson cloning (New England Biolabs) to generate pSL814. pSL814 was injected with *odr-1::rfp* to make the extrachromosomal arrays in strains UD709 and UD710. pSL814 was injected with $p_{myo-2}::mCherry$ to make the extrachromosomal arrays in strains UD716, UD717, UD825, UD826.

Synchronized L1 animals were washed off normal NGM plates with distilled water approximately two hours before P-cell nuclear migration began. Next, the L1 larvae were transferred to NGM+auxin plates with 1 mM 3-indoleacetic acid (IAA; Sigma #I2886) and kept in the dark. After P-cell nuclear migration was completed, the L1 larvae were washed off the NGM+auxin plates with M9 buffer and transferred to an NGM plate. For experiments done at 15°C, embryos were left on the plates to develop for 29 hours and then the resulting L1s were washed onto NGM + auxin plates and left to develop for 8 hours before being washed off onto NGM plates without auxin to develop to the L4 stage. For experiments done at 20°C, embryos developed into L1s on NGM plates for 18 hours and placed on NGM with auxin plates for 7 hours. For experiments done at 25°C, embryos developed into L1s for 12 hours and then placed on NGM with auxin plates for 6 hours. These timings were determined by using the marker $p_{hlh-3}::nls::tdTOMATO$ (pSL619) to visualize P-cell nuclei throughout development. Once animals reached the L4 stage, the number of UNC-47::GFP marked GABA neurons were quantified.

To synchronize *C. elegans* for imaging, 3-5 plates of gravid animals were bleached and eggs were pelleted and resuspended in M9 solution for 12-16 hours at room temperature on a rocker. After starvation, L1s were plated onto NGM plates seeded with OP50 and grown at room temperature for 12 hours. After 12 hours, L1s were washed off the plates with M9 and mounted onto 2% agarose slides with 1mM tetramisole solution.

Microscopy Imaging

Images were taken on a Zeiss LSM 980 with Airyscan using 20x objective and the Zeiss Zen Blue software which was provided by the MCB light imaging microscopy core and by NIH grant S10OD026702.

Statistical Analysis

Graphs of GABA neuron counts were created by using Prism (version 9). Student t-test was used to determine statistical significance. Error bars are 95% confidence intervals.

References

Aceto, D., Beers, M., & Kemphues, K. J. (2006). Interaction of PAR-6 with CDC-42 is required for maintenance but not establishment of PAR asymmetry in C. elegans. *Developmental Biology*, *299*(2), 386–397. PubMed. https://doi.org/10.1016/j.ydbio.2006.08.002

Alan, J. K., Struckhoff, E. C., & Lundquist, E. A. (2013). Multiple cytoskeletal pathways and PI3K signaling mediate CDC-42-induced neuronal protrusion in C. elegans. *Small GTPases*, *4*(4), 208–220. https://doi.org/10.4161/sgtp.26602

Arribere, J. A., Bell, R. T., Fu, B. X. H., Artiles, K. L., Hartman, P. S., & Fire, A. Z. (2014). Efficient Marker-Free Recovery of Custom Genetic Modifications with CRISPR/Cas9 in Caenorhabditis elegans. *Genetics*, *198*(3), 837–846. https://doi.org/10.1534/genetics.114.169730

Barbier, L., Sáez, P. J., Attia, R., Lennon-Duménil, A.-M., Lavi, I., Piel, M., & Vargas, P. (2019). Myosin II Activity Is Selectively Needed for Migration in Highly Confined Microenvironments in Mature Dendritic Cells. *Frontiers in Immunology*, *10*. https://www.frontiersin.org/articles/10.3389/fimmu.2019.00747

Bell, E. S., Shah, P., Zuela-Sopilniak, N., Kim, D., Varlet, A.-A., Morival, J. L. P., McGregor, A. L., Isermann, P., Davidson, P. M., Elacqua, J. J., Lakins, J. N., Vahdat, L., Weaver, V. M., Smolka, M. B., Span, P. N., & Lammerding, J. (2022). Low lamin A levels enhance confined cell migration and metastatic capacity in breast cancer. *Oncogene*, *41*(36), 4211–4230. https://doi.org/10.1038/s41388-022-02420-9

Bone, C. R., Chang, Y.-T., Cain, N. E., Murphy, S. P., & Starr, D. A. (2016). Nuclei migrate through constricted spaces using microtubule motors and actin networks in C. elegans hypodermal cells. *Development*, *143*(22), 4193–4202. https://doi.org/10.1242/dev.141192

Bone, C. R., & Starr, D. A. (2016). Nuclear migration events throughout development. *Journal of Cell Science*, *129*(10), 1951–1961. https://doi.org/10.1242/jcs.179788

Brenner, S. (1974). THE GENETICS OF CAENORHABDITIS ELEGANS. *Genetics*, *77*(1), 71–94. https://doi.org/10.1093/genetics/77.1.71

C. elegans Deletion Mutant Consortium. (2012). Large-scale screening for targeted knockouts in the Caenorhabditis elegans genome. *G3 (Bethesda, Md.)*, *2*(11), 1415–1425. PubMed. https://doi.org/10.1534/g3.112.003830

Carlier, M.-F., Ducruix, A., & Pantaloni, D. (1999). Signalling to actin: The Cdc42-N-WASP-Arp2/3 connection. *Chemistry & Biology*, *6*(9), R235–R240. https://doi.org/10.1016/S1074-5521(99)80107-0

Castiglioni, V. G., Pires, H. R., Rosas Bertolini, R., Riga, A., Kerver, J., & Boxem, M. (2020). Epidermal PAR-6 and PKC-3 are essential for larval development of C. elegans and organize non-centrosomal microtubules. *ELife*, *9*, e62067. https://doi.org/10.7554/eLife.62067

Chan, E., & Nance, J. (2013). Mechanisms of CDC-42 activation during contact-induced cell polarization. *Journal of Cell Science*, *126*(7), 1692–1702. https://doi.org/10.1242/jcs.124594

Chang, Y.-T., Dranow, D., Kuhn, J., Meyerzon, M., Ngo, M., Ratner, D., Warltier, K., & Starr, D. A. (2013). Toca-1 Is in a Novel Pathway That Functions in Parallel with a SUN-KASH Nuclear Envelope Bridge to Move Nuclei in Caenorhabditis elegans. *Genetics*, *193*(1), 187–200. https://doi.org/10.1534/genetics.112.146589

Cox, E. A., & Hardin, J. (2004). Sticky worms: Adhesion complexes in C. elegans. *Journal of Cell Science*, *117*(10), 1885–1897. https://doi.org/10.1242/jcs.01176

Davidson, P. M., Denais, C., Bakshi, M. C., & Lammerding, J. (2014). Nuclear Deformability Constitutes a Rate-Limiting Step During Cell Migration in 3-D Environments. *Cellular and Molecular Bioengineering*, *7*(3), 293–306. https://doi.org/10.1007/s12195-014-0342-y

Davidson, P. M., Sliz, J., Isermann, P., Denais, C., & Lammerding, J. (2015). Design of a microfluidic device to quantify dynamic intra-nuclear deformation during cell migration through confining environments. *Integrative Biology*, *7*(12), 1534–1546. https://doi.org/10.1039/c5ib00200a

Denais, C. M., Gilbert, R. M., Isermann, P., McGregor, A. L., te Lindert, M., Weigelin, B., Davidson, P. M., Friedl, P., Wolf, K., & Lammerding, J. (2016). Nuclear envelope rupture and repair during cancer cell migration. *Science*, *352*(6283), 353–358. https://doi.org/10.1126/science.aad7297

Doitsidou, M., Jarriault, S., & Poole, R. J. (2016). Next-Generation Sequencing-Based Approaches for Mutation Mapping and Identification in Caenorhabditis elegans. *Genetics*, *204*(2), 451–474. https://doi.org/10.1534/genetics.115.186197

Etienne-Manneville, S. (2004). Cdc42—The centre of polarity. *Journal of Cell Science*, *117*(8), 1291–1300. https://doi.org/10.1242/jcs.01115

Farboud, B., Severson, A. F., & Meyer, B. J. (2019). Strategies for Efficient Genome Editing Using CRISPR-Cas9. *Genetics*, *211*(2), 431–457. https://doi.org/10.1534/genetics.118.301775

Fire, A., Xu, S., Montgomery, M. K., Kostas, S. A., Driver, S. E., & Mello, C. C. (1998). Potent and specific genetic interference by double-stranded RNA in Caenorhabditis elegans. *Nature*, *391*(6669), 806–811. https://doi.org/10.1038/35888

Francis, R., & Waterston, R. H. (1991). Muscle cell attachment in Caenorhabditis elegans. *Journal of Cell Biology*, *114*(3), 465–479. https://doi.org/10.1083/jcb.114.3.465

Fricke, R., Gohl, C., Dharmalingam, E., Grevelhörster, A., Zahedi, B., Harden, N., Kessels, M., Qualmann, B., & Bogdan, S. (2009). Drosophila Cip4/Toca-1 Integrates Membrane Trafficking and Actin Dynamics through WASP and SCAR/WAVE. *Current Biology*, *19*(17), 1429–1437. https://doi.org/10.1016/j.cub.2009.07.058

Fridolfsson, H. N., Herrera, L. A., Brandt, J. N., Cain, N. E., Hermann, G. J., & Starr, D. A. (2018). Genetic Analysis of Nuclear Migration and Anchorage to Study LINC Complexes

During Development of Caenorhabditis elegans. *Methods in Molecular Biology (Clifton, N.J.)*, *1840*, 163–180. PubMed. https://doi.org/10.1007/978-1-4939-8691-0_13

Fridolfsson, H. N., Ly, N., Meyerzon, M., & Starr, D. A. (2010). UNC-83 coordinates kinesin-1 and dynein activities at the nuclear envelope during nuclear migration. *Developmental Biology*, *338*(2), 237–250. https://doi.org/10.1016/j.ydbio.2009.12.004

Fridolfsson, H. N., & Starr, D. A. (2010). Kinesin-1 and dynein at the nuclear envelope mediate the bidirectional migrations of nuclei. *The Journal of Cell Biology*, *191*(1), 115–128. PubMed. https://doi.org/10.1083/jcb.201004118

Friedl, P., Wolf, K., & Lammerding, J. (2011). Nuclear mechanics during cell migration. *Cell Structure and Dynamics*, *23*(1), 55–64. https://doi.org/10.1016/j.ceb.2010.10.015

Fu, Y., Chin, L. K., Bourouina, T., Liu, A. Q., & VanDongen, A. M. J. (2012). Nuclear deformation during breast cancer cell transmigration. *Lab on a Chip*, *12*(19), 3774–3778. https://doi.org/10.1039/C2LC40477J

Gally, C., Wissler, F., Zahreddine, H., Quintin, S., Landmann, F., & Labouesse, M. (2009). Myosin II regulation during C. elegans embryonic elongation:LET-502/ROCK, MRCK-1 and PAK-1, three kinases with different roles. *Development*, *136*(18), 3109–3119. https://doi.org/10.1242/dev.039412

Gerlitz, G. (2020). The Emerging Roles of Heterochromatin in Cell Migration. *Frontiers in Cell and Developmental Biology*, *8*. https://www.frontiersin.org/articles/10.3389/fcell.2020.00394

Giuliani, C., Troglio, F., Bai, Z., Patel, F. B., Zucconi, A., Malabarba, M. G., Disanza, A., Stradal, T. B., Cassata, G., Confalonieri, S., Hardin, J. D., Soto, M. C., Grant, B. D., & Scita, G. (2009). Requirements for F-BAR Proteins TOCA-1 and TOCA-2 in Actin Dynamics and Membrane Trafficking during Caenorhabditis elegans Oocyte Growth and Embryonic Epidermal Morphogenesis. *PLOS Genetics*, *5*(10), e1000675. https://doi.org/10.1371/journal.pgen.1000675

Gotta, M., Abraham, M. C., & Ahringer, J. (2001). CDC-42 controls early cell polarity and spindle orientation in C. elegans. *Current Biology*, *11*(7), 482–488. https://doi.org/10.1016/S0960-9822(01)00142-7

Gujar, M. R., Stricker, A. M., & Lundquist, E. A. (2019). RHO-1 and the Rho GEF RHGF-1 interact with UNC-6/Netrin signaling to regulate growth cone protrusion and microtubule organization in Caenorhabditis elegans. *PLOS Genetics*, *15*(6), e1007960. https://doi.org/10.1371/journal.pgen.1007960

Hall, A. (1998). Rho GTPases and the Actin Cytoskeleton. *Science*, *279*(5350), 509–514. https://doi.org/10.1126/science.279.5350.509

Hao, H., Kalra, S., Jameson, L. E., Guerrero, L. A., Cain, N. E., Bolivar, J., & Starr, D. A. (2021). The Nesprin-1/-2 ortholog ANC-1 regulates organelle positioning in C. elegans independently from its KASH or actin-binding domains. *ELife*, *10*, e61069. https://doi.org/10.7554/eLife.61069

Herrera, L. A., & Starr, D. A. (2018). The E3 Ubiquitin Ligase MIB-1 Is Necessary To Form the Nuclear Halo in Caenorhabditis elegans Sperm. *G3 (Bethesda, Md.)*, *8*(7), 2465–2470. PubMed. https://doi.org/10.1534/g3.118.200426

Ho, H.-Y. H., Rohatgi, R., Lebensohn, A. M., Le Ma, Li, J., Gygi, S. P., & Kirschner, M. W. (2004). Toca-1 Mediates Cdc42-Dependent Actin Nucleation by Activating the N-WASP-WIP Complex. *Cell*, *118*(2), 203–216. https://doi.org/10.1016/j.cell.2004.06.027

Ho, J., Venecia A. Valdez, Ma, L., & Starr, D. A. (2018). *Characterizing Dynein's Role in P-cell Nuclear Migration using an Auxin-Induced Degradation System*. https://doi.org/10.17912/W2W96J

Horvitz, H. R., & Sulston, J. E. (1980). ISOLATION AND GENETIC CHARACTERIZATION OF CELL-LINEAGE MUTANTS OF THE NEMATODE CAENORHABDITIS ELEGANS. *Genetics*, *96*(2), 435–454. https://doi.org/10.1093/genetics/96.2.435

Kalukula, Y., Stephens, A. D., Lammerding, J., & Gabriele, S. (2022). Mechanics and functional consequences of nuclear deformations. *Nature Reviews. Molecular Cell Biology*, *23*(9), 583–602. PubMed. https://doi.org/10.1038/s41580-022-00480-z

Kamath, R. S., Fraser, A. G., Dong, Y., Poulin, G., Durbin, R., Gotta, M., Kanapin, A., Le Bot, N., Moreno, S., Sohrmann, M., Welchman, D. P., Zipperlen, P., & Ahringer, J. (2003). Systematic functional analysis of the Caenorhabditis elegans genome using RNAi. *Nature*, *421*(6920), 231–237. https://doi.org/10.1038/nature01278

Kelpsch, D. J., & Tootle, T. L. (2018). Nuclear Actin: From Discovery to Function. *Anatomical Record (Hoboken, N.J. : 2007)*, *301*(12), 1999–2013. PubMed. https://doi.org/10.1002/ar.23959

Kengaku, M. (2018). Cytoskeletal control of nuclear migration in neurons and non-neuronal cells. *Proceedings of the Japan Academy. Series B, Physical and Biological Sciences*, *94*(9), 337–349. PubMed. https://doi.org/10.2183/pjab.94.022

Kumfer, K. T., Cook, S. J., Squirrell, J. M., Eliceiri, K. W., Peel, N., O'Connell, K. F., & White, J. G. (2010). CGEF-1 and CHIN-1 Regulate CDC-42 Activity during Asymmetric Division in the Caenorhabditis elegans Embryo. *Molecular Biology of the Cell*, *21*(2), 266–277. https://doi.org/10.1091/mbc.e09-01-0060

Lämmermann, T., Bader, B. L., Monkley, S. J., Worbs, T., Wedlich-Söldner, R., Hirsch, K., Keller, M., Förster, R., Critchley, D. R., Fässler, R., & Sixt, M. (2008). Rapid leukocyte migration by integrin-independent flowing and squeezing. *Nature*, *453*(7191), 51–55. https://doi.org/10.1038/nature06887

Lawson, C. D., & Ridley, A. J. (2017). Rho GTPase signaling complexes in cell migration and invasion. *Journal of Cell Biology*, *217*(2), 447–457. https://doi.org/10.1083/jcb.201612069

L'Etoile, N. D., & Bargmann, C. I. (2000). Olfaction and Odor Discrimination Are Mediated by the C. elegans Guanylyl Cyclase ODR-1. *Neuron*, *25*(3), 575–586. https://doi.org/10.1016/S0896-6273(00)81061-2

Liu, J., Zhang, X., Cheng, Y., & Cao, X. (2021). Dendritic cell migration in inflammation and immunity. *Cellular & Molecular Immunology*, *18*(11), 2461–2471. https://doi.org/10.1038/s41423-021-00726-4

Luxton, G., Gomes, E., Folker, E., Vintinner, E., & Gundersen, G. (2010). Linear Arrays of Nuclear Envelope Proteins Harness Retrograde Actin Flow for Nuclear Movement. *Science (New York, N.Y.)*, *329*, 956–959. https://doi.org/10.1126/science.1189072

Ma, L., Rohatgi, R., & Kirschner, M. W. (1998). The Arp2/3 complex mediates actin polymerization induced by the small GTP-binding protein Cdc42. *Proceedings of the National Academy of Sciences*, *95*(26), 15362–15367. https://doi.org/10.1073/pnas.95.26.15362

Malone, C. J., Fixsen, W. D., Horvitz, H. R., & Han, M. (1999). UNC-84 localizes to the nuclear envelope and is required for nuclear migration and anchoring during C. elegans development. *Development*, *126*(14), 3171–3181. https://doi.org/10.1242/dev.126.14.3171

McGee, M. D., Rillo, R., Anderson, A. S., & Starr, D. A. (2006). UNC-83 Is a KASH Protein Required for Nuclear Migration and Is Recruited to the Outer Nuclear Membrane by a Physical Interaction with the SUN Protein UNC-84. *Molecular Biology of the Cell*, *17*(4), 1790–1801. https://doi.org/10.1091/mbc.e05-09-0894

McIntire, S. L., Reimer, R. J., Schuske, K., Edwards, R. H., & Jorgensen, E. M. (1997). Identification and characterization of the vesicular GABA transporter. *Nature*, *389*(6653), 870–876. https://doi.org/10.1038/39908

Meyerzon, M., Fridolfsson, H. N., Ly, N., McNally, F. J., & Starr, D. A. (2009). UNC-83 is a nuclear-specific cargo adaptor for kinesin-1-mediated nuclear migration. *Development*, *136*(16), 2725–2733. https://doi.org/10.1242/dev.038596

Minevich, G., Park, D. S., Blankenberg, D., Poole, R. J., & Hobert, O. (2012). CloudMap: A Cloud-Based Pipeline for Analysis of Mutant Genome Sequences. *Genetics*, *192*(4), 1249–1269. https://doi.org/10.1534/genetics.112.144204

Norris, A. D., Sundararajan, L., Morgan, D. E., Roberts, Z. J., & Lundquist, E. A. (2014). The UNC-6/Netrin receptors UNC-40/DCC and UNC-5 inhibit growth cone filopodial protrusion via UNC-73/Trio, Rac-like GTPases and UNC-33/CRMP. *Development*, *141*(22), 4395–4405. https://doi.org/10.1242/dev.110437

Paix, A., Folkmann, A., Rasoloson, D., & Seydoux, G. (2015). High Efficiency, Homology-Directed Genome Editing in Caenorhabditis elegans Using CRISPR-Cas9 Ribonucleoprotein Complexes. *Genetics*, *201*(1), 47–54. https://doi.org/10.1534/genetics.115.179382

Paix, A., Folkmann, A., & Seydoux, G. (2017). Precision genome editing using CRISPR-Cas9 and linear repair templates in C. elegans. *CRISPR-Cas Systems for Genome Engineering and Investigation*, *121–122*, 86–93. https://doi.org/10.1016/j.ymeth.2017.03.023

Raab, M., Gentili, M., de Belly, H., Thiam, H.-R., Vargas, P., Jimenez, A. J., Lautenschlaeger, F., Voituriez, R., Lennon-Duménil, A.-M., Manel, N., & Piel, M. (2016). ESCRT III repairs

nuclear envelope ruptures during cell migration to limit DNA damage and cell death. *Science*, *352*(6283), 359–362. https://doi.org/10.1126/science.aad7611

Raduwan, H., Sasidharan, S., Burgos, L. C., Wallace, A. G., & Soto, M. C. (2020). RhoGAP RGA-8 supports morphogenesis in C. elegans by polarizing epithelia. *Biology Open*, *9*(11), bio056911. https://doi.org/10.1242/bio.056911

Raftopoulou, M., & Hall, A. (2004). Cell migration: Rho GTPases lead the way. *Developmental Biology*, *265*(1), 23–32. https://doi.org/10.1016/j.ydbio.2003.06.003

Ramesh, N., Antón, I. M., Hartwig, J. H., & Geha, R. S. (1997). WIP, a protein associated with Wiskott–Aldrich syndrome protein, induces actin polymerization and redistribution in lymphoid cells. *Proceedings of the National Academy of Sciences*, *94*(26), 14671–14676. https://doi.org/10.1073/pnas.94.26.14671

Reiner, D. J., & Lundquist, E. A. (2018). Small GTPases. *WormBook : The Online Review of C. Elegans Biology*, *2018*, 1–65. PubMed. https://doi.org/10.1895/wormbook.1.67.2

Renkawitz, J., Kopf, A., Stopp, J., de Vries, I., Driscoll, M. K., Merrin, J., Hauschild, R., Welf, E. S., Danuser, G., Fiolka, R., & Sixt, M. (2019). Nuclear positioning facilitates amoeboid migration along the path of least resistance. *Nature*, *568*(7753), 546–550. https://doi.org/10.1038/s41586-019-1087-5

Ridley, A. J. (2015). Rho GTPase signalling in cell migration. *Cell Adhesion and Migration*, *36*, 103–112. https://doi.org/10.1016/j.ceb.2015.08.005

Rodriguez, J., Peglion, F., Martin, J., Hubatsch, L., Reich, J., Hirani, N., Gubieda, A. G., Roffey, J., Fernandes, A. R., St Johnston, D., Ahringer, J., & Goehring, N. W. (2017). aPKC Cycles between Functionally Distinct PAR Protein Assemblies to Drive Cell Polarity. *Developmental Cell*, *42*(4), 400-415.e9. https://doi.org/10.1016/j.devcel.2017.07.007

Rohatgi, R., Ho, H. H., & Kirschner, M. W. (2000). Mechanism of N-Wasp Activation by Cdc42 and Phosphatidylinositol 4,5-Bisphosphate. *Journal of Cell Biology*, *150*(6), 1299–1310. https://doi.org/10.1083/jcb.150.6.1299

Rohatgi, R., Ma, L., Miki, H., Lopez, M., Kirchhausen, T., Takenawa, T., & Kirschner, M. W. (1999). The Interaction between N-WASP and the Arp2/3 Complex Links Cdc42-Dependent Signals to Actin Assembly. *Cell*, *97*(2), 221–231. https://doi.org/10.1016/S0092-8674(00)80732-1

Rossman, K. L., Der, C. J., & Sondek, J. (2005). GEF means go: Turning on RHO GTPases with guanine nucleotide-exchange factors. *Nature Reviews Molecular Cell Biology*, *6*(2), 167–180. https://doi.org/10.1038/nrm1587

Salvermoser, M., Begandt, D., Alon, R., & Walzog, B. (2018). Nuclear Deformation During Neutrophil Migration at Sites of Inflammation. *Frontiers in Immunology*, *9*, 2680–2680. PubMed. https://doi.org/10.3389/fimmu.2018.02680

Sawa, M., Suetsugu, S., Sugimoto, A., Miki, H., Yamamoto, M., & Takenawa, T. (2003). Essential role of the C. elegans Arp2/3 complex in cell migration during ventral enclosure. *Journal of Cell Science*, *116*(8), 1505–1518. https://doi.org/10.1242/jcs.00362

Schmidt, A., & Hall, A. (2002). Guanine nucleotide exchange factors for Rho GTPases: Turning on the switch. *Genes & Development*, *16*(13), 1587–1609. https://doi.org/10.1101/gad.1003302

Spencer, A. G., Orita, S., Malone, C. J., & Han, M. (2001). A RHO GTPase-mediated pathway is required during P cell migration in Caenorhabditis elegans. *Proceedings of the National Academy of Sciences*, *98*(23), 13132–13137. https://doi.org/10.1073/pnas.241504098

Starr, D. A., & Fridolfsson, H. N. (2010). Interactions Between Nuclei and the Cytoskeleton Are Mediated by SUN-KASH Nuclear-Envelope Bridges. *Annual Review of Cell and Developmental Biology*, *26*(1), 421–444. https://doi.org/10.1146/annurev-cellbio-100109-104037

Starr, D. A., Hermann, G. J., Malone, C. J., Fixsen, W., Priess, J. R., Horvitz, H. R., & Han, M. (2001). Unc-83 encodes a novel component of the nuclear envelope and is essential for proper nuclear migration. *Development*, *128*(24), 5039–5050. https://doi.org/10.1242/dev.128.24.5039

Stephens, A. D., Liu, P. Z., Banigan, E. J., Almassalha, L. M., Backman, V., Adam, S. A., Goldman, R. D., & Marko, J. F. (2018). Chromatin histone modifications and rigidity affect nuclear morphology independent of lamins. *Molecular Biology of the Cell*, *29*(2), 220–233. https://doi.org/10.1091/mbc.E17-06-0410

Sulston, J. E., & Horvitz, H. R. (1977). Post-embryonic cell lineages of the nematode, Caenorhabditis elegans. *Developmental Biology*, *56*(1), 110–156. https://doi.org/10.1016/0012-1606(77)90158-0

Sulston, J. E., & Horvitz, H. R. (1981). Abnormal cell lineages in mutants of the nematode Caenorhabditis elegans. *Developmental Biology*, *82*(1), 41–55. https://doi.org/10.1016/0012-1606(81)90427-9

Swift, J., Ivanovska, I. L., Buxboim, A., Harada, T., Dingal, P. C. D. P., Pinter, J., Pajerowski, J. D., Spinler, K. R., Shin, J.-W., Tewari, M., Rehfeldt, F., Speicher, D. W., & Discher, D. E. (2013). Nuclear Lamin-A Scales with Tissue Stiffness and Enhances Matrix-Directed Differentiation. *Science*, *341*(6149), 1240104. https://doi.org/10.1126/science.1240104

Thiam, H.-R., Vargas, P., Carpi, N., Crespo, C. L., Raab, M., Terriac, E., King, M. C., Jacobelli, J., Alberts, A. S., Stradal, T., Lennon-Dumenil, A.-M., & Piel, M. (2016). Perinuclear Arp2/3-driven actin polymerization enables nuclear deformation to facilitate cell migration through complex environments. *Nature Communications*, *7*(1), 10997. https://doi.org/10.1038/ncomms10997

Wang, S.-C., Low, T. Y. F., Nishimura, Y., Gole, L., Yu, W., & Motegi, F. (2017). Cortical forces and CDC-42 control clustering of PAR proteins for Caenorhabditis elegans embryonic polarization. *Nature Cell Biology*, *19*(8), 988–995. https://doi.org/10.1038/ncb3577

Watson, J. R., Owen, D., & Mott, H. R. (2017). Cdc42 in actin dynamics: An ordered pathway governed by complex equilibria and directional effector handover. *Small GTPases*, *8*(4), 237–244. PubMed. https://doi.org/10.1080/21541248.2016.1215657

Wolf, K., te Lindert, M., Krause, M., Alexander, S., te Riet, J., Willis, A. L., Hoffman, R. M., Figdor, C. G., Weiss, S. J., & Friedl, P. (2013). Physical limits of cell migration: Control by ECM space and nuclear deformation and tuning by proteolysis and traction force. *Journal of Cell Biology*, *201*(7), 1069–1084. https://doi.org/10.1083/jcb.201210152

Zhang, L., Ward, J. D., Cheng, Z., & Dernburg, A. F. (2015). The auxin-inducible degradation (AID) system enables versatile conditional protein depletion in C. elegans. *Development*, *142*(24), 4374–4384. https://doi.org/10.1242/dev.129635

Zhu, R., Liu, C., & Gundersen, G. G. (2018). Nuclear positioning in migrating fibroblasts. *Seminars in Cell & Developmental Biology*, *82*, 41–50. PubMed. https://doi.org/10.1016/j.semcdb.2017.11.006

Ziel, J. W., Matus, D. Q., & Sherwood, D. R. (2009). An expression screen for RhoGEF genes involved in C. elegans gonadogenesis. *Gene Expression Patterns*, *9*(6), 397–403. https://doi.org/10.1016/j.gep.2009.06.005

Chapter V

<u>Future Directions</u>

Overview

    As a whole, this dissertation conveys the significance of using *C. elegans* P cells as an *in vivo* model to study nuclear migration. This dissertation, along with previous data from our lab, showed that microtubule and actin structures facilitate nuclear migration. Because there is high conservation between *C. elegans* proteins and mammalian proteins, these studies help further our understanding of confined nuclear migration which is important in the function of immune cells and metastatic cancer cells. In this final Chapter, I will discuss future experiments to advance our knowledge of nuclear migration *in vivo*.

Observe microtubule and actin dynamics during nuclear migration

    P-cell nuclear migration is a highly dynamic process and valuable information can be obtained from being able to visual this process as it occurs. We know that during nuclear migration, microtubules are polarized in the direction of migration with the nuclei migrating towards the minus end of microtubules (Bone et al., 2016; Ho et al., 2018). We have also observed actin bundles behind the nucleus and actin fibers oriented in the direction of migration in the constriction (Ma et al., in preparation). However, these images were taken from animals that were immobilized between an agarose pad and a coverslip, which causes stress for the animals and make them more likely to halt P-cell nuclear migration. Therefore, we have not been able to observe microtubule or actin dynamics during active P-cell nuclear migration. The main struggle with live imaging of this process is that the animals are sensitive to constant pressure, require a food source in order to be imaged over a longer period of time, and L1s do not respond as efficiently to paralytics such as tetramisole as their adult counterparts. With the emergence of microfluidic devices, it is becoming easier to overcome these challenges.

The first microfluidic device that we tried to use was from the company vivoVerse Inc. (formerly Newormics). This device has channels that are small enough to hold L1-L2 stage animals in the same orientation by applying constant pressure (Gokce et al., 2017). While this chip was able to immobilize animals without the use of paralytics, the constant pressure and lack of food source prevented the animals from undergoing nuclear migration. The second microfluidic device that we tried also has channels that can fit L1-L2 stage animals, provides a food source, and allows us to apply pressure only during imaging through the use of a hydraulic valve (Figure 4.1) (Berger et al., 2021). Another advantage of this device is worms can be loaded into the chip hours beforehand and allowed to grow and develop in the device, instead of having to load the animals right before imaging which usually stresses the animals causing them to halt nuclear migration. A disadvantage to this device is not all the animals are oriented in the same direction and animals that are facing away from the food source may arrest and go into daur stage and not undergo nuclear migration. Despite the disadvantages, our lab has been able to capture time-lapse videos of P-cell nuclear migration using this microfluidic device (Figure 4.2). While further optimization will be required, this device will finally allow the lab to capture videos of P-cell nuclear migration.

An area of interest in our lab is determining why mutations in microtubule and actin regulators in the absence of the LINC complex lead to temperature sensitive phenotypes of P-cell nuclear migration. Using the microfluidic device, we can film microtubule and actin dynamics at different temperature to determine if the cytoskeletal structures different from temperature to temperature. A hypothesis for why we see a temperature sensitive phenotype is because some cytoskeletal structures may be either more dynamic or more stable at different temperatures. When the LINC complex is disrupted and animals are grown at 20°C, there is a P-cell nuclear

migration defect. However, this defect is suppressed at 15°C. Perhaps microtubules networks play a more prominent role at 20°C because they are more stable at higher temperatures. Alternatively, actin structures, which seem to be involved in suppressing the defect of LINC mutants at lower temperatures, may be more stable at lower temperatures and more dynamic at higher temperatures. Tagging microtubule components and actin components and observing microtubule and actin dynamics at different temperatures will reveal how these cytoskeletal structures change during this process. Additionally, because both microtubule and actin structures are involved in nuclear migration, it's possible that one pathway may regulate the other. Perhaps disrupting microtubule structures make actin structures more stable and therefore actin is able to suppress the nuclear migration defect in the absence of LINC. In addition to imaging *wild-type* animals, we can image *unc-84(n369)* null mutants and ARX-3/NMY-2 knockdown mutants and observe how microtubule and actin structures are affected.

Observe nuclear migration kinetics

We also would be interested in measuring kinetics of nuclear migration. Another hypothesis for why we see this temperature sensitive phenotype is the nucleus migrates slower at lower temperatures and thus allows more time for cytoskeletal structures to act upon it. While the whole process of nuclear migration takes a longer time to complete at lower temperatures, it is unclear if the rate of nuclear migration is slower or if cytoskeletal structures take a longer time to polarize and orient at lower temperatures. If the rate of nuclear migration is slower, *unc-84(n369)* induced defects may be suppressed at lower temperatures because actin structures are either more stable at lower temperatures or slower rate of nuclear migration allows actin structures more time to act on the nucleus. By this logic, the nucleus migrates faster at higher temperature and actin structures are unstable and unable to polarize quickly enough to efficiently facilitate

nuclear migration. With the microfluidic chip, we can inject a P-cell nuclear marker *into wild-type*, *unc-84(n369)* mutant, ARX-3 knockdown mutant, and the NMY-2 knockdown mutants in order to measure the rate of nuclear migration.

Observe movement of protein localization

Our model for P-cell nuclear migration contains multiple microtubule and actin regulators. In Chapter II and III, I talked about the importance of DHC-1, CGEF-1D, CDC-42, ARX-3(Arp2/3), and NMY-2 in P-cell nuclear migration. While there is a lot of data that allows us to genetically determine if these genes function in the same or different pathway, we are lacking in data that tell us the mechanisms of how these proteins function during this process. In order to probe how these proteins function, we need to first determine where these proteins localize throughout the duration of P-cell nuclear migration.

I initially used the split-GFP method where I endogenously tagged CGEF-1D, CDC-42, and NMY-2 with the eleventh beta strand of GFP and then express GFP1-10 on an extrachromosomal array under the control of a P-cell specific promoter (Cabantous et al., 2005; Hefel & Smolikove, 2019; Noma et al., 2017). Unfortunately, overexpression of GFP1-10 alone led to significant GFP signal that is much brighter than background fluorescence signal, which is an issue that has been seen in other systems (Feng et al., 2017). Because of the tissue-specific advantage of the split-GFP method in imaging proteins that are expressed throughout the body, it is still worth it to optimize this method moving forward. There are several ways we can improve this system. First, there have been success in increasing the fluorescence ratio of the protein interests and background fluorescence by endogenously adding multiple, tandem GFP11 tags (He et al., 2019; Hefel & Smolikove, 2019). This can improve fluorescence signal of proteins that are expressed too low for detection with just one fluorescent tag. Another method to improve

the signal to noise ratio is by using split-mNeonGreen2(mNG) as the fluorescent tag instead of split-GFP. The brightness of mNG has been reported to be two times brighter than split-GFP (Cranfill et al., 2016). Additionally, while expression of GFP1-10 in mammalian cells has been reported to fluoresce at a level higher than background signal, expression of split-mNG2 alone does not show above background level signals (Feng et al., 2017). Another way around overexpression of GFP1-10 is by inserting a single copy of the construct at an endogenous locus (Goudeau et al., 2021; Hefel & Smolikove, 2019). There are several methods to achieve this such as Mos1-mediated Single Copy Insertion (mosSCI) or by using Flp recombinase-mediated cassette exchange (RMCE) (Frøkjaer-Jensen et al., 2008; Nonet, 2020). These methods will allow us to generate lines of tissue-specific expression of GFP1-10 which can also be a powerful tool for the *C. elegans* field.

Once we are able to optimize the split-fluorescent protein method, we can observe localization of CGEF-1D, CDC-42, Arp2/3 complex and NMY-2 over the duration of P-cell nuclear migration with the use of the microfluidic device. As mentioned in Chapter III, it is likely that CGEF-1D functions by activating CDC-42 instead of the other Rho GTPases so I would expect colocalization of CGEF-1D and CDC-42 right before and during nuclear migration. Previous data from our lab show that there is actin enrichment in the constriction and behind the nucleus during nuclear migration, therefore I predict CGEF-1D/CDC-42 and the Arp2/3 complex will be localized near and in the constriction to generate branched actin and deform the nucleus as it migrates through the constriction. I also predict that the actin enrichment behind the nucleus are actomyosin structures and that NMY-2 will be localized at the rear of the nucleus. It is also unclear if CDC-42 also regulates NMY-2, and if so, then I would also predict CDC-42 will localize at the rear of the nucleus in addition to being localized in the constriction.

Once we can determine where these proteins are localized during this process and if any of them co-localize with each other, then we can start to build a mechanism model for this process.

Determine if branched actin and actomyosin are in the same pathway

In Chapter III, I show that CDC-42, ARX-3 and NMY-2 are necessary for nuclear migration in the absence of the LINC complex at 15°C. As a known regulator of actin, CDC-42 could be regulating either ARX-3 or NMY-2 or both proteins (Figure 4.3). Once activated by a GEF, CDC-42 binds to and activates WAVE/WASP, which then activates the Arp2/3 complex to generate branched actin (Ramesh et al., 1997; Rohatgi et al., 1999, 2000; Watson et al., 2017). Another downstream effector of active CDC-42 is myotonic dystrophy kinase-related Cdc42-binding kinase (MRCK) (Zhao & Manser, 2015). CDC-42 functions by recruiting MRCK and once activated, MRCK can regulate the phosphorylation of myosin light chain MLC and activate NMY-2 (Zhao & Manser, 2015). This is one way in which CDC-42 and NMY-2 can function in the same pathway. Another hypothesis is actomyosin contractions are required for redistribution of CDC-42 so that it can function where it needs to. To test if CDC-42 exclusively regulates ARX-3 or NMY-2 is to generate the *degron::cdc-42; degron::arx-3; unc-84(n369)* and *degron::cdc-42; degron::nmy-2; unc-84(n369)* triple mutants and compare their GABA counts to that of the respective double mutants *degron::arx-3; unc-84(n369)* and *degron::nmy-2; unc-84(n369)*. If the triple mutants are similar to the double mutants, that would suggest they are in the same pathway. However, if the triple mutants are worse than the double mutants, that would suggest that CDC-42 is either in a different pathway than ARX-3 or NMY-2, or that CDC-42 regulates both ARX-3 and NMY-2. To test if CDC-42 regulates both proteins, we can generate the *degron::cdc-42; degron::arx-3; degron::nmy-2; unc-84(n369)* quadruple mutant and the *degron::arx-3; degron::nmy-2; unc-84(n369)* triple mutant and compare the GABA counts

between the two mutants. If CDC-42 regulates both the Arp2/3 complex and NMY-2, then I would expect the quadruple mutant to look similar to the triple mutant as CDC-42 would be acting upstream of both the Arp2/3 complex and NMY-2. We could also compare the *degron::arx-3; degron::nmy-2; unc-84(n369)* triple mutant to the *degron::cdc-42::unc-84(n369)* double mutant and if CDC-42 regulates the Arp2/3 complex and NMY-2, then the triple would look similar to the double. Alternatively, if CDC-42 does not regulate NMY-2, we could test if RHO-1 regulates NMY-2, seeing as myosin light chain kinase (MLCK) is an effector of RHO-1 and MLCK functions by phosphorylating NMY-2 to regulate actomyosin contractions (Kelley et al., 2018; Totsukawa et al., 2000).

With an optimized protocol for the microfluidic device, we can visualize where these proteins are localized with respect to each other to further determine the mechanism of the actin-based pathway. In my model, the Arp2/3 complex and NMY-2 function at different spaces. If CDC-42 regulates the Arp2/3 complex, NMY-2, or both, I would expect to see co-localization between CDC-42 and ARX-3 and/or CDC-42 and NMY-2.

Identify what other RhoGTPases are activated by CGEF-1

In Chapter III, I showed data suggesting CGEF-1 activates CDC-42 but it also might function by activating the other RhoGTPases. While the constitutively active versions of RHO-1, MIG-2, and CED-10 did not rescue the nuclear migration defect of the *cgef-1(yc3); unc-84(n369)* double mutant, this does not prove that they are not involved. Unlike *cdc-42*, there are viable null and loss-of function alleles of *mig-2* and *ced-10. mig-2(mu28)* and *ced-10(n3246)* are null and loss-of-function alleles that on their own do not lead to a P-cell migration failure (Spencer et al., 2001). Future directions should be to cross these alleles into an *unc-84(n369)* background and assay for P-cell nuclear migration. To also make sure *mig-2* and *ced-10* are not

acting redundantly, we should also generate the *unc-84(n369); mig-2(mu28); ced-10(n3246)* triple mutant and assay for nuclear migration. Because RHO-1 is essential for embryogenesis, we could use the auxin-inducible degradation system to knockdown RHO-1 in P cells during nuclear migration in an *unc-84(n369)* background and assay for nuclear migration. These experiments would tell us if MIG-2, CED-10, and RHO-1 are necessary for P-cell nuclear migration in the absence of LINC.

Determine which domains of CGEF-1 are involved in function and localization

To further characterize CGEF-1, we can do more analysis on the domains of CGEF-1. Most RhoGEFs have the canonical Dbl homology (DH) domain followed by the pleckstrin homology (PH) domain. The DH domain is the catalytic domain that interacts with RhoGTPases and facilitates the exchange of GDP for GTP. The PH domain can interact with lipids and can serve as a docking site for other proteins in order to enhance the activity of the DH domain. Domains outside of the DH-PH domain can be involved in protein-protein and protein-lipid interactions that can regulate the activity of the DH-PH domain, involved in localization, or in localizing other proteins (Cook et al., 2014; Hoffman & Cerione, 2002; Rossman et al., 2005). Using CRISPR, we can delete different domains of cgef-1d and assay for P-cell nuclear migration defects. We can also look at protein localization of these different domain deletion mutants and determine if any of these domains are necessary for proper localization of the protein.

Determine the role of nuclear actin in P-cell nuclear migration

In Chapter I, I discussed the different factors that contribute to nuclear stiffness and deformation include lamin and heterochromatin levels. Another factor that has not been as

extensively studied in confined nuclear migration is nuclear actin. Nuclear actin has been shown to affect transcription, chromatin organization, and nuclear structure (Kelpsch & Tootle, 2018). Knockout of β-actin in mouse embryonic fibroblasts led to increased levels of H3K9me3 and Heterochromatin protein (HP) and these effects were partially rescued by expression of NLS-tagged β-actin (Xie et al., 2018). The LINC complex has also been shown to be able to regulate nuclear actin in mammalian fibroblasts. When fibroblasts were stimulated by fibronectin, nuclear actin polymerized within 30 minutes and there was a loss of actin formation when Sun1 and Sun2 was knocked-down (Plessner et al., 2015). The nuclear envelope protein Emerin has also been shown to stimulate actin polymerization *in vitro* and may be helping to create an actin network at the nuclear periphery to provide structural support at the nuclear envelope (Holaska et al., 2004). In addition to nuclear envelope proteins, lamin has also been shown be able to interact with actin *in vitro* and can bind and bundle filamentous actin (Simon et al., 2010). Interestingly, *Xenopus laevis* oocyte, which usually does not express exportin 6, contain high levels of nuclear actin and ectopic expression of exportin 6 led to more fragile nuclei suggesting nuclear actin is required for nuclear structure (Bohnsack et al., 2006).

While it is clear nuclear actin plays a role in nuclear structure and interacts with proteins that are known to affect nuclear stiffness, there is very little research on the role of nuclear actin in confined nuclear migration. I propose that we study nuclear actin in P-cell nuclear migration. We can add fluorescent tags to ARX-2 and NMY-2 and observe their dynamic during nuclear migration. The company Chromotek sells a plasmid that codes for NLS-tagged actin (Chromotek, #Acg-n) that we can use to label nuclear actin and observe nuclear actin dynamic using the microfluidic device to determine if actin structures form in the nucleus. Nuclear actin structures are distinct from cytoplasmic actin. While nuclear actin can also be found as

monomers, filamentous actin has been describes as rods, fibrillar bodies, nuclear bundles, paracrystals, filaments, and bars (Kelpsch & Tootle, 2018). I hypothesize actin filaments will form at the nuclear periphery during nuclear migration to provide structural support for the nucleus. We can also ascertain if nuclear actin affects lamin organization or levels of heterochromatin to regulate nuclear stiffness. To do so, we can knockdown the Arp2/3 complex or NMY-2 and observe fluorescently tagged lamin to determine if nuclear actin affects lamin organization. We can also look at enrichment and localization of heterochromatin protein 1 (HP1) in the knockdown mutants as an indication of heterochromatin levels and organization.

Summary

Confined nuclear migration is an important process to study because it is the rate-limiting step for cell migration through constricted spaces, which is required in many diverse biological processes. Because this field of study is dominated by *in vitro* techniques to study this process, there is a need for an *in vivo* model to study confined nuclear migration. In Chapter I of this dissertation, I've reviewed several nuclear migration events *in vivo*, the significance of actin in *C. elegans* development, and proposed the use of P-cell nuclear migration as a model for studying nuclear migration *in vivo*. In Chapter II, I show that dynein is necessary for P-cell nuclear migration which highlights the importance of cytoskeletal elements such as microtubules and motor proteins in this dynamic process. In Chapter III, I show that actin regulators such as CDC-42, Arp2/3 complex, and non-muscle myosin are necessary for P-cell nuclear migration and proposed the existence of two cytoskeletal pathways involved in this process—a microtubule-based pathway and an actin-based pathway. In Chapter IV, I describe the different avenues future experiments can take to further our understanding of nuclear migration through constrictions *in vivo*. These future directions mainly focus on live-imaging P-cell nuclear

migration and observing cytoskeletal dynamics and proteins localization. Towards the end of this Chapter, I bring up the possibility of studying nuclear actin during this process which would be an area of great interest as studies on nuclear actin is not as extensive as cytoplasmic actin. While all of the data in this dissertation focuses on elements outside of the nucleus, it's just as important to study elements inside the nucleus. My lab member Ellen Gregory has already shown that chromatin remodelers play a significant role in nuclear migration. Hopefully future lab members will be able to further characterize the different pathways involved in P-cell nuclear migration both outside and inside the nucleus.
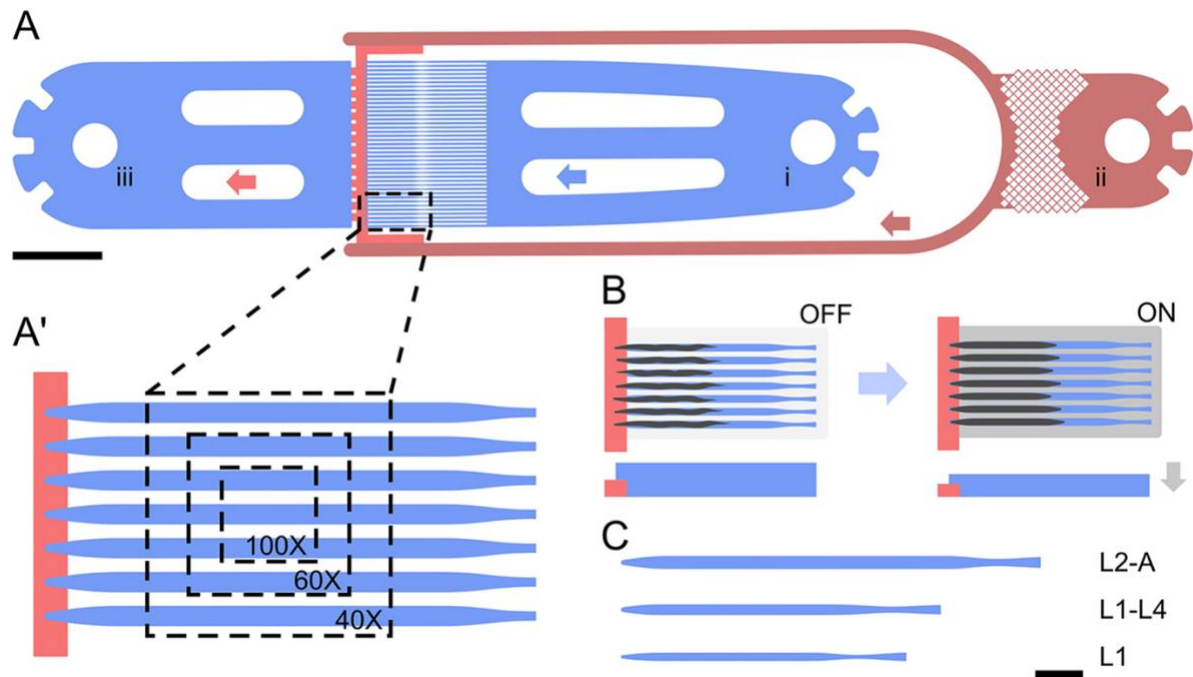
Figures

Figure 4.1

Figure 4.1: Microfluidic chip (Berger et al., 2021). (A) Overview of the microfluidic device. Animals are flowed into the device through the inlet (i) and pushed into parallel channels (A'). E. coli food source is flowed into the device through the inlet (ii) and flows to a channel that runs perpendicular to the worm channels (red arrow shows direction of food flow). Liquid leaves the device through the outlet (iii). (B) A hydraulic valve (not pictured) runs perpendicular to the worm channels and sits on top of the worm channels. When the valve is off, the worms are loosely held in the channels, which have bigger dimensions than the worms to allow for growth. When the valve is on, the animals get pressed onto the cover glass and are immobilized for image acquisition. (C) There are microfluidic devices with different size channels for worms in different growth stages.
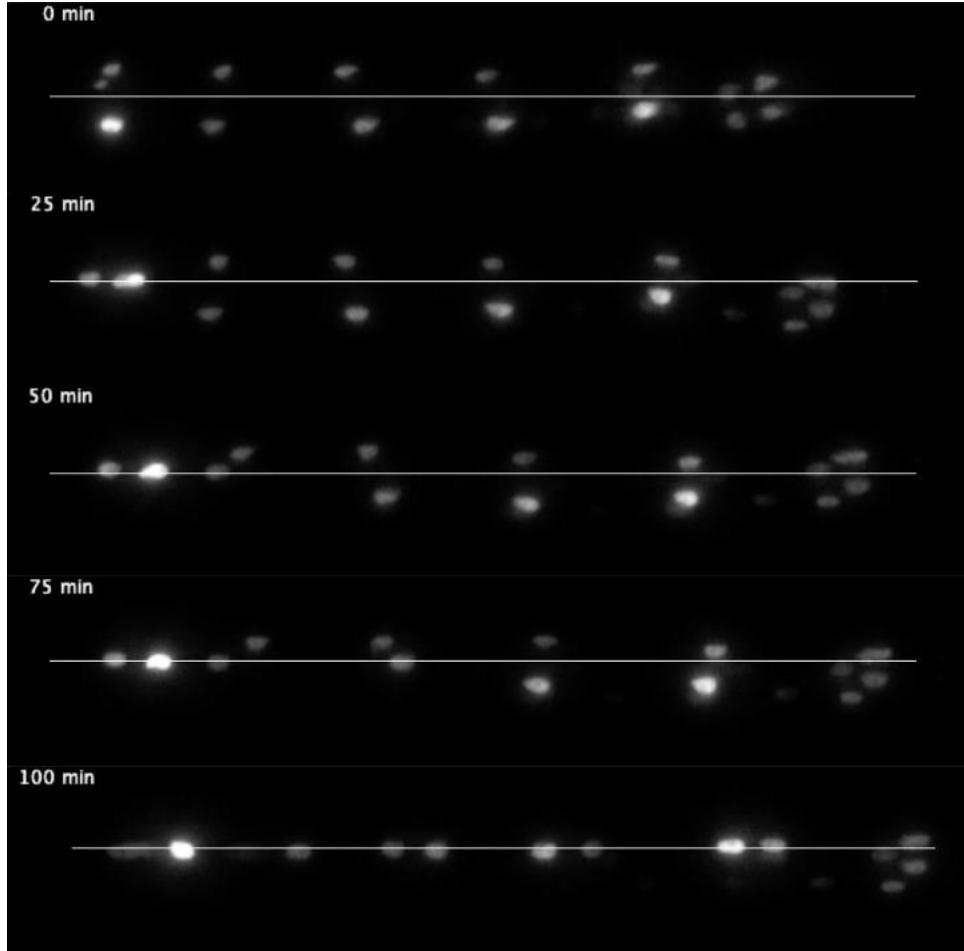
Figure 4.2

Figure 4.2: Timelapse video of P-cell nuclear migration using microfluidic chip from

Figure 1. L1s that expressed NLS::tdTomato under the P-cell specific promoter, *hlh-3*, were

flowed into the microfluidic device and imaged. Images show the animals from a dorsal view,

with the ventral cord depicted by a white horizonal line. P-cell nuclei can be seen as six nuclei on

either side of the white line. During nuclear migration, the labeled nuclei can be seen migrating

to the ventral cord (white line) starting with the anterior pair at timepoint 0 min and ending with

nuclear migration of the most posterior pair at timepoint 100 min. P-cell nuclear migration

occurred over the course of ~100 min at room temperature. Images taken by Simon Berger.
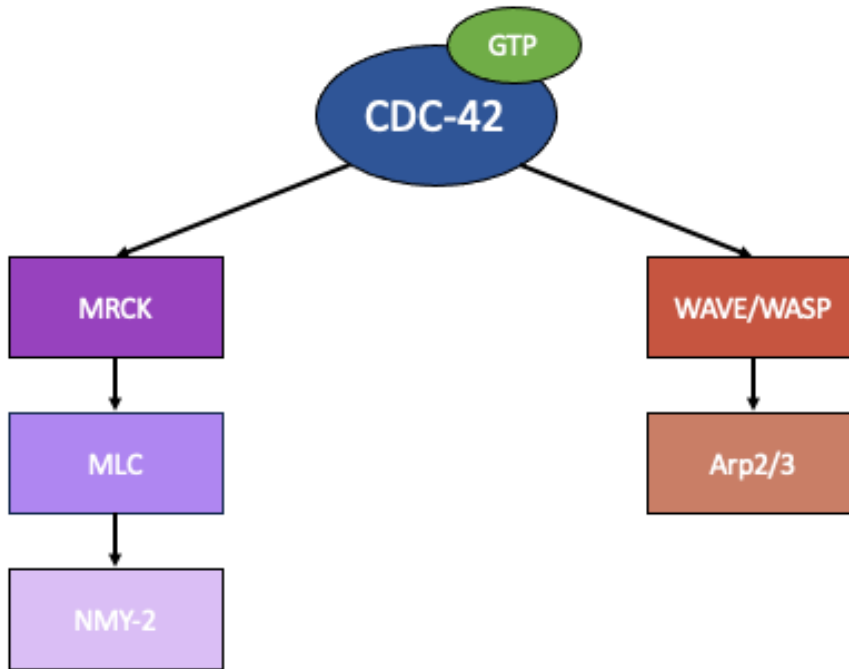
Figure 4.3

Figure 4.3: Downstream effectors of activated CDC-42. Once CDC-42 is activated by a GEF

protein, it can activate downstream effectors depending on the context. Potential effectors are

MRCK (myotonic dystrophy kinase-related Cdc42-binding kinase) and WAVE/WASP. On the

left, once activated, MRCK can activate MLC (myosin light chain), which can activate NMY-2

(non-muscle myosin 2) to generate actomyosin contractions. On the right, once activated,

WAVE/WASP can activate the Arp2/3 complex to generate branched actin.

References

Berger, S., Spiri, S., deMello, A., & Hajnal, A. (2021). Microfluidic-based imaging of complete Caenorhabditis elegans larval development. *Development*, *148*(18), dev199674. https://doi.org/10.1242/dev.199674

Bohnsack, M. T., Stüven, T., Kuhn, C., Cordes, V. C., & Görlich, D. (2006). A selective block of nuclear actin export stabilizes the giant nuclei of Xenopus oocytes. *Nature Cell Biology*, *8*(3), 257–263. https://doi.org/10.1038/ncb1357

Bone, C. R., Chang, Y.-T., Cain, N. E., Murphy, S. P., & Starr, D. A. (2016). Nuclei migrate through constricted spaces using microtubule motors and actin networks in C. elegans hypodermal cells. *Development*, *143*(22), 4193–4202. https://doi.org/10.1242/dev.141192

Cabantous, S., Terwilliger, T. C., & Waldo, G. S. (2005). Protein tagging and detection with engineered self-assembling fragments of green fluorescent protein. *Nature Biotechnology*, *23*(1), 102–107. https://doi.org/10.1038/nbt1044

Cook, D. R., Rossman, K. L., & Der, C. J. (2014). Rho guanine nucleotide exchange factors: Regulators of Rho GTPase activity in development and disease. *Oncogene*, *33*(31), 4021–4035. https://doi.org/10.1038/onc.2013.362

Cranfill, P. J., Sell, B. R., Baird, M. A., Allen, J. R., Lavagnino, Z., de Gruiter, H. M., Kremers, G.-J., Davidson, M. W., Ustione, A., & Piston, D. W. (2016). Quantitative assessment of fluorescent proteins. *Nature Methods*, *13*(7), 557–562. https://doi.org/10.1038/nmeth.3891

Feng, S., Sekine, S., Pessino, V., Li, H., Leonetti, M. D., & Huang, B. (2017). Improved split fluorescent proteins for endogenous protein labeling. *Nature Communications*, *8*(1), 370. https://doi.org/10.1038/s41467-017-00494-8

Frøkjaer-Jensen, C., Davis, M. W., Hopkins, C. E., Newman, B. J., Thummel, J. M., Olesen, S.-P., Grunnet, M., & Jorgensen, E. M. (2008). Single-copy insertion of transgenes in Caenorhabditis elegans. *Nature Genetics*, *40*(11), 1375–1383. PubMed. https://doi.org/10.1038/ng.248

Gokce, S. K., Hegarty, E. M., Mondal, S., Zhao, P., Ghorashian, N., Hilliard, M. A., & Ben-Yakar, A. (2017). A multi-trap microfluidic chip enabling longitudinal studies of nerve regeneration in Caenorhabditis elegans. *Scientific Reports*, *7*(1), 9837. https://doi.org/10.1038/s41598-017-10302-4

Goudeau, J., Sharp, C. S., Paw, J., Savy, L., Leonetti, M. D., York, A. G., Updike, D. L., Kenyon, C., & Ingaramo, M. (2021). Split-wrmScarlet and split-sfGFP: tools for faster, easier fluorescent labeling of endogenous proteins in Caenorhabditis elegans. *Genetics*, *217*(4), iyab014. https://doi.org/10.1093/genetics/iyab014

He, S., Cuentas-Condori, A., & Miller, D. M., III. (2019). NATF (Native and Tissue-Specific Fluorescence): A Strategy for Bright, Tissue-Specific GFP Labeling of Native Proteins in Caenorhabditis elegans. *Genetics*, *212*(2), 387–395. https://doi.org/10.1534/genetics.119.302063

Hefel, A., & Smolikove, S. (2019). Tissue-Specific Split sfGFP System for Streamlined Expression of GFP Tagged Proteins in the Caenorhabditis elegans Germline. *G3 (Bethesda, Md.)*, *9*(6), 1933–1943. PubMed. https://doi.org/10.1534/g3.119.400162

Ho, J., Venecia A. Valdez, Ma, L., & Starr, D. A. (2018). *Characterizing Dynein's Role in P-cell Nuclear Migration using an Auxin-Induced Degradation System*. https://doi.org/10.17912/W2W96J

Hoffman, G. R., & Cerione, R. A. (2002). Signaling to the Rho GTPases: Networking with the DH domain. *FEBS Letters*, *513*(1), 85–91. https://doi.org/10.1016/S0014-5793(01)03310-5

Holaska, J. M., Kowalski, A. K., & Wilson, K. L. (2004). Emerin Caps the Pointed End of Actin Filaments: Evidence for an Actin Cortical Network at the Nuclear Inner Membrane. *PLOS Biology*, *2*(9), e231. https://doi.org/10.1371/journal.pbio.0020231

Kelley, C. A., Wirshing, A. C. E., Zaidel-Bar, R., & Cram, E. J. (2018). The myosin light-chain kinase MLCK-1 relocalizes during Caenorhabditis elegans ovulation to promote actomyosin bundle assembly and drive contraction. *Molecular Biology of the Cell*, *29*(16), 1975–1991. https://doi.org/10.1091/mbc.E18-01-0056

Kelpsch, D. J., & Tootle, T. L. (2018). Nuclear Actin: From Discovery to Function. *Anatomical Record (Hoboken, N.J. : 2007)*, *301*(12), 1999–2013. PubMed. https://doi.org/10.1002/ar.23959

Noma, K., Goncharov, A., Ellisman, M. H., & Jin, Y. (2017). Microtubule-dependent ribosome localization in C. elegans neurons. *ELife*, *6*, e26376. https://doi.org/10.7554/eLife.26376

Nonet, M. L. (2020). Efficient Transgenesis in Caenorhabditis elegans Using Flp Recombinase-Mediated Cassette Exchange. *Genetics*, *215*(4), 903–921. https://doi.org/10.1534/genetics.120.303388

Plessner, M., Melak, M., Chinchilla, P., Baarlink, C., & Grosse, R. (2015). Nuclear F-actin Formation and Reorganization upon Cell Spreading * ♦. *Journal of Biological Chemistry*, *290*(18), 11209–11216. https://doi.org/10.1074/jbc.M114.627166

Ramesh, N., Antón, I. M., Hartwig, J. H., & Geha, R. S. (1997). WIP, a protein associated with Wiskott–Aldrich syndrome protein, induces actin polymerization and redistribution in lymphoid cells. *Proceedings of the National Academy of Sciences*, *94*(26), 14671–14676. https://doi.org/10.1073/pnas.94.26.14671

Rohatgi, R., Ho, H. H., & Kirschner, M. W. (2000). Mechanism of N-Wasp Activation by Cdc42 and Phosphatidylinositol 4,5-Bisphosphate. *Journal of Cell Biology*, *150*(6), 1299–1310. https://doi.org/10.1083/jcb.150.6.1299

Rohatgi, R., Ma, L., Miki, H., Lopez, M., Kirchhausen, T., Takenawa, T., & Kirschner, M. W. (1999). The Interaction between N-WASP and the Arp2/3 Complex Links Cdc42-Dependent Signals to Actin Assembly. *Cell*, *97*(2), 221–231. https://doi.org/10.1016/S0092-8674(00)80732-1

Rossman, K. L., Der, C. J., & Sondek, J. (2005). GEF means go: Turning on RHO GTPases with guanine nucleotide-exchange factors. *Nature Reviews Molecular Cell Biology*, *6*(2), 167–180. https://doi.org/10.1038/nrm1587

Simon, D. N., Zastrow, M. S., & Wilson, K. L. (2010). Direct actin binding to A- and B-type lamin tails and actin filament bundling by the lamin A tail. *Nucleus (Austin, Tex.)*, *1*(3), 264–272. PubMed. https://doi.org/10.4161/nucl.1.3.11799

Totsukawa, G., Yamakita, Y., Yamashiro, S., Hartshorne, D. J., Sasaki, Y., & Matsumura, F. (2000). Distinct Roles of Rock (Rho-Kinase) and Mlck in Spatial Regulation of Mlc Phosphorylation for Assembly of Stress Fibers and Focal Adhesions in 3t3 Fibroblasts. *Journal of Cell Biology*, *150*(4), 797–806. https://doi.org/10.1083/jcb.150.4.797

Watson, J. R., Owen, D., & Mott, H. R. (2017). Cdc42 in actin dynamics: An ordered pathway governed by complex equilibria and directional effector handover. *Small GTPases*, *8*(4), 237–244. PubMed. https://doi.org/10.1080/21541248.2016.1215657

Xie, X., Almuzzaini, B., Drou, N., Kremb, S., Yousif, A., Farrants, A.-K. Ö., Gunsalus, K., & Percipalle, P. (2018). β-Actin-dependent global chromatin organization and gene expression programs control cellular identity. *The FASEB Journal*, *32*(3), 1296–1314. https://doi.org/10.1096/fj.201700753R

Zhao, Z., & Manser, E. (2015). Myotonic dystrophy kinase-related Cdc42-binding kinases (MRCK), the ROCK-like effectors of Cdc42 and Rac1. *Small GTPases*, *6*(2), 81–88. PubMed. https://doi.org/10.1080/21541248.2014.1000699

Ziel, J. W., Matus, D. Q., & Sherwood, D. R. (2009). An expression screen for RhoGEF genes involved in C. elegans gonadogenesis. *Gene Expression Patterns*, *9*(6), 397–403. https://doi.org/10.1016/j.gep.2009.06.005